

LAKEHEAD UNIVERSITY

ATTITUDE CONTROL FOR  
A QUADROTOR UAV  
USING ADAPTIVE FUZZY BACKSTEPPING

by

Kaiyu Zhao

Under the Supervision of Dr. Xiaoping Liu

*For Fulfilling the Partial Requirements of the Master of Science  
in the Electrical and Computer Engineering*

Lakehead University, Thunder Bay, Ontario, Canada

Sept. 2017

# Acknowledgments

Foremost, I would like to express a sincere appreciation to my supervisor Dr. Xiaoping Liu for his supervision during my study period of Master's degree at Lakehead University. From the very beginning of my thesis, Dr. Xiaoping Liu has devoted all his passion to help and support me. I was inspired by his enthusiasm on control theory, and motivated by his guidance with practical implementation. It is Dr. Liu who expands my horizon in engineering field and guided me to various possibilities. When I was stuck in a problem which I could not handle, Dr. Liu always taught me patiently with good manner. Without the constant help from Dr. Liu, this thesis would have not gone smoothly. Besides my supervisor, I would also like to show sincere thanks to Dr. Krishnamoorthy Natarajan, Dr. Mohammad Uddin, Dr. Abdelhamid Tayebi, and Dr. Wilson Wang for their feedback and comments during my thesis progress. And thank you sincerely for taking your time reviewing my thesis paper.

I would like to forward my sincere gratitude to my previous graduate fellow students Mr. Xiao Cui and Mr. Miaomiao Wang. We shared the similar platform with different control strategies. They have done a great job in this research area before I started my research topic. They led me to familiarize with the quadrotor in the contents that are easy to understand. They built my confidence and increased my interest. They gave me various suggestions from their previous experiences, which saved my time and effort. We still share new ideas on our research area after they graduated. I would also like to thank my colleagues in my lab, Mr. Renjie Yin, Mr. Zhengqi Wang, Mr. Tianqi Xi, and Miss Ning Che. Thank you for all the help with my research and daily life in Thunder Bay and wish you all the best in your future lives at Lakehead University. I feel obliged to have these close friends who are talented and generous.

Last but not the least, I would like to thank my family, my father, my mother and my boy friend. They have given me their great understanding and support for my study and life at Lakehead University. It is their loves that support me to overcome various obstacles.

Sincerely

Kaiyu Zhao

## Abstract

With improvements on automation, computer, electronics and other technologies, applications of unmanned aerial vehicles (UAVs) have expanded from pure military field to civilian areas. As a multirotor aircraft, a quadrotor UAV has the advantages of simple structure, small size, high manoeuvrability, etc. On the basis of summarizing the current research situation of the quadrotor UAV, a deep research has been conducted on the attitude control system of the quadrotor UAV and two controllers are proposed to generate a stable performance: Back-stepping controller, adaptive fuzzy back-stepping nonlinear controller.

The quadrotor UAV consists of two pairs of rotors and propellers, which can generate thrust and air drag. The dynamic model is derived using the Euler-Lagrangian method and Newton method with 6 degrees of freedom. To represent the model of the quadrotor, Euler angles representation is first derived. However, facing the gimbal lock drawback of Euler angles representation, unit quaternion representation is then discussed afterwards.

In normal situations, model parameter uncertainties and external disturbances would affect the system output. Due to this problem, an adaptive fuzzy strategy is designed to approximate the uncertain model using back-stepping techniques with the Lyapunov stability theorem. Firstly, simulations are used to prove the mathematical feasibility. And then experimental results will be provided to illustrate the satisfactory performances of the proposed approach in real time.

# Contents

<b>1</b>	<b>Introduction</b>	<b>1</b>
1.1	Overview of Quadrotor UAVs . . . . .	1
1.2	Attitude Control . . . . .	4
1.3	Thesis Motivation . . . . .	5
1.4	Thesis Outline . . . . .	5
<b>2</b>	<b>Background and Preliminaries</b>	<b>7</b>
2.1	Flight Principles and Aerodynamics . . . . .	7
2.2	Attitude Representation . . . . .	9
2.2.1	Rotational Representation . . . . .	11
2.2.2	Euler Angle Representation . . . . .	11
2.2.3	Unit Quaternion Representation . . . . .	13
2.2.4	Relations between Attitude Representation . . . . .	15
<b>3</b>	<b>UAV Quadrotor Dynamics</b>	<b>17</b>
3.1	Dynamic Model with Euler Lagrangian Formalism . . . . .	17
3.2	Dynamic Model with Newton-Euler Formalism . . . . .	20
<b>4</b>	<b>Experimental Platform</b>	<b>23</b>
4.1	The frame of the Quadrotor . . . . .	23
4.2	Main Controller . . . . .	24

---

4.3	Communication Subsystem . . . . .	27
4.4	Propulsion Subsystem . . . . .	28
<b>5</b>	<b>Controller Design with Back-stepping Technique</b>	<b>33</b>
5.1	Backstepping Design with Euler Angle Representation . . . . .	33
5.1.1	Controller Design . . . . .	33
5.1.2	Simulation Results . . . . .	36
5.2	Fuzzy Adaptive Integral Backstepping Design with Euler Angle Representation	37
5.2.1	Controller Design . . . . .	37
5.2.2	Simulation Results . . . . .	54
5.3	Backstepping Design with Unit Quaternion Representation . . . . .	55
5.3.1	Controller Design . . . . .	55
5.3.2	Experimental Results . . . . .	59
5.4	Adaptive Fuzzy Backstepping Design with Quaternion Representation . . . . .	61
5.4.1	Controller Design . . . . .	61
5.4.2	Experimental Results . . . . .	73
<b>6</b>	<b>Conclusion</b>	<b>76</b>
6.1	Achievements of the Thesis . . . . .	76
6.2	Future Work . . . . .	77

# List of Figures

1.1	DJI Phantom 4 . . . . .	2
1.2	Parrot AR. Drone 2.0 . . . . .	2
1.3	Hover Camera . . . . .	3
2.1	(a) ”+” Structure of the Quadrotor; (b) ”x” Structure of the Quadrotor . . . . .	7
2.2	(a) Raise; (b) Hover; (a) Down . . . . .	8
2.3	(a) Left; (b) Right . . . . .	9
2.4	(a) Forward; (b) Backward . . . . .	9
2.5	(a) Clockwise; (b) Counterclockwise . . . . .	10
2.6	Coordinate System . . . . .	10
2.7	Roll, Pitch, and Yaw Motion . . . . .	12
2.8	Rotate the x-y-z Frame Around x Axis . . . . .	12
2.9	Rotate the x-y-z Frame Around y Axis . . . . .	13
2.10	Rotate the x-y-z Frame Around z Axis . . . . .	13
4.1	Experimental Platform . . . . .	23
4.2	Overview of the Quadrotor Platform . . . . .	24
4.3	The Frame . . . . .	24
4.4	Arduino Interface . . . . .	25
4.5	APM 2.6 and Ports . . . . .	25

4.6	3DR UBlox GPS with Compass Model . . . . .	27
4.7	3DR Power Module . . . . .	27
4.8	(a) RC Transmitter; (b) RC Reciever . . . . .	28
4.9	3DR Telemetry Radio . . . . .	28
4.10	Propulsion System . . . . .	29
4.11	BLDC motor . . . . .	29
4.12	ESC . . . . .	30
4.13	Propeller . . . . .	30
4.14	LiPo Battery . . . . .	31
5.1	Backstepping Controller with Euler Angle Representation . . . . .	36
5.2	$\phi$ , $\theta$ , and $\psi$ with Backstepping Controller . . . . .	37
5.3	Tracking Errors with Backstepping Controller . . . . .	37
5.4	Angular Velocities with Backstepping Controller . . . . .	38
5.5	The Fuzzy Sets for $\dot{\phi}$ . . . . .	40
5.6	The Fuzzy Sets for $\dot{\theta}$ . . . . .	41
5.7	The Fuzzy Sets for $\dot{\psi}$ . . . . .	41
5.8	The Fuzzy Logic Estimator for $\dot{\theta}\dot{\psi} \left( \frac{I_{\theta}-I_{\psi}}{I_{\phi}} \right)$ . . . . .	43
5.9	The Fuzzy Logic Estimator for $\dot{\phi}\dot{\psi} \left( \frac{I_{\psi}-I_{\phi}}{I_{\theta}} \right)$ . . . . .	44
5.10	The Fuzzy Logic Estimator for $\dot{\phi}\dot{\theta} \left( \frac{I_{\phi}-I_{\theta}}{I_{\psi}} \right)$ . . . . .	44
5.11	Adaptive Fuzzy Integral Backsteppig Controller with Euler Angle Representation	54
5.12	$\phi$ , $\theta$ , and $\psi$ with Fuzzy Adaptive Integral Backstepping Controller . . . . .	54
5.13	Tracking Errors with Fuzzy Adaptive Integral Backstepping Controller . . . . .	55
5.14	Angular Velocities with Fuzzy Adaptive Integral Backstepping Controller . . . . .	55
5.15	Tracking for $\phi$ , $\theta$ , and $\psi$ with Fuzzy Adaptive Integral Backstepping Controller	56
5.16	Backsteppig Controller with Unit Quaternion Representation . . . . .	59

5.17	Separate Tests with Backstepping Controller-Quaternion Representation . . .	60
5.18	$\phi$ , $\theta$ , and $\psi$ with Backstepping Controller-Quaternion Representation . . . .	60
5.19	Angular Velocities with Backstepping Controller-Quaternion Representation .	61
5.20	The Fuzzy Sets for $\omega_1$ . . . . .	62
5.21	The Fuzzy Sets for $\omega_2$ . . . . .	63
5.22	The Fuzzy Sets for $\omega_3$ . . . . .	63
5.23	The Fuzzy Logic Estimator for $\left(\frac{I_\theta - I_\psi}{I_\phi}\right) \omega_2 \omega_3$ . . . . .	65
5.24	The Fuzzy Logic Estimator for $\left(\frac{I_\psi - I_\phi}{I_\theta}\right) \omega_1 \omega_3$ . . . . .	66
5.25	The Fuzzy Logic Estimator for $\left(\frac{I_\phi - I_\theta}{I_\psi}\right) \omega_1 \omega_2$ . . . . .	66
5.26	Adaptive Fuzzy Backstepping Controller with Unit Quaternion Representation	73
5.27	Separate Tests with Adaptive Fuzzy Backstepping Controller . . . . .	74
5.28	$\phi$ , $\theta$ , and $\psi$ with Adaptive Fuzzy Backstepping Controller . . . . .	74
5.29	Angular Velocities with Adaptive Fuzzy Backstepping Controller . . . . .	75

# List of Tables

4.1	800KV Motor Specification . . . . .	29
4.2	ESC Specification . . . . .	30
4.3	Propeller Parameters . . . . .	31
4.4	3300mAh LiPo Battery Specification . . . . .	31

# List of Abbreviations

<b>UAV</b>	–	Unmanned Aerial Vehicle.
<b>IC</b>	–	Integrated Circuit.
<b>LQR</b>	–	Linear Quadratic Regulator .
<b>PID</b>	–	Proportional Integral Derivative .
<b>FLS</b>	–	Fuzzy Logic System.
<b>FLC</b>	–	Fuzzy Logic Controller.
<b>DCM</b>	–	Direction Cosine Matrix.
<b>DSP</b>	–	Digital Signal Processor.
<b>APM</b>	–	Ardupilot Mega.
<b>PM</b>	–	Power Module.
<b>RC</b>	–	Remote Control.
<b>PPM</b>	–	Pulse Position Modulation.
<b>BLDC</b>	–	Brushless DC.
<b>LiPo</b>	–	Lithium Polymer.
<b>ESC</b>	–	Electronic Speed Controller.
<b>GPS</b>	–	Global Positioning System.
<b>OSP</b>	–	Open-Source Projects.
<b>APM</b>	–	Arduino Pilot Module.
<b>ESC</b>	–	Electronics Speed Control.
<b>IDE</b>	–	Integrated Development Environment .
<b>I2C</b>	–	Inter Integral Circuit.
<b>USB</b>	–	Universal Serial Bus.
<b>IMU</b>	–	Inertial Measurement Unit.
<b>PPM</b>	–	Pulse Position Modulation.
<b>CPU</b>	–	Central Processing Unit.
<b>MPU</b>	–	Inertial Measurement Unit.
<b>LiPo</b>	–	Lithium Polymer.

# Chapter 1

## Introduction

### 1.1 Overview of Quadrotor UAVs

Unmanned Aerial Vehicle (UAV) is a kind of vehicle which is able to fly autonomously. UAV is controlled by wireless remote control device with its own programmable control device in accordance with the predetermined procedures to achieve flight independence. In recent years, with the declining cost of hardware and the smaller size of IC chips, the application of UAVs is no longer confined to the military area. It has been widely applied in the civil and commercial fields, such as construction, utilities and telecom, public safety, agriculture, surveying and mapping as well.

According to the layout of the body and the shape of airfoils, UAVs can be divided into airships, fixed wing and rotary wing machine [1]. According to the number of rotors, it can also be divided into single rotor (eg. helicopter) and multi-rotor UAVs. So UAVs with four (called quadrotor), six, and eight rotors are called multi-rotor UAVs. Usually, the number of rotors of UAV is even numbers. The reason for this feature is basically aim to compromise the positive and negative rotational torque in order to maintain the stability of UAVs.

The technology of fixed wing UAVs has become relatively mature in the last decade, while, comparing to this high tech, multiple rotor UAVs have the advantages of greater trust-weight ratio, small volume, light weight, simple construction, simple operation of vertical take-off and landing, small operating environment. Comparing to the fixed wing helicopter, drones which are controlled by changing angular velocity of four motors do not need the swashplate. According to the introduction in [2] and [3], the first attempt to realize a quadrotor was Louis and Jacques Breguet from France in 1907. More attempts had been made after that. In 1922, Dr. George de Bothezat and Ivan Jerome (US Air Service) developed an X-shaped structure helicopter with six-bladed motors. They reached maximum 5 meters with reliability problems. A breakthrough was made in 1958. A vertical take-off and landing quadrotor named Curtiss-Wright VZ-7 was designed by the Curtiss-Wright company for the US Army since it was controlled by changing the thrust of each rotor. Because of the special construction and flying principle, the drone system is a nonlinear and under-actuated

system, which will bring various challenges to control design. In this thesis, a quadrotor will be studied intensively.

Nowadays, quadrotor is widely used not only for institutions, but also for individuals as personal interest. Many companies are catching up with the trend. A variety of quadrotors have been designed for commercial use. Here are some brief introductions of three well-known companies with their products.

Fig. 1.1 shows the world's most popular quadrotor named DJI Phantom 4, which is developed by a company named DJI located in China. This company was founded in 2006 by Frank Wang. They mainly intend to develop stable multi-rotor control systems for different kinds of platforms with heavy payloads and/or perfect photography function. A survey had shown that the DJI occupied more than 50 percentage of average market share in consumer quadrotor market over the world.



Figure 1.1: DJI Phantom 4

Fig. 1.2 illustrates a quadrotor called AR. Drone 2.0, which is designed by a French company located in Paris. It used to be known for its expertise in wireless devices. The company shocked the hobbyist market by developing a drone which can be controlled by a cell phone application although this technique has been widely adapted by many developed companies nowadays.



Figure 1.2: Parrot AR. Drone 2.0

Fig. 1.3 shows a small and foldable quadrotor, named hover camera, which is designed by a Chinese company named Zero Zero Robotics. The main feature of this drone is that there is no need for control because it is able to hover in the air following a person automatically and capture perspectives on its own while the person is moving. Also, different from other inconvenient relative big size quadrotors, the hover camera weights only 238 grams and can

be easily folded for carrying around in any of your bags. [4]

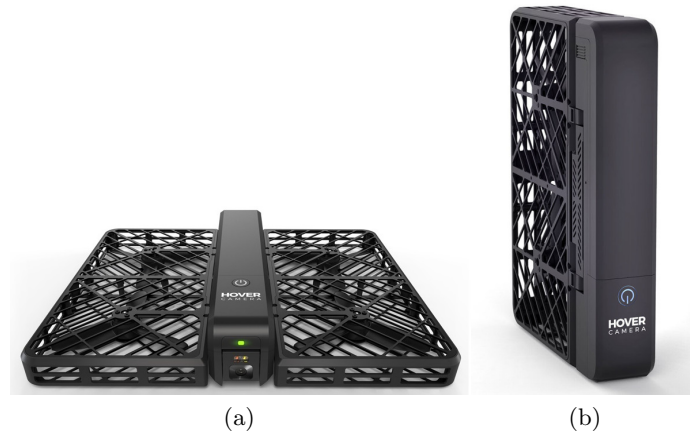


Figure 1.3: Hover Camera

Quadrotor UAV is a multidisciplinary cross technology, including control system theory, advanced sensor tech, computer science and so on. The current research fields are as follow:

- *Quadrotor Dynamics*

Quadrotor is an under-actuated, strong coupling, multi-variable and nonlinear complex system. The impact of gravity, gyroscope and other physical effects including air turbulence is valid from different situations. As a consequence, to get the rigid dynamic model for a quadrotor can be complicated in some way.

- *GPS system*

Navigation system is the "eyes" of UAVs. It is mainly used for detecting the position and attitude of a UAV in the geographic coordinate system and return feedback data to the flight control system. Navigation system in general can be divided into two categories: autonomous and independent. In the field of military, UAVs usually need to perform a variety of complex tasks, such as automatic approach landing, automatic searching, and stuff delivery. These tasks are mainly dependent on whether the navigation system provides accurate position and attitude information. But the precision of current single navigation systems does not meet the requirements. With the development of science and technology, the researchers put forward a variety of navigation technologies.

- *UAV Cooperative Mission*

When facing increasingly complex application environments, single quadrotor itself seems unlikely to satisfy the demand of usage. So, multiple drones working together can not only increase the efficiency, but also complete a multidimensional complex task.

- *Advanced Control Algorithm*

An effective control algorithm is the key to guarantee the stability of quadrotors. However, because of the nonlinearity and under-actuated property of quadrotors, it's not easy to design a controller to maintain a stable attitude while flying. So, how to improve the stability of the control system of quadrotors has increasingly popular in recent years.

## 1.2 Attitude Control

Due to an increasing demand for quadrotors adapting to different usages, various advanced control algorithms have been developed in recent years: Linear Quadratic Regulator (LQR), Proportional Integral Derivative (PID), sliding mode control, back-stepping design, fuzzy logic control, and neural networks control, etc. [5]. Each method has its own advantages and disadvantages.

In [1], based on quaternion representation, some comparisons of control methods were made, such as PD, LQR, and back-stepping control theory. Multiple simulations were verified by adding noise, applying actuator restriction, and so on. Integral of absolute errors, settling time, and maximum overshoots were compared when applying various external disturbances. An integral back-stepping control strategy was discussed in [6] for path tracking problem, which is based on quaternion representation as well. External disturbance and parameters uncertainty were taken into account. Several simulations were conducted to test the stability of the control algorithm. In [7], a back-stepping-based inverse optimal attitude controller was proposed. Under input torque limitation, it has the advantage of faster convergence with less control effort. Also, the controller was tested on a real quadrotor and effective experimental results were achieved.

A trajectory tracking back-stepping control strategy was proposed in [8] by using decoupling quaternion parametrization. And experimental results showed a good performance. In [9], two approaches were addressed to solve the trajectory tracking problem. Sliding mode controller dealt with entire multiple input and multiple output system rather than subsystem. Combined with block-backstepping method, attitude and altitude controllers were designed. The simulation results showed a good tracking performance and attenuation to external disturbances. A nonlinear proportional squared control strategy with a quaternion based Madwick complementary filter was discussed in [10].

As for nonlinear under-actuated systems, classical back-stepping technique has been widely use since it was first proposed in 1990 and fully developed by Krstic, Kanellakopoulos and Kotovic in 1995 [11]. It has the advantages of flexibility and global stability. However, by utilizing back-stepping technique, an accurate dynamic model is required [12]. In recent years, an increasing number of approximator-based adaptive control strategies have been designed to extend the applicability of classical back-stepping control scheme without full knowledge of system dynamic and to compensate model uncertainties [13]. To deal with nonlinear complex systems, fuzzy-logic approximator dealing with unknown functions was proposed in [12]. Adaptive fuzzy part is mainly constructed in the frame of back-stepping technique.

In [14], an adaptive fuzzy back-stepping controller was constructed for trajectory tracking problems. Simulation results showed that all signals were semi-globally uniformly ultimately bounded and tracking errors were around the neighborhood of the origin, but no experimental data were collected. Fuzzy logic and neural networks, which are included in intelligent control algorithms, share similar derivation processes for controller design. Where an adaptive back-stepping controller based on neural networks technique was presented in [15], considering unmodeled dynamics. The proposed method concentrated on tracking desired position and yaw motion while maintaining roll and pitch stability. Simulations showed a relative satisfactory control performance when changing masses and lengths of quadrotor. In order to prevent a drift when being subjected to wind disturbances and other oscillations, [16] proposed a method with fuzzy membership centers. Simulations illustrated a good control performance and robust stability.

### 1.3 Thesis Motivation

Quadrotors is an electronic platform which has been really popular around the world these days. From the very beginning of the research, a topic corresponding quadrotors is proposed with fully interests and curiosities. To make a quadrotor fly stably, several issues should be considered, such as electronic parts of the real quadrotor platform, a mature aerodynamic model, practical control strategies, and other related preliminaries and background knowledge. Under the inspiration of [14, 17–21], a quadrotor with emphasis on the controller design is illustrated in this thesis. To describe a flying quadrotor correctly, the Euler angle representation was first utilized in simulations for theoretical verification. Considering about the singularity problem of the Euler angle representation, a unit quaternion representation is chosen and implemented to the experimental quadrotor platform after comparing 3 methods of representations. As for the dynamic model, Euler Lagrangian method and Newton-Euler approach are discussed along with 2 different attitude representations. The back-stepping technique is utilized throughout the design. Since the quadrotor is an under-actuated, strong coupling, multi-variable and nonlinear complex system with parameter uncertainties, an adaptive fuzzy system is employed. The adaptive laws which are used for tuning the adjustable parameters are derived from Lyapunov theorem. Also, the measurement of inertial moments with unreliable or imprecise sensors may influence the final results of controllers. A adaptive fuzzy back-stepping controller based on quaternion representation is proposed to the experimental platform.

### 1.4 Thesis Outline

In this thesis, Chapter 1 gives a brief introduction of UAV quadrotors and some relevant knowledge around the research field. Chapter 2 illustrates the aerodynamics of a quadrotor and flight principles. Euler angle and quaternion representations will be discussed as well. Chapter 3 consists of two kinds of methods to describe dynamic models. Chapter 4 shows some brief description of hardware platform which is used in this thesis. Several controller

strategies are proposed in Chapter 5 with corresponding simulation results and experimental results. In the end, Chapter 6 summarizes the whole work in this thesis and gives some suggestions for the future work around this thesis.

## Chapter 2

# Background and Preliminaries

### 2.1 Flight Principles and Aerodynamics

A quadrotor UAV is composed of two equal mass cross mechanical arms. Brushless motors are installed at the end of the arms in order to generate four thrust forces for the drone. In terms of layout, quadrotors can be divided into two categories: '+' and 'x' as shown in Fig.2.1. '+' structure is common in this field since it's easier to incorporate a camera. In this paper, a platform is set up according to this common sense and we use '+' structure to explain the flight principle of quadrotors.

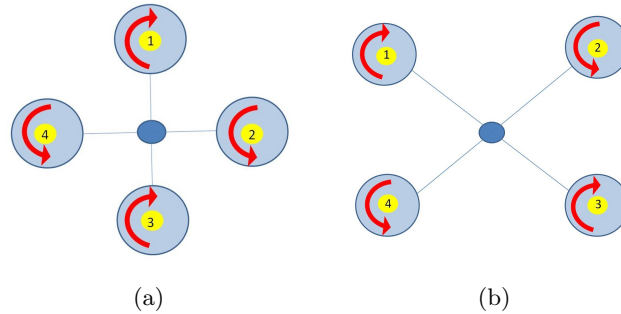


Figure 2.1: (a) '+' Structure of the Quadrotor; (b) 'x' Structure of the Quadrotor

The aerodynamics of the propellers should be considered in this thesis. Following the description in [22,23], it can be seen that, with the rotation of the motors, the propellers not only create thrust, but also generate drag factors on the quadrotor. These drag factors can influence the stability of the quadrotor by controlling the yaw angle. As shown in Fig.2.1, motor 1 and motor 3 form one pair and rotate in clockwise with clockwise propellers to create a counterclockwise air drag, while motor 2 and motor 4 form another pair and rotate in counterclockwise with counterclockwise propellers to create a clockwise air drag. It is this special structure that produces torque to offset each other at the same time, unlike traditional helicopters which rely on a tail to counter-balance the plasma torque.

With the flight principle as mentioned, it can be observed that motors  $M_i (i = 1, 2, 3, 4)$  produce forces  $T_i$ ,

$$T_i = b\Omega_i^2. \quad (2.1)$$

where  $b$  is the thrust factor.  $\Omega_1, \Omega_2, \Omega_3$ , and  $\Omega_4$  are the angular velocities of 4 motors respectively. The total vertical force  $U_1$  is the sum of thrust generated by 4 motors:

$$U_1 = \sum_{i=1}^4 T_i = b(\Omega_1^2 + \Omega_2^2 + \Omega_3^2 + \Omega_4^2) \quad (2.2)$$

The yaw torque  $\tau_\psi$  is the sum of 4 reaction torque from motors  $i$  caused by shaft acceleration and blade drag:  $\tau_\psi = \tau_{M_1} + \tau_{M_2} + \tau_{M_3} + \tau_{M_4}$ . At the equilibrium point, the aerodynamic torque produced by each pair of motors will be cancelled out.

The attitude of a quadrotor consists of: hover, raise, down, forward, backward and rotation. We also call them roll, pitch and yaw motion. As shown in Fig.2.1, the attitude and the movement of the quadrotor is controlled by four motors which change their rotational speeds to generate different thrust and torsion.

- *Hover, raise and down*

As shown in Fig.2.2, when the four motors rotate at the same speed and the total thrust is bigger than the gravity, the quadrotor will ascend, otherwise it will descend. If the total thrust is equal to the gravity, the quadrotor will remain in hover state.

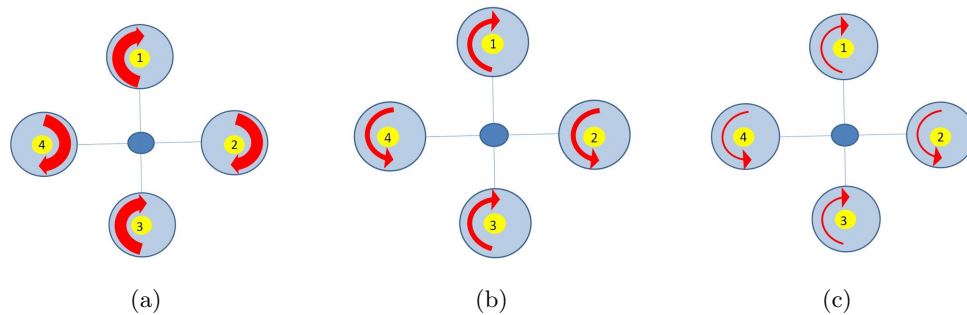


Figure 2.2: (a) Raise; (b) Hover; (a) Down

- *Roll motion*

As shown in Fig.2.3, when maintaining the speeds of motors 1 and 3, increasing the speed of motor 2, and decreasing the speed of motor 4, the thrust of motor 2 is greater than gravity. The quadrotor will gain a roll angle and fly to the left. Otherwise it will forward to right.

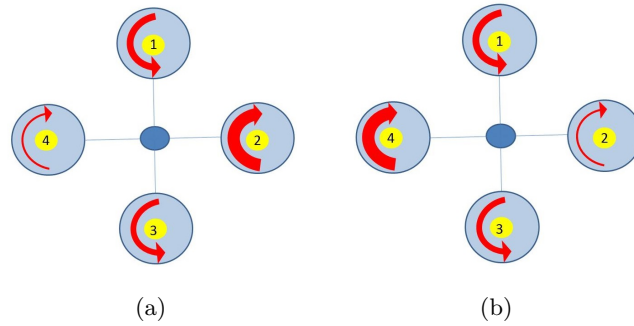


Figure 2.3: (a) Left; (b) Right

- *Pitch motion*

As shown in Fig.2.4, if motors 2 and 4 maintain their speeds, motor 3 increases its speed, and motor 1 reduces its speed, then the thrust of motor 3 is greater than gravity. The quadrotor will gain a pitch angle and fly forward. Otherwise it will fly backward.

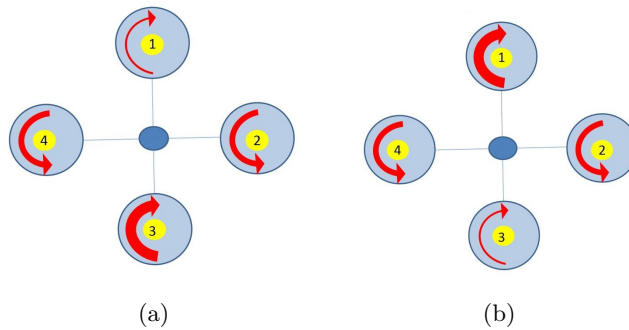


Figure 2.4: (a) Forward; (b) Backward

- *Yaw motion*

As shown in Fig.2.5, the difference speed between two pairs of motors will cause yaw motion. Increasing the rotation speeds of motors 2 and 4, which make the counterclockwise reverse torque greater than the clockwise reverse torque, the whole body will rotate in counterclockwise, which is called yaw motion. Instead, by increasing the speeds of motors 1 and 3, it will do the clockwise yaw motion.

## 2.2 Attitude Representation

When describing a rigid body, it's important to establish a well designed body representation. In this section, three kinds of attitude representations will be discussed in details. To sum up, advantages and disadvantages all appear at the same time. Euler angle representation is widely used among attitude control in the last several decades due to its simple structure

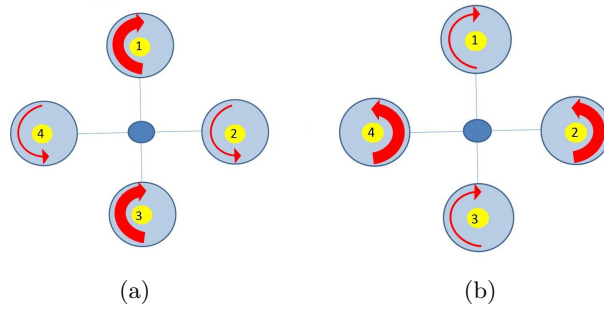


Figure 2.5: (a) Clockwise; (b) Counterclockwise

and understandability. But, *gimbal lock* is the main drawback when applied to aircrafts. Although Direction Cosine Matrix (DCM) does not have the *gimbal lock* problem, a highly computational expensive problem will occur. As a whole, the quaternion representation is considered to be the best attitude representation which is free of these two problems.

Generally, the motion of a rigid body is a combination of translational and rotational motions. Assume that the center of mass and the body-fixed frame are coincident. In order to know where the rigid body is in the three dimensional space, as shown in Fig.2.6, two kinds of coordinate systems are used. One is the inertial frame  $I$ , which is commonly attached to the Earth coordinate system. Another is the body-fixed frame  $B$ , which is attached to the quadrotor. The reason for generating two coordinate systems is as follows: When the quadrotor is flying, the coordinate is changing at the same time. So it's hard to get the accurate state of the quadrotor. However, the inertial frame  $I$  is fixed, which can be used as the reference.

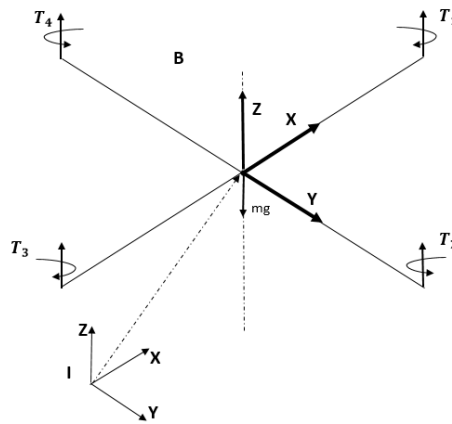


Figure 2.6: Coordinate System

### 2.2.1 Rotational Representation

Rotation Matrix, which is known as the Direction Cosine Matrix (DCM) as well, is one of the most popular representations for describing a rigid body. It is used to transform the coordinate system between the inertial frame  $I$  and the body-fixed frame  $B$ . Assume that  $R$  represents a rotation from the inertial frame  $I$  to the body-fixed frame  $B$ . Let  $v_I \in \mathbb{R}^3$  be the vector in the inertial coordinates,  $v_B \in \mathbb{R}^3$  be the same vector expressed in the body-fixed coordinates. Then the following relation holds:

$$v_B = R^T v_I \quad (2.3)$$

A quadrotor can be rotated about 3 orthogonal axes, Here are the matrices for the rotation by  $\phi$  around the x-axis,  $\theta$  around the y-axis, and  $\psi$  around the z-axis:

$$R_x = \begin{bmatrix} 1 & 0 & 0 \\ 0 & \cos \phi & -\sin \phi \\ 0 & \sin \phi & \cos \phi \end{bmatrix}, R_y = \begin{bmatrix} \cos \theta & 0 & \sin \theta \\ 0 & 1 & 0 \\ -\sin \theta & 0 & \cos \theta \end{bmatrix}, R_z = \begin{bmatrix} \cos \psi & -\sin \psi & 0 \\ \sin \psi & \cos \psi & 0 \\ 0 & 0 & 1 \end{bmatrix} \quad (2.4)$$

A single rotation about any arbitrary axis can be written in terms of the rotation about the  $z$ ,  $x$  and  $y$  axis by multiplying the 3 matrices as shown below.

$$R = R_x R_y R_z = \begin{bmatrix} \cos \theta \cos \psi & \sin \phi \sin \theta \cos \psi - \cos \phi \sin \psi & \sin \phi \sin \psi + \cos \phi \sin \theta \cos \psi \\ \cos \theta \sin \psi & \cos \phi \cos \psi + \sin \phi \sin \theta \sin \psi & \cos \phi \sin \theta \sin \psi - \cos \psi \sin \phi \\ -\sin \theta & \cos \theta \sin \phi & \cos \theta \cos \phi \end{bmatrix} \quad (2.5)$$

The *special orthogonal group* of  $3 \times 3$  rotation matrices is denoted by  $SO(3)$  where

$$SO(3) = \{R \in \mathbb{R}^{3 \times 3} \mid R^T R = R R^T = I_3\} \quad (2.6)$$

with  $I_3$  being a 3-by-3 identity matrix.

The following property of the rotation matrix can be easily verified.

$$\det(R) = \pm 1 \quad (2.7)$$

The rotation matrix is called *proper* if  $\det(R) = 1$  and *improper* if  $\det(R) = -1$ . We restrict our analyses to *proper* rotation, since *improper* rotation is not a rigid body transformation.

### 2.2.2 Euler Angle Representation

The Euler angles are introduced by Leonard Euler to represent the orientation of a rigid body with respect to the inertial frame  $I$  in a 3 dimensional space. The most common way

to describe the attitude of a rigid body is definitely the three Euler angles, because they are easy to understand and easy to visualize how the body rotates. They use the minimum parameterizing variables to represent attitude motion. In most of the time, Euler angles are given by  $\phi$ ,  $\theta$ ,  $\psi$ , which are named as the roll, pitch and yaw and represent the angles relative to the  $x$ ,  $y$  and  $z$  axes, as seen in Fig. 2.7.

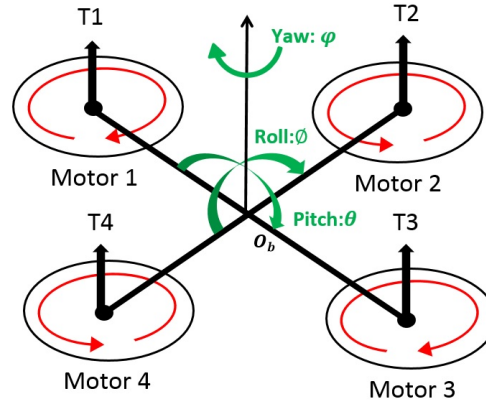


Figure 2.7: Roll, Pitch, and Yaw Motion

There are 12 sets of Euler angles:  $xyx, xzx, yxy, yzy, zxz, zyz, xyz, xzy, yxz, yzx, zxy, zyx$ . But the most common Euler angles for denoting orientations with respect to the inertial frame is  $zyx$  with the rotation of  $\psi, \theta, \phi$ . Rotating the  $x$ - $y$ - $z$  frame around its  $x$  axis is shown in Fig.2.8. Rotating the  $x$ - $y$ - $z$  frame around its  $y$  axis is displayed in Fig.2.9. Rotating the  $x$ - $y$ - $z$  frame around its  $z$  axis is described in Fig.2.10.

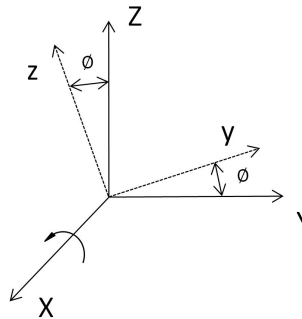


Figure 2.8: Rotate the  $x$ - $y$ - $z$  Frame Around  $x$  Axis

Euler angle representation is widely used in the UAV field for its clear definitions. However, it has an inherent disadvantage, which is known as singularity problem or *gimbal lock*. The *gimbal lock* occurs when two of the rotational axes align and lock together [1, 24]. Then, one degree of freedom will be lost. Also, highly complex computation is another disadvantage of Euler angle representation because it contains many trigonometric functions.

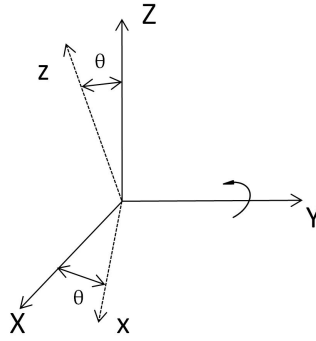


Figure 2.9: Rotate the x-y-z Frame Around y Axis

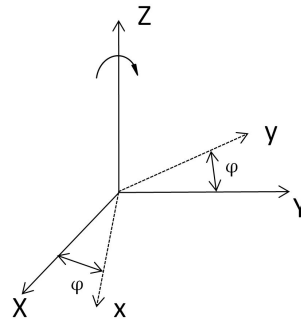


Figure 2.10: Rotate the x-y-z Frame Around z Axis

### 2.2.3 Unit Quaternion Representation

Because of the *gimbal lock* and singularity problems, unit quaternion is becoming more popular these days. Quaternion was first devised by William Rowan Hamilton, a 19th century Irish mathematician. It belongs to the quaternion space  $H$ , which can be shown in different ways. Here, it is defined as a vector of four components as shown in (2.8)

$$Q = \begin{bmatrix} q_0 \\ q \end{bmatrix} = \begin{bmatrix} q_0 \\ q_1 \\ q_2 \\ q_3 \end{bmatrix} \quad (2.8)$$

where  $Q \in \mathbb{R}^4$  is the quaternion,  $q \in \mathbb{R}^3$  is the vector and  $q_0 \in \mathbb{R}$  is the scalar part. The physical meaning of the quaternion is to change the orientation of the vector and scale the length [25]. The quaternion can also be written as:

$$Q = \begin{bmatrix} \cos \frac{\alpha}{2} \\ \hat{k} \sin \frac{\alpha}{2} \end{bmatrix} \quad (2.9)$$

which represents a rotation about an arbitrary vector  $\hat{k} \in \mathbb{R}^3$  by a given angle  $\alpha$ . It is worth noting that the quaternions  $q$  and  $-q$  describe the same orientation, which denote two

different directions of rotation. When  $|\alpha| \leq \pi$ ,  $q_0$  will be non-negative and the quaternion representation will be unique.

A quaternion is called the unit quaternion if

$$q_0^2 + q^T q = q_0^2 + q_1^2 + q_2^2 + q_3^2 = 1 \quad (2.10)$$

The unit quaternion will be used in this thesis. The inverse of a quaternion is defined by:

$$Q^{-1} = \begin{bmatrix} q_0 \\ -q \end{bmatrix} \quad (2.11)$$

The norm of a quaternion is defined by:

$$\|q\| = \sqrt{q_0^2 + q_1^2 + q_2^2 + q_3^2} \quad (2.12)$$

To calculate multiplication of two quaternions, two quaternion are defined as

$$Q_1 = \begin{bmatrix} q_0 \\ q \end{bmatrix}, Q_2 = \begin{bmatrix} p_0 \\ p \end{bmatrix} \quad (2.13)$$

Then, the quaternion multiplication is defined by

$$Q_1 \odot Q_2 = \begin{bmatrix} p_0 q_0 - q^T p \\ q_0 p + p_0 q + q \times p \end{bmatrix} = \begin{bmatrix} p_0 q_0 - q^T p \\ p_1 q_0 - p_2 q_3 + p_3 q_2 + q_1 p_0 \\ p_1 q_3 - p_3 q_1 + p_2 q_0 + p_0 q_2 \\ p_2 q_1 - p_1 q_2 + p_3 q_0 + p_0 q_3 \end{bmatrix} \quad (2.14)$$

As a result, the following relation will be used when an error between  $Q_1$  and  $Q_2$  is required.

$$Q_1^{-1} \odot Q_2 = \begin{bmatrix} q_0 \\ -q \end{bmatrix} \odot \begin{bmatrix} p_0 \\ p \end{bmatrix} \quad (2.15)$$

$$= \begin{bmatrix} p_0 q_0 + q^T p \\ q_0 p - p_0 q - q \times p \end{bmatrix} = \begin{bmatrix} p_0 q_0 + q^T p \\ p_1 q_0 + p_2 q_3 - p_3 q_2 - q_1 p_0 \\ p_3 q_1 - p_1 q_3 + p_2 q_0 - p_0 q_2 \\ p_1 q_2 - p_2 q_1 + p_3 q_0 - p_0 q_3 \end{bmatrix} \quad (2.16)$$

where  $\odot$  denotes the quaternion product and  $\times$  denotes the vector cross product.

The quaternion  $Q_I = [1 \ 0 \ 0 \ 0]^T$  is called the identity quaternion. The following relation can be easily proofed.

$$Q \odot Q^{-1} = Q^{-1} \odot Q = Q_I \quad (2.17)$$

Note that the quaternion product is not commutative, which means that the results of multiplication rely on the order it is done.

### 2.2.4 Relations between Attitude Representation

Transformation from Euler angles to rotation matrix can be derived as follows [26, 27]:

$$R = R_x R_y R_z = \begin{bmatrix} c\theta c\psi & s\phi s\theta c\psi - c\phi s\psi & c\phi s\theta c\psi + s\phi s\psi \\ c\theta s\psi & s\phi s\theta s\psi + c\phi c\psi & c\phi s\theta s\psi - s\phi c\psi \\ -s\theta & s\phi c\theta & c\phi c\theta \end{bmatrix} \quad (2.18)$$

where  $c$  and  $s$  represent cosine and sine operators respectively,  $R_x$ ,  $R_y$ , and  $R_z$  are the rotation around x, y, and z axis respectively, defined by

$$R_x = \begin{bmatrix} 1 & 0 & 0 \\ 0 & \cos \phi & -\sin \phi \\ 0 & \sin \phi & \cos \phi \end{bmatrix}, R_y = \begin{bmatrix} \cos \theta & 0 & \sin \theta \\ 0 & 1 & 0 \\ -\sin \theta & 0 & \cos \theta \end{bmatrix}, R_z = \begin{bmatrix} \cos \psi & -\sin \psi & 0 \\ \sin \psi & \cos \psi & 0 \\ 0 & 0 & 1 \end{bmatrix} \quad (2.19)$$

The rotation matrix can be parameterized by quaternion. The rotation matrix  $R$  is related to the unit quaternion through Rodriguez formula  $R = R(Q)$ , where

$$\begin{aligned} R(Q) &= (q_0^2 - q^T q)I + 2q_0 S(q) + 2qq^T \\ &= \begin{bmatrix} 1 - 2(q_2^2 + q_3^2) & 2(q_1 q_2 - q_0 q_3) & 2(q_0 q_2 + q_1 q_3) \\ 2(q_1 q_2 + q_0 q_3) & 1 - 2(q_1^2 + q_3^2) & 2(q_2 q_3 - q_0 q_1) \\ 2(q_1 q_3 - q_0 q_2) & 2(q_0 q_1 + q_2 q_3) & 1 - 2(q_1^2 + q_2^2) \end{bmatrix} \end{aligned} \quad (2.20)$$

with  $Q = \begin{bmatrix} q_0 \\ q \end{bmatrix}$ ,  $q = [q_1 \quad q_2 \quad q_3]^T \in \mathbb{R}^3$  and  $S(\cdot)$  being a skew symmetric matrix [6] defined by

$$S(q) = \begin{bmatrix} 0 & -q_3 & q_2 \\ q_3 & 0 & -q_1 \\ -q_2 & q_1 & 0 \end{bmatrix} \quad (2.21)$$

It can be verified that  $S(q) \in SO(3)$  where  $SO(3)$  represents a group of  $3 \times 3$  skew symmetric matrices defined by  $SO(3) = \{S \in \mathbb{R}^{3 \times 3} \mid S^T = -S\}$ . It has the following useful properties,

which will be used later.

$$S(x)y = -S(y)x = x \times y \quad (2.22)$$

$$S(x)x = 0 \quad (2.23)$$

$$S(S(x)y) = S(x)S(y) - S(y)S(x) = yx^T - xy^T \quad (2.24)$$

$$S(Ry) = RS(y)R^T \quad (2.25)$$

where  $\times$  denotes the vector cross product.

It should be noted that the rotation associated with  $Q$  is the same as the rotation associated with  $-Q$ . In other words, two quaternions  $Q$  and  $-Q$  denote the same rotation matrix, that is,

$$R(Q) = R(-Q) \quad (2.26)$$

The form that maps Euler angles to their corresponding unit quaternion is given by

$$Q = \begin{bmatrix} q_0 \\ q \end{bmatrix} = \begin{bmatrix} c_{\phi/2}c_{\theta/2}c_{\psi/2} + s_{\phi/2}s_{\theta/2}s_{\psi/2} \\ -c_{\phi/2}s_{\theta/2}s_{\psi/2} + c_{\theta/2}c_{\psi/2}s_{\phi/2} \\ c_{\phi/2}c_{\psi/2}s_{\theta/2} + s_{\phi/2}c_{\theta/2}s_{\psi/2} \\ c_{\phi/2}c_{\theta/2}s_{\psi/2} - s_{\phi/2}c_{\psi/2}s_{\theta/2} \end{bmatrix} \quad (2.27)$$

where  $c$  and  $s$  represent as cosine and sine operators respectively. Also, Euler angles can be presented by unit quaternion as following:

$$\begin{bmatrix} \phi \\ \theta \\ \psi \end{bmatrix} = \begin{bmatrix} atan2(2(q_0q_1 + q_2q_3), 1 - 2(q_1^2 + q_2^2)) \\ asin(2(q_0q_2 - q_3q_1)) \\ atan2(2(q_0q_3 + q_1q_2), 1 - 2(q_2^2 + q_3^2)) \end{bmatrix}$$

where  $atan2()$  and  $asin()$  denote the four-quadrant inverse tangent and the inverse sine.

## Chapter 3

# UAV Quadrotor Dynamics

The dynamic model of an unmanned aerial vehicle is the basic of flight control. The accuracy of modeling is crucial to the design of controllers. To get the dynamics model of a quadrotor, a couple of factors need to be taken into consideration, such as, aerodynamics effects, internal dynamics of four engines, changing variables, flexible wings and so on. Therefore, it's not easy to describe a complicated structure with a simple modeling method because the quadrotor is a multi output multi input under-actuated nonlinear system. In this chapter, a simplified model is constructed for a quadrotor by using the minimum number of states with the main factors that should be taken into account.

Before starting to build a model, a few assumptions are made: [7, 28, 29]

- The quadrotor is a rigid body.
- The body is symmetrical.
- The origin of the body fixed-frame is at the center of mass.
- The propellers are rigid.

In this chapter, two approaches, Euler-Lagrange and Newton-Euler, are discussed for obtaining a simple aerodynamic model of the quadrotor. In order to avoid singularity of the Euler angles, as a consequence, Newton-Euler Equations method is utilized to establish dynamic model based on unit quaternion representation. The models derived here will be used in later chapters for designing control strategies to get a stable attitude control system.

### 3.1 Dynamic Model with Euler Lagrangian Formalism

In this section, under the inspiration of [18, 30–33], the quadrotor is modelled by Euler-Lagrange formalism and the model can be divided into two parts, one for translational

motion and the other for rotational motion. The generalized coordinates of the quadrotor are  $q = (x, y, z, \phi, \theta, \psi) \in \mathbb{R}^6$ . Define a translational vector  $\zeta = (x, y, z) \in \mathbb{R}^3$ , which represents the corresponding position of the quadrotor with respect to the inertial frame. Similarly, define a rotational vector  $\eta = (\phi, \theta, \psi) \in \mathbb{R}^3$ , which is the Euler angles representing the orientation of the quadrotor.  $\phi$  represents the roll angle around x-axis,  $\theta$  denotes the pitch angle around y-axis and  $\psi$  is the yaw angle around z-axis. Assume the Euler angles are bounded as follows.

$$\begin{aligned} \text{roll} & : & -90^\circ \leq \phi \leq 90^\circ \\ \text{pitch} & : & -90^\circ \leq \theta \leq 90^\circ \\ \text{yaw} & : & -180^\circ \leq \psi < 180^\circ \end{aligned} \quad (3.1)$$

The translational kinetic energy  $T_{trans}$  and rotational kinetic energy  $T_{rot}$  are defined as follows:

$$T_{trans} = \frac{1}{2} m \dot{\zeta}^T \dot{\zeta} \quad (3.2)$$

$$T_{rot} = \frac{1}{2} \dot{\eta}^T I \dot{\eta} \quad (3.3)$$

where  $m$  is the mass of the quadrotor and  $I$  is the inertial matrix with respect to the inertial frame  $I$ . The total potential energy is given by

$$U = mgz \quad (3.4)$$

where  $g$  is the acceleration due to gravity and  $z$  is the altitude of the quadrotor.

Then, the Lagrangian function is represented by

$$\begin{aligned} L(q, \dot{q}) & = T_{trans} + T_{rot} - U \\ & = \frac{1}{2} m \dot{\zeta}^T \dot{\zeta} + \frac{1}{2} \dot{\eta}^T I \dot{\eta} - mgz \end{aligned} \quad (3.5)$$

According to Euler Lagrangian theory, the following equation is obtained.

$$(F_\zeta, \tau) = \frac{d}{dt} \left( \frac{\partial L}{\partial \dot{q}} \right) - \frac{\partial L}{\partial q} \quad (3.6)$$

where  $\tau = [\tau_\phi \ \tau_\theta \ \tau_\psi]^T$  represents the moment vector and  $F_\zeta$  denotes the translational force vector expressed in the body frame  $B$ , which can be obtained by  $F_\zeta = R F_R$  with  $F_R$  expressed in the inertial frame  $I$ . Here,  $R$  is the rotation matrix defined by (2.5).

$F_R = [0 \ 0 \ U_1]$ , where  $U_1$  is the total vertical force which is the sum of thrust generated by 4 motors, that is,

$$U_1 = \sum_{i=1}^4 T_i = b(\Omega_1^2 + \Omega_2^2 + \Omega_3^2 + \Omega_4^2) \quad (3.7)$$

where  $b$  is the thrust factor which is defined in Chapter 4.  $\Omega_1, \Omega_2, \Omega_3$ , and  $\Omega_4$  are the angular velocities of 4 motors respectively. Thus, the 4 inputs are given by:

$$\begin{bmatrix} U_1 \\ \tau_\phi \\ \tau_\theta \\ \tau_\psi \end{bmatrix} = \begin{bmatrix} b(\Omega_1^2 + \Omega_2^2 + \Omega_3^2 + \Omega_4^2) \\ bl(\Omega_2^2 - \Omega_4^2) \\ bl(\Omega_1^2 - \Omega_3^2) \\ k(\Omega_1^2 - \Omega_2^2 + \Omega_3^2 - \Omega_4^2) \end{bmatrix} \quad (3.8)$$

where  $l$  is the distance from the center mass of the quadrotor to the location of the motor shaft which is defined in Chapter 4 and  $k$  is the air drag factor.  $bl(\Omega_2^2 - \Omega_4^2)$  represents the thrust imbalance between motor 4 and motor 2.  $bl(\Omega_1^2 - \Omega_3^2)$  represents the thrust imbalance between motor 3 and motor 1.  $k(\Omega_1^2 - \Omega_2^2 + \Omega_3^2 - \Omega_4^2)$  represents the difference of thrust between motors (1,3) and motors (2,4).

The Euler-Lagrange equation in (3.6) can be expressed as

$$\begin{aligned} F_\zeta &= \frac{d}{dt} \left( \frac{\partial L_{trans}}{\partial \dot{\zeta}} \right) - \frac{\partial L_{trans}}{\partial \zeta} \\ \tau &= \frac{d}{dt} \left( \frac{\partial L_{rot}}{\partial \dot{\eta}} \right) - \frac{\partial L_{rot}}{\partial \eta} \end{aligned} \quad (3.9)$$

After some mathematical manipulations, the final dynamic model is derived as

$$\begin{aligned} F_\zeta &= m\ddot{\zeta} + mg\hat{z} \\ \tau &= I\ddot{\eta} + \dot{I}\dot{\eta} - \frac{1}{2} \frac{\partial}{\partial t} (\dot{\eta}^T I \dot{\eta}) \end{aligned} \quad (3.10)$$

which can be also rewritten as

$$\begin{bmatrix} \ddot{x} \\ \ddot{y} \\ \ddot{z} \end{bmatrix} = \begin{bmatrix} \cos \phi \sin \theta \cos \psi + \sin \phi \sin \psi \\ \cos \phi \sin \theta \sin \psi - \sin \phi \cos \psi \\ \cos \phi \cos \theta \end{bmatrix} \frac{U_1}{m} + \begin{bmatrix} 0 \\ 0 \\ -g \end{bmatrix} \quad (3.11)$$

$$\begin{bmatrix} \ddot{\phi} \\ \ddot{\theta} \\ \ddot{\psi} \end{bmatrix} = \begin{bmatrix} \dot{\theta}\dot{\psi} \left( \frac{I_\theta - I_\psi}{I_\phi} \right) - \frac{J_x}{I_\phi} \dot{\theta}\dot{\Omega} \\ \dot{\phi}\dot{\psi} \left( \frac{I_\psi - I_\phi}{I_\theta} \right) + \frac{J_x}{I_\theta} \dot{\phi}\dot{\Omega} \\ \dot{\phi}\dot{\theta} \left( \frac{I_\phi - I_\theta}{I_\psi} \right) \end{bmatrix} + \begin{bmatrix} \frac{l}{I_\phi} & 0 & 0 \\ 0 & \frac{l}{I_\theta} & 0 \\ 0 & 0 & \frac{1}{I_\psi} \end{bmatrix} \begin{bmatrix} \tau_\phi \\ \tau_\theta \\ \tau_\psi \end{bmatrix} \quad (3.12)$$

where

$g \in \mathbb{R}$  : gravitational constant,

$I_\phi \in \mathbb{R}$  : moment of inertia of the quadrotor with respect to  $x$  axis in the body frame  $B$ ,

$I_\theta \in \mathbb{R}$  : moment of inertia of the quadrotor with respect to  $y$  axis in the body frame  $B$ ,

$I_\psi \in \mathbb{R}$  : moment of inertia of the quadrotor with respect to  $z$  axis in the body frame  $B$ ,

$\tau_\phi \in \mathbb{R}$  : the torque around the body center in roll direction with respect to body frame  $B$ ,

$\tau_\theta \in \mathbb{R}$  : the torque around the body center in pitch direction with respect to body frame  $B$ ,

$\tau_\psi \in \mathbb{R}$  : the torque around the body center in yaw direction with respect to body frame  $B$ ,

$m \in \mathbb{R}$  : mass of the quadrotor,

$J_r \in \mathbb{R}$  : the moment inertia of the motor,

$\Omega$  : the difference of motor speed which can be represented as follows:

$$\Omega = \sum_{i=1}^4 (-1)^{i+1} (\omega \times \hat{z}) \Omega_i \quad (3.13)$$

$$= \Omega_1 - \Omega_2 - \Omega_3 + \Omega_4 \quad (3.14)$$

where  $\Omega_i \in \mathbb{R}$  is the angular velocity of motor  $i$ ,  $i = 1, 2, 3, 4$ ,  $\omega = [\omega_1 \ \omega_2 \ \omega_3]^T \in \mathbb{R}^3$  is the angular velocity vector of the quadrotor with respect to the body frame  $B$ , and  $\hat{z} = [0 \ 0 \ 1]^T \in \mathbb{R}^3$  is the unit vector expressed in frame  $I$ .

## 3.2 Dynamic Model with Newton-Euler Formalism

Based on the assumptions and preliminaries given before, a singularity problem may occur with the Euler angle representation. To solve this puzzler, by using Newton-Euler formalism and quaternion kinematics [28, 34], a mathematical model will be re-established as follows.

$$\dot{p} = v \quad (3.15)$$

$$\dot{v} = g\hat{z} - \frac{U_1}{m} R^T \hat{z} \quad (3.16)$$

$$\dot{R} = RS(\omega) \quad (3.17)$$

$$I_B \dot{\omega} = -\omega \times I_B \omega - G_a + \tau \quad (3.18)$$

where

$p = [x \ y \ z]^T \in \mathbb{R}^3$ : the coordinates of the center of mass of the body-fixed frame (frame  $B$ ) with respect to the inertial frame  $I$ ,

$v = [v_1 \ v_2 \ v_3]^T \in \mathbb{R}^3$ : the translational velocity vector of the quadrotor with respect to the inertial frame  $I$ ,

$g \in \mathbb{R}$ : the gravitational constant,

$\hat{z} = [0 \ 0 \ 1]^T \in \mathbb{R}^3$ : the unit vector expressed in the inertial frame  $I$ ,

$U_1 \in \mathbb{R}$ : the total thrust generated by 4 motors along the  $z$  axis of the fixed-body frame  $B$ , see (3.7) for definition.

$m \in \mathbb{R}$ : the mass of the quadrotor,

$R \in SO(3)$ : the rotation matrix which represents the attitude of the quadrotor with respect to the inertial frame  $I$ ,

$\omega = [\omega_1 \ \omega_2 \ \omega_3]^T$ : the angular velocity vector of the quadrotor with respect to the body frame  $B$ ,

$I_B = \text{diag}(I_\phi, I_\theta, I_\psi) \in \mathbb{R}^{3 \times 3}$ : the inertia matrix of the quadrotor with respect to the fixed-body frame  $B$ ,

$\tau = [\tau_\phi \ \tau_\theta \ \tau_\psi]^T \in \mathbb{R}^3$ : the quadrotor input torque vector, which can be determined by (3.8),

$S(\omega)$ : the skew symmetric matrix, which is defined in (2.21) and is rewritten below for convenience,

$$S(\omega) = \begin{bmatrix} 0 & -\omega_3 & \omega_2 \\ \omega_3 & 0 & -\omega_1 \\ -\omega_2 & \omega_1 & 0 \end{bmatrix} \quad (3.19)$$

$G_a \in \mathbb{R}$ : the gyroscopic torque, which will be explained in details below.

The gyroscopic torque  $G_a$  in (3.18) is related to the rotation of the motors and angular velocity of the quadrotor, which can be determined by

$$\begin{aligned} G_a &= \sum_{i=1}^4 (-1)^{i+1} J_r(\omega \times \hat{z}) \Omega_i \\ &= \begin{bmatrix} \omega_2 J_r(\Omega_1 - \Omega_2 - \Omega_3 + \Omega_4) \\ -\omega_1 J_r(\Omega_1 - \Omega_2 - \Omega_3 + \Omega_4) \\ 0 \end{bmatrix} \end{aligned} \quad (3.20)$$

where  $\Omega_i \in \mathbb{R}$  is the angular velocity of motor  $i$ ,  $i = 1, 2, 3, 4$  and  $J_r \in \mathbb{R}$  is the moment inertia of motor  $i$ ,  $i = 1, 2, 3, 4$ .

Let  $\tau_{M_i} \in \mathbb{R}$  denote the torque generated by motor  $i, i = 1, 2, 3, 4$ . Then, according to the Newton second law,  $\Omega_i$  satisfies the following dynamic equation [35]

$$J_r \dot{\Omega}_i = \tau_{M_i} - Q_i \quad (3.21)$$

where  $Q_i$  is the propeller reactive torque generated by the propeller motion, which is calculated by

$$Q_i = k\Omega_i^2 \quad (3.22)$$

with  $k > 0$  denoting the drag factor in free air. When in the equilibrium point  $\dot{\Omega}_i = 0$ , then  $Q_i = \tau_{M_i}$ .

The attitude dynamics (3.17) can be represented by using the unit quaternion as follows.

$$\begin{aligned} \dot{Q} &= \frac{1}{2} Q \odot Q_\omega \\ &= \frac{1}{2} \begin{bmatrix} -q^T \\ q_0 I_{3 \times 3} + s(q) \end{bmatrix} \omega \\ &= \frac{1}{2} A(q_0, q) \omega \end{aligned} \quad (3.23)$$

where  $Q = [q_0 \ q_1 \ q_2 \ q_3]^T$ .

Using (3.17)-(3.18), the quadrotor dynamical model can also be represented by Euler angles as follows.

$$\begin{aligned} \dot{\phi} &= \omega_1 + \omega_2 \sin \phi \tan \theta + \omega_3 \cos \phi \tan \theta \\ \dot{\theta} &= \omega_2 \cos \phi - \omega_3 \sin \phi \\ \dot{\psi} &= \omega_2 \sin \phi \sec \theta + \omega_3 \cos \phi \sec \theta \\ \dot{\omega}_1 &= \left( \frac{I_\theta - I_\psi}{I_\phi} \right) \omega_2 \omega_3 + \frac{1}{I_\phi} \tau_\phi - \frac{J_r}{I_\phi} \omega_2 (\Omega_1 - \Omega_2 - \Omega_3 + \Omega_4) \\ \dot{\omega}_2 &= \left( \frac{I_\psi - I_\phi}{I_\theta} \right) \omega_1 \omega_3 + \frac{1}{I_\theta} \tau_\theta + \frac{J_r}{I_\theta} \omega_1 (\Omega_1 - \Omega_2 - \Omega_3 + \Omega_4) \\ \dot{\omega}_3 &= \left( \frac{I_\phi - I_\theta}{I_\psi} \right) \omega_1 \omega_2 + \frac{1}{I_\psi} \tau_\psi \end{aligned} \quad (3.24)$$

## Chapter 4

# Experimental Platform



Figure 4.1: Experimental Platform

In order to implement a controller into a real proper UAV quadrotor structure, we first combine experimental requirements with other researchers' experiences [7], and then come up with the desired quadrotor experimental platform which is presented in Fig. 4.1. The entire platform has been divided into 4 parts: the frame, main controller, communication subsystem, and propulsion subsystem. The overview of the experimental structure is shown in Fig. 4.2. Most of the experimental parts are purchased in [36].

### 4.1 The frame of the Quadrotor

As shown in Fig. 4.3, a 600 size quadrotor fame is selected which has a rigid and robust construction. The metal part is fabricated from solid T6 aluminum where the booms are also made from heavy duty thick T6 aluminum. Considering the weight of the quadrotor, carbon fiber is regarded as the best material due to its light weight and notable strength. So, the middle part of this frame is made from carbon fiber and glass-filled nylon which makes this frame strong enough for potential external strike [37]. For more details, please refer to [36].

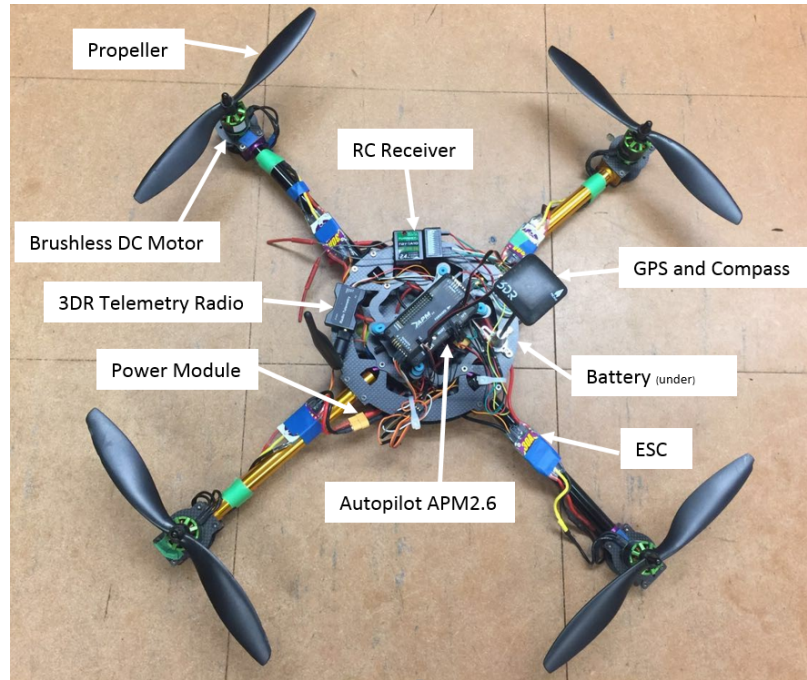


Figure 4.2: Overview of the Quadrotor Platform



Figure 4.3: The Frame

## 4.2 Main Controller

Autopilot is the core part that can be the brain of the quadrotor. All the computing tasks are processed onboard, including data acquisition and filtering, motors' control, wireless remote control, and real-time control, etc. Basically, most of the flight controllers include gyroscopes, accelerometer, barometric pressure sensors, compass and other electronics. Many research institutions have designed a couple of onboard controllers based on microcontroller or digital signal processor (DSP).

It is worth mentioning that some open-source projects (OSP) have good performance, such as, OpenPilot, Paparazzi, Pixhawk and APM2.6 [19]. Before choosing a flight controller, we need to decide what sort of flying function is suitable, freestyle, aerial photography or

autonomous missions. OpenPilot is an OSP developed by RC hobbyists. Not only fixed-wing aircraft, but also helicopter can be embedded on the OpenPilot OSP. Various data can be found on the internet, which can help users make drones fly. Paparazzi was designed in 2003 by ENAC University. The Paparazzi team developed nine autopilot hardware systems to support outdoor flying mission with flight-path scripting.

By comparing integrated hardware processing performance, software development difficulty, price and other factors, we chose Ardupilot Mega (APM) 2.6 to be the ideal autopilot system. The APM 2.6 is a simple and ready-to-use autopilot system designed by 3D Robotics. Arduino is compatible with other software, which is used throughout our programming and implementation. Arduino includes both the open-source microcontroller circuit and the Integrated Development Environment (IDE). Arduino is a developed platform which includes various of driver libraries for diverse sensors and actuators. It is intuitive, free to download, and compatible with Windows and Mac OS. More than 100 libraries are available for signal analysis and hardware accessories. The overview of the Arduino IDE is shown in Fig. 4.4 . Ardupilot and its attached accessories are shown in Fig.4.5.

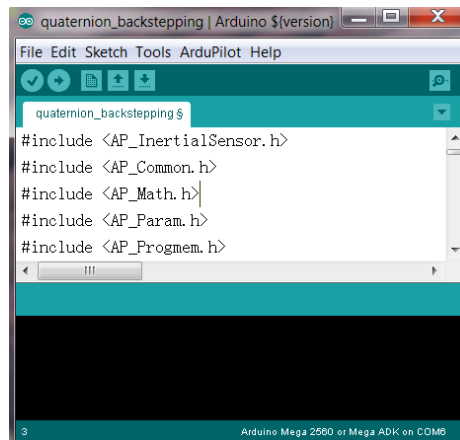


Figure 4.4: Arduino Interface

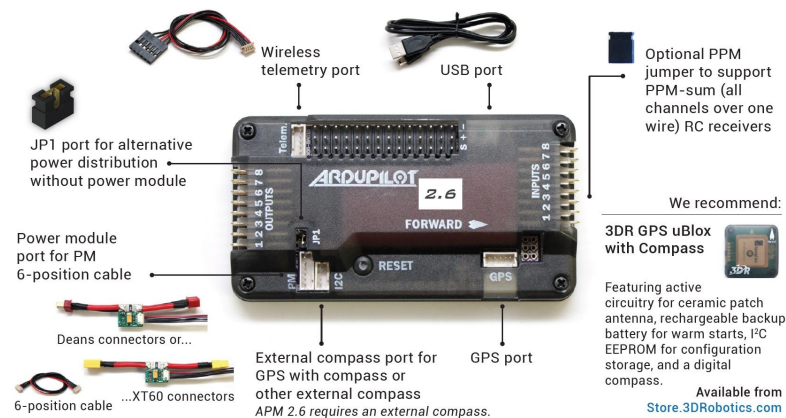


Figure 4.5: APM 2.6 and Ports

Atmel ATMEGA 2560 and ATMEGA 32U chips are onboard for controller processing and

USB measurement, respectively. 3-axis gyroscope, magnetometer and accelerometer are also included on the chip MPU 6050 for motion tracking. An upgraded MS5611-01BA03 barometric pressure sensor provides air pressure reading data for altitude measurement. Also, there are various ports onboard for function expanding. Such as: wireless telemetry port, Universal Serial Bus (USB) port, Global Positioning System (GPS) port, Inter Integral Circuit ( $I^2C$ ) port for GPS external compass, power module (PM) port and 8 channels digital input and output.

- *Microcontroller: Atmel Atmega 2560*

The Atmel Atmega 2560 is a high-performance, low-power 8-bit AVR RISC-based microcontroller with 256KB ISP flash memory, 8KB SRAM and 4KB EEPROM. It also combines with 86 general purpose I/O lines and 32 general purpose working registers. The controller also has real-time counters, six flexible timer/counters with compare modes, and a JTAG interface for on-chip debugging. The Atmega 2560 also achieves a throughput approaching 1 MIPS per MHz allowing the system designer to balance power consumption and processing speed [38].

- *Inertial Measurement Unit: MPU 6050*

The motion processing unit MPU 6050 from InvenSense Inc. is the world's first 6-axis onboard digital motion processor, which has the built-in gyroscope and accelerometer and is capable of processing complex fusions or functions. The 3-axis accelerometer has a full-scale of  $\pm 2g$ ,  $\pm 4g$ ,  $\pm 8g$  and  $\pm 16g$ . Also, the MPU 6050 features a programmable 3-axis gyroscope with a full-scale range of  $\pm 250$ ,  $\pm 500$ ,  $\pm 1000$ , and  $\pm 2000$ /sec(dps) on chip. As for communication, it can be accessed with external magnetometers or other sensors by a 400KHz Inter Integral Circuit so that the devices can gather a full set of sensor data without intervention from the system processor.

- *3DR UBlox GPS and HMC5883L Digital Compass*

The accuracy of compass data is significant for quadrotors. Before launching APM 2.6, there is an old series of autopilot named APM 2.5. These two controllers have the exact same hardware and sensors and the only difference between them is that the compass unit is taken off from APM 2.6 since the GPS and compass unit can be easily influenced by noise sources. Afterwards, the 3DR UBlox GPS with a compass model is recommended as shown in Fig.4.6. It is made by ceramic patch antenna, with rechargeable 3V backup battery for warm starts and Inter Integral Circuit EEPROM for configuration storage. The APM port is attached to the GPS port by 6-position-to-5-position cable. The APM  $I^2C$  port is attached to the GPS MAG port, and  $I^2C$  communication between the APM and the speed controller is 50Hz. One more thing needs to be mentioned here: The GPS module should be mounted at least 10 cm away from the main control module and battery to reduce interferences from the magnetic field.

- *3DR Power Module(PM)*

The APM 2.6 needs to be powered by a steady clean voltage and sufficient current. So, in this thesis, we use a power module shown in Fig.4.7. It is produced by 3DR aim to monitor the voltage and current of the battery and avoid uncertainties. It can

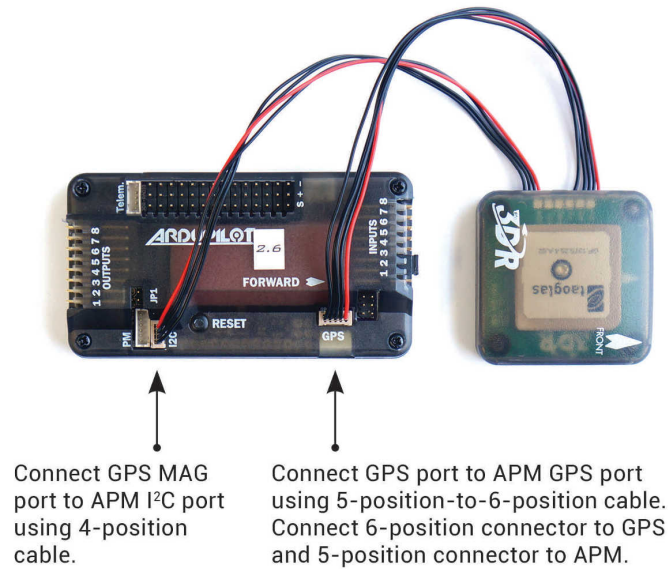


Figure 4.6: 3DR UBlox GPS with Compass Model

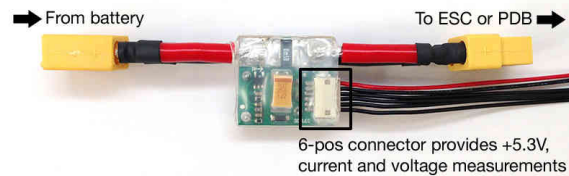


Figure 4.7: 3DR Power Module

convert a 5.37V and 2.25A power from LiPo battery which will reduce the chances of brown-out and compensate the interferences of compass. One port is connected to the battery, and the other port connects to one ESC.

### 4.3 Communication Subsystem

The remote control (RC) transmitter and RC radio receiver, shown in Fig. 4.8, are considered as an essential part of a quadrotor platform. According to several researchers' papers, we chose Turnigy TGY-i10 which has 10 channels with 2.4 GHz bandwidth, although only 4 channels have been used in this thesis: throttle, yaw, roll and pitch. The transmitter is equipped with a high sensitivity receiver which can generate Pulse Position Modulation (PPM) between each other. For further development, an extra channel will be involved when flight mode is switching. As shown in Fig. 4.8, the throttle stick will not return to the middle position when removing the finger. On the contract, the roll, pitch and yaw sticks will return to the center automatically and the value of roll, pitch and yaw in the center is 0. From experimental results, the PPM value of these 4 stick vary from the minimum 1001 to the maximum 2003.



Figure 4.8: (a) RC Transmitter; (b) RC Receiver

- *3DR Telemetry Radio*

As for wireless data transfer, we chose 3DR 915Mhz telemetry radio for data transmitting and receiving, shown in Fig. 4.9. This radio connector allows us to communicate the ground station (computer) with quadrotor wireless. Also, we can change tasks, tune the flight, and view data while the quadrotor is flying. It is the easiest way to setup the connection between the quadrotor and ground station, just like USB as a ready-to-use electronic device.



Figure 4.9: 3DR Telemetry Radio

## 4.4 Propulsion Subsystem

Electrical propulsion is a better means of propulsion due to its advantage of zero gaseous emissions, low heat and less audible noise. In general, an electrical propulsion subsystem converts electrical energy to mechanical power in the form of thrust, which consists of 4 parts: propeller, motor, electronic speed controller(ESC), electrical power source. In this thesis, brushless DC (BLDC) motors are selected to generate thrust for the quadrotor, which are combined with corresponding electronic speed controller(ESC). Different from fixed wing aircraft, a quadrotor is an energy-consuming equipment depending entirely on the four motors. Thus, we choose Lithium-Polymer Battery to be the electrical power source. Each component has its own performance characteristics and maximum efficiency. The choice of

these components is the key of the entire propulsion system. Each of the component should meet the demand of experimental platform effectively [39]. A diagram of the quadrotor electrical propulsion system is presented in Fig. 4.10.

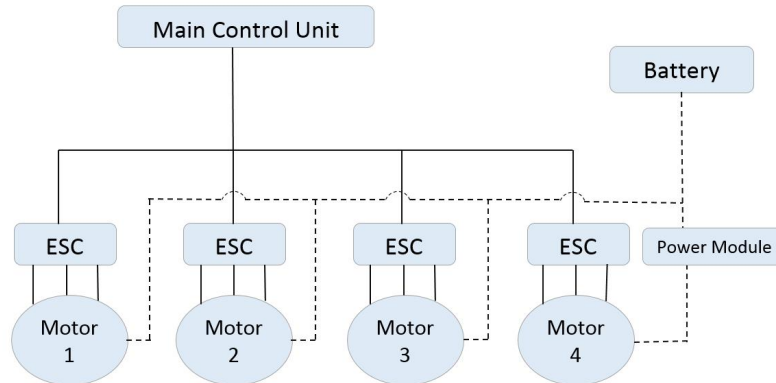


Figure 4.10: Propulsion System

- *Brushless DC motor(BLDC)*



Figure 4.11: BLDC motor

When comparing to DC motors with brushes, BLDC motors have a couple of advantages, for example: high efficiency, lower noise, faster speed, bigger torque and longer operating duration [40]. The motor shown in Fig.4.11 is chosen for the experimental quadrotor and its basic parameters are given in Table 4.1. For more details, please refer to [36].

Table 4.1: 800KV Motor Specification

KV(RPM/V)	Max Current	Max Power	Cel Count	Suggested ESC	Connector
800KV	20A	222W	2-3S LiPo	Afro 20A	3mm Bullet

- *Electronic Speed Controller(ESC)*

Since the BLDC motors have 3-phases, one can not just apply power source directly to them to make them spin. Motors need some phase control electronics to generate 3 high frequency signals. So, ESC is then made to do this job. The ESC is just a motor controller board with power source input and 3-pharse outputs for the motors. To control a quadrotor, the frequency of the signals should be higher than 200Hz, then it



Figure 4.12: ESC

is possible to vary the speed of motors quick enough for stabilization. Also, the current of the ESC should be about 20A or more. The ESC shown in Fig.4.12 is chosen for the experimental quadrotor and its basic parameters are given in Table 4.2. For more details, please refer to [36].

Table 4.2: ESC Specification

Current	Voltage Range	Freq.	Battery Eliminator Circuit	Weight	Size
30A	2-4s Lipoly	1KHz	0.5A Linear	26.5g	50x25x11mm

- *Propeller*



Figure 4.13: Propeller

When choosing the proper size of the propellers, we should consider a couple of influential factors, such as: the duration of battery, the mass, the throttle of motors, etc. Also, we should take the aerodynamics model into account, which was discussed in Section 2.1. There are five aerodynamic factors which act on each motor, such as ground effect, horizontal force ( or hub force ), rolling moment, thrust force and drag moment [41]. As for this thesis, as shown in Fig.4.13, the following two main factors are taken into consideration: thrust force and drag moment. The steady-state thrust generated by a hovering motor which is not translating horizontally or vertically in a free air can be rewritten by momentum theory as [18]:

$$T_i = b\Omega_i^2 = \frac{4C_T\rho r_i^4\Omega_i^2}{\pi^4}, i = 1, 2, 3, 4; \quad (4.1)$$

where  $b$  is the thrust factor,  $C_T$  is the coefficient of trust that depends on motor geometry and characteristics, which can be found in [42],  $\rho$  is the air density,  $r$  is the

radius of motor disk area when the propeller is spinning. A quadrotor is influenced by not only thrust forces from individual motors, but also balancing drag moment. The reactive torque can be derived as follows [43]:

$$Q_i = k\Omega_i^2 = \frac{4C_P\rho r^5\Omega_i^2}{\pi^3}, i = 1, 2, 3, 4; \quad (4.2)$$

where  $k$  is the drag factor. The parameters in (4.1) and (4.2) are provided in Table 4.3.

Table 4.3: Propeller Parameters

Name	Parameter	Value	Units
Thrust Coefficient	$C_T$	0.1225	-
Power Coefficient	$C_P$	0.051	-
Air Density	$\rho$	1.225	$kg/m^3$
Radius	$r$	0.124	m

From (4.1), (4.2), and Table 4.3, the thrust factor  $b$  and drag factor  $k$  can be determined as

$$b = \frac{4C_T\rho r^4}{\pi^4} = 1.347323e^{-5} \quad (4.3)$$

$$k = \frac{4C_P\rho r^5}{\pi^3} = 2.1783e^{-7} \quad (4.4)$$

Taking all the factors into account, we chose four  $10V \times 4.7$  propeller blades including two pairs of CCW and CW in this quadrotor platform.

- *Electrical Power Source*

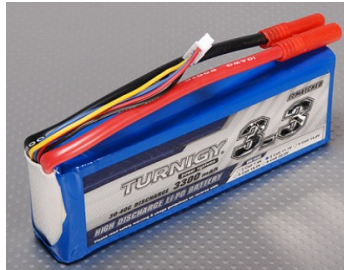


Figure 4.14: LiPo Battery

Table 4.4: 3300mAh LiPo Battery Specification

Capacity	Configuration	Constant Discharge	Pack Weight	Discharge Plug
3300mAh	11.1v (3Cell)	30C	297g	4mm Bullet-connector

Because of the advantages of lighter and higher electrical capacity, Lithium Polymer (LiPo) battery has become the most popular electrical power source for quadrotors

recently. Unlike other kinds of batteries, LiPo battery is rated at 3.7V per cell. The higher capability the battery has, the heavier it will be. So, in this thesis, regarding the weight and the time range of operation, a Turnigy nano-tech 3300 mAh high discharge LiPo battery with 3 cells, as shown in Fig.4.14, has been used in the experimental platform. Table 4.4 has shown the corresponding parameters. Another situation that should be mentioned is the discharge rate, referred to equation (4.5) [44]. It is important to make sure that the total amount of current drawn by motors will not exceed the MaxSource. Discharge rate is the speed of a battery when discharging. The discharge rate and capacity of the LiPo battery can be found in Table 4.4. For more details, please refer to [36].

$$MaxSource = DischargeRate \times Capacity \quad (4.5)$$

$$99A = 30C \times 3300mAh \quad (4.6)$$

The maximum speed of motor is related to motor specifications and the voltage of battery, which is expressed as follows:

$$\Omega_{max} = 11.1V \times 800KV \times \frac{2\pi}{60} = 1065.6rad/s \quad (4.7)$$

The maximum total thrust shown in (4.1) can be derived as (4.8) by using (4.3).

$$T_{total} = 4b\Omega_{max}^2 = 4 \times 1.347323e^{-5} \times (1065.6)^2 = 49.96N = 5.098kg \quad (4.8)$$

It means that the total weight of the quadrotor can not be heavier than 5.098kg. It can fly normally as the actual weight of the quadrotor is 1.535kg.

## Chapter 5

# Controller Design with Back-stepping Technique

In this Chapter, 4 controllers based on back-stepping technique are proposed. Controllers with Euler angle representation are tested by simulations and controllers with unit quaternion representation are tested by a real quadrotor platform. The main objective of the proposed controllers is to guarantee that the angles  $\phi$ ,  $\theta$ , and  $\psi$  follow the desired attitude trajectory accurately. To sum up, the attitude of the quadrotor need to be stabilized with satisfactory performance.

### 5.1 Backstepping Design with Euler Angle Representation

#### 5.1.1 Controller Design

In this section, inspired by [18], a backstepping controller with Euler angle representation is proposed. Backstepping technique is widely use due to the fact that both Lyapunov function and global stabilizing controller can be constructed by a recursive procedure for a class of nonlinear uncertain systems in the strict feedback firm, which is more general than the matching conditions. Also, high order systems can be transformed to several low order systems, so the system structure is clear and easy to follow. As attitude control, let  $\phi_d$ ,  $\theta_d$ ,  $\psi_d$  and  $\dot{\phi}_d$ ,  $\dot{\theta}_d$ ,  $\dot{\psi}_d$  represent the desired roll, pitch, and yaw angles and their derivatives, respectively. Define the errors as follows

$$\begin{aligned} e_1 &= \phi - \phi_d \\ e_2 &= \dot{\phi} - \dot{\phi}_d = \dot{e}_1 \\ e_3 &= \theta - \theta_d \\ e_4 &= \dot{\theta} - \dot{\theta}_d = \dot{e}_3 \\ e_5 &= \psi - \psi_d \\ e_6 &= \dot{\psi} - \dot{\psi}_d = \dot{e}_5 \end{aligned} \tag{5.1}$$

Step 1:

Define a positive definite Lyapunov function  $V_1$  by

$$V_1 = \frac{1}{2}e_1^2 + \frac{1}{2}e_3^2 + \frac{1}{2}e_5^2 \quad (5.2)$$

Its derivative with respect to time is derived as

$$\begin{aligned} \dot{V}_1 &= e_1\dot{e}_1 + e_3\dot{e}_3 + e_5\dot{e}_5 \\ &= e_1e_2 + e_3e_4 + e_5e_6 \\ &= e_1e_2 - k_1e_1^2 + k_1e_1^2 + e_3e_4 - k_3e_3^2 + k_3e_3^2 + e_5e_6 - k_5e_5^2 + k_5e_5^2 \\ &= -k_1e_1^2 - k_3e_3^2 - k_5e_5^2 + e_1(e_2 + k_1e_1) + e_3(e_4 + k_3e_3) + e_5(e_6 + k_5e_5) \\ &= -k_1e_1^2 - k_3e_3^2 - k_5e_5^2 + e_1\bar{e}_2 + e_3\bar{e}_4 + e_5\bar{e}_6 \end{aligned} \quad (5.3)$$

where  $k_1, k_3,$  and  $k_5$  are the positive gains and

$$\begin{aligned} \bar{e}_2 &= e_2 + k_1e_1 \\ \bar{e}_4 &= e_4 + k_3e_3 \\ \bar{e}_6 &= e_6 + k_5e_5 \end{aligned} \quad (5.4)$$

Note that  $-k_1e_1, -k_3e_3,$  and  $-k_5e_5$  are the virtual control part of backstepping control procedure. When errors  $e_2, e_4, e_6$  equal their corresponding virtual control,  $\dot{V}_1 = -k_1e_1^2 - k_3e_3^2 - k_5e_5^2 < 0$  is a negative definite.

Step 2

Define a positive definite function  $V_2$  by

$$V_2 = V_1 + \frac{1}{2}\bar{e}_2^2 + \frac{1}{2}\bar{e}_4^2 + \frac{1}{2}\bar{e}_6^2 \quad (5.5)$$

Differentiating it with respect to time yields

$$\begin{aligned} \dot{V}_2 &= \dot{V}_1 + \bar{e}_2\dot{\bar{e}}_2 + \bar{e}_4\dot{\bar{e}}_4 + \bar{e}_6\dot{\bar{e}}_6 \\ &= -k_1e_1^2 - k_3e_3^2 - k_5e_5^2 + e_1\bar{e}_2 + e_3\bar{e}_4 + e_5\bar{e}_6 \\ &\quad + \bar{e}_2\dot{\bar{e}}_2 + k_2\bar{e}_2^2 - k_2\bar{e}_2^2 + \bar{e}_4\dot{\bar{e}}_4 + k_4\bar{e}_4^2 - k_4\bar{e}_4^2 + \bar{e}_6\dot{\bar{e}}_6 + k_6\bar{e}_6^2 - k_6\bar{e}_6^2 \\ &= -k_1e_1^2 - k_2\bar{e}_2^2 - k_3e_3^2 - k_4\bar{e}_4^2 - k_5e_5^2 - k_6\bar{e}_6^2 \\ &\quad + \bar{e}_2(e_1 + \dot{\bar{e}}_2 + k_2\bar{e}_2) + \bar{e}_4(e_3 + \dot{\bar{e}}_4 + k_4\bar{e}_4) + \bar{e}_6(e_5 + \dot{\bar{e}}_6 + k_6\bar{e}_6) \end{aligned} \quad (5.6)$$

where  $k_2, k_4,$  and  $k_6$  are the positive gains. By using (5.1) and (3.12), the derivatives of  $\bar{e}_2,$

$\bar{e}_4$ , and  $\bar{e}_6$  in (5.4) can be expressed as

$$\begin{aligned}\dot{\bar{e}}_2 &= \dot{e}_2 + k_1 \dot{e}_1 \\ &= \ddot{\phi} - \ddot{\phi}_d + k_1 e_2 \\ &= \dot{\theta} \dot{\psi} \left( \frac{I_\theta - I_\psi}{I_\phi} \right) - \frac{J_r}{I_\phi} \dot{\theta} \Omega + \frac{l}{I_\phi} \tau_\phi - \ddot{\phi}_d + k_1 e_2\end{aligned}\quad (5.7)$$

$$\begin{aligned}\dot{\bar{e}}_4 &= \dot{e}_4 + k_3 \dot{e}_3 \\ &= \ddot{\theta} - \ddot{\theta}_d + k_3 e_4 \\ &= \dot{\phi} \dot{\psi} \left( \frac{I_\psi - I_\phi}{I_\theta} \right) + \frac{J_r}{I_\theta} \dot{\phi} \Omega + \frac{l}{I_\theta} \tau_\theta - \ddot{\theta}_d + k_3 e_4\end{aligned}\quad (5.8)$$

$$\begin{aligned}\dot{\bar{e}}_6 &= \dot{e}_6 + k_5 \dot{e}_5 \\ &= \ddot{\psi} - \ddot{\psi}_d + k_5 e_6 \\ &= \dot{\phi} \dot{\theta} \left( \frac{I_\phi - I_\theta}{I_\psi} \right) + \frac{1}{I_\psi} \tau_\psi - \ddot{\psi}_d + k_5 e_6\end{aligned}\quad (5.9)$$

Then, by substituting (5.7), (5.8), (5.9) into (5.6),  $\dot{V}_2$  can be rewritten as

$$\begin{aligned}\dot{V}_2 &= -k_1 e_1^2 - k_2 \bar{e}_2^2 - k_3 e_3^2 - k_4 \bar{e}_4^2 - k_5 e_5^2 - k_2 \bar{e}_6^2 \\ &\quad + \bar{e}_2 (e_1 + \dot{e}_2 + k_2 \bar{e}_2) + \bar{e}_4 (e_3 + \dot{e}_4 + k_4 \bar{e}_4) + \bar{e}_6 (e_5 + \dot{e}_6 + k_6 \bar{e}_6) \\ &= -k_1 e_1^2 - k_2 \bar{e}_2^2 - k_3 e_3^2 - k_4 \bar{e}_4^2 - k_5 e_5^2 - k_2 \bar{e}_6^2 \\ &\quad + \bar{e}_2 \left[ e_1 + \dot{\theta} \dot{\psi} \left( \frac{I_\theta - I_\psi}{I_\phi} \right) - \frac{J_r}{I_\phi} \dot{\theta} \Omega + \frac{l}{I_\phi} \tau_\phi - \ddot{\phi}_d + k_1 e_2 + k_2 \bar{e}_2 \right] \\ &\quad + \bar{e}_4 \left[ e_3 + \dot{\phi} \dot{\psi} \left( \frac{I_\psi - I_\phi}{I_\theta} \right) + \frac{J_r}{I_\theta} \dot{\phi} \Omega + \frac{l}{I_\theta} \tau_\theta - \ddot{\theta}_d + k_3 e_4 + k_4 \bar{e}_4 \right] \\ &\quad + \bar{e}_6 \left[ e_5 + \dot{\phi} \dot{\theta} \left( \frac{I_\phi - I_\theta}{I_\psi} \right) + \frac{1}{I_\psi} \tau_\psi - \ddot{\psi}_d + k_5 e_6 + k_6 \bar{e}_6 \right]\end{aligned}\quad (5.10)$$

Note that if the last three parts equal zero, then  $\dot{V}_2$  becomes

$$\dot{V}_2 = -k_1 e_1^2 - k_2 \bar{e}_2^2 - k_3 e_3^2 - k_4 \bar{e}_4^2 - k_5 e_5^2 - k_2 \bar{e}_6^2 < 0 \quad (5.11)$$

which is a negative definite. Setting the last 3 parts in (5.10) to zero gives

$$\begin{aligned}\tau_\phi &= \frac{I_\phi}{l} \left[ -\dot{\theta} \dot{\psi} \left( \frac{I_\theta - I_\psi}{I_\phi} \right) + \frac{J_r}{I_\phi} \dot{\theta} \Omega + \ddot{\phi}_d - k_1 e_2 - k_2 \bar{e}_2 - e_1 \right] \\ \tau_\theta &= \frac{I_\theta}{l} \left[ -\dot{\phi} \dot{\psi} \left( \frac{I_\psi - I_\phi}{I_\theta} \right) - \frac{J_r}{I_\theta} \dot{\phi} \Omega + \ddot{\theta}_d - k_3 e_4 - k_4 \bar{e}_4 - e_3 \right] \\ \tau_\psi &= I_\psi \left[ -\dot{\phi} \dot{\theta} \left( \frac{I_\phi - I_\theta}{I_\psi} \right) + \ddot{\psi}_d - k_5 e_6 - k_6 \bar{e}_6 - e_5 \right]\end{aligned}\quad (5.12)$$

Substituting (5.4) into (5.12) produces

$$\begin{aligned}\tau_\phi &= \frac{I_\phi}{l} \left[ -\dot{\theta}\dot{\psi} \left( \frac{I_\theta - I_\psi}{I_\phi} \right) + \frac{J_r}{I_\phi} \dot{\theta}\Omega - (k_1 k_2 + 1)e_1 - (k_1 + k_2)e_2 \right] \\ \tau_\theta &= \frac{I_\theta}{l} \left[ -\dot{\phi}\dot{\psi} \left( \frac{I_\psi - I_\phi}{I_\theta} \right) - \frac{J_r}{I_\theta} \dot{\phi}\Omega - (k_3 k_4 + 1)e_3 - (k_3 + k_4)e_4 \right] \\ \tau_\psi &= I_\psi \left[ -\dot{\phi}\dot{\theta} \left( \frac{I_\phi - I_\theta}{I_\psi} \right) - (k_5 k_6 + 1)e_5 - (k_5 + k_6)e_6 \right]\end{aligned}\quad (5.13)$$

Substituting (3.8) into (5.13) results in the following

$$\begin{aligned}bl(\Omega_2^2 - \Omega_4^2) - \frac{J_r}{l} \dot{\theta}\Omega &= \frac{I_\phi}{l} \left[ -\dot{\theta}\dot{\psi} \left( \frac{I_\theta - I_\psi}{I_\phi} \right) - (k_1 k_2 + 1)e_1 - (k_1 + k_2)e_2 \right] \\ bl(\Omega_1^2 - \Omega_3^2) + \frac{J_r}{l} \dot{\phi}\Omega &= \frac{I_\theta}{l} \left[ -\dot{\phi}\dot{\psi} \left( \frac{I_\psi - I_\phi}{I_\theta} \right) - (k_3 k_4 + 1)e_3 - (k_3 + k_4)e_4 \right] \\ k(\Omega_1^2 - \Omega_2^2 + \Omega_3^2 - \Omega_4^2) &= I_\psi \left[ -\dot{\phi}\dot{\theta} \left( \frac{I_\phi - I_\theta}{I_\psi} \right) - (k_5 k_6 + 1)e_5 - (k_5 + k_6)e_6 \right]\end{aligned}\quad (5.14)$$

where  $\Omega = \Omega_1 - \Omega_2 - \Omega_3 + \Omega_4$ . It is clear that the motor speeds  $\Omega_1, \Omega_2, \Omega_3$ , and  $\Omega_4$  can be solved from (5.14) numerically. By tuning the gains  $k_1, \dots, k_6$  properly and controlling the motor speeds, the quadrotor can be stabilized around the desired attitude. The block diagram of the backstepping controller with Euler angle representation is shown in Fig. 5.1.

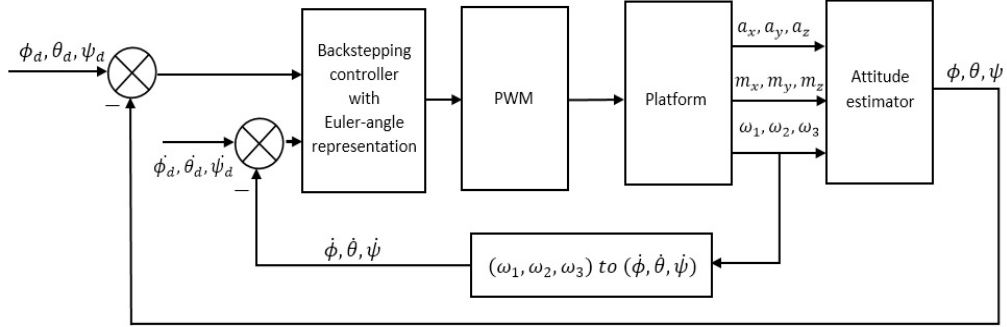


Figure 5.1: Backstepping Controller with Euler Angle Representation

### 5.1.2 Simulation Results

In this section, some simulations are conducted for the backstepping controller based on Euler angle representation. After several times of testing, a couple of relative satisfactory gains have been chosen as  $k_1 = k_3 = k_5 = 2$ ,  $k_2 = k_4 = k_6 = 100$ , which are tuned by trial and error method. The inertial Euler angles are chosen randomly as 0.2, 0.1, and 0.3 rad. Matlab Simulink environment is used for the model coding. The physical parameters of the quadrotor in the simulation are derived from the real quadrotor platform. The simulation results are shown in Figs. 5.2- 5.4. As shown in Fig. 5.3, all the three angles are able to

follow the corresponding desired angles with the satisfactory tracking errors. The system can be stabilized within 3s. The simulation results which are provided in this section illustrate the stability property and good performance of the proposed controller.

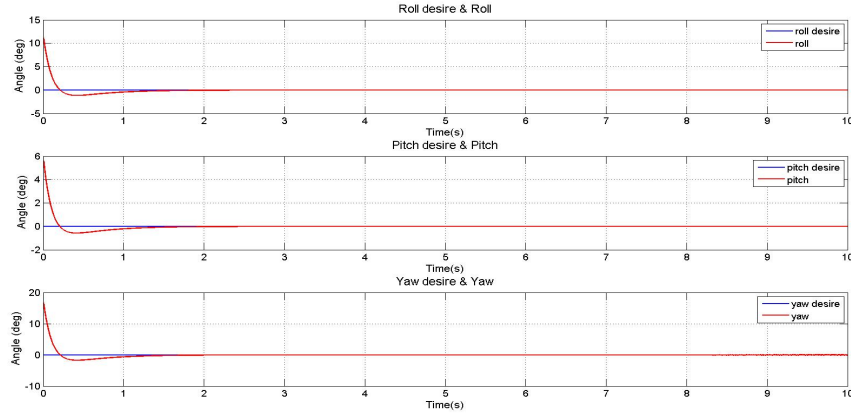


Figure 5.2:  $\phi$ ,  $\theta$ , and  $\psi$  with Backstepping Controller

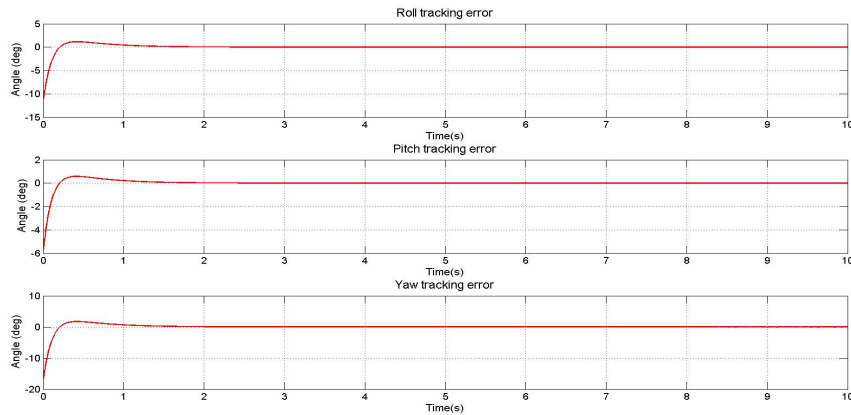


Figure 5.3: Tracking Errors with Backstepping Controller

## 5.2 Fuzzy Adaptive Integral Backstepping Design with Euler Angle Representation

### 5.2.1 Controller Design

Fuzzy logic controllers (FLCs) are currently being used in quadrotors for its complex dynamics and uncertainties [45]. In this quadrotor platform, there are a few issues that should be taken into consideration. When discussing the mathematical model, it is assumed

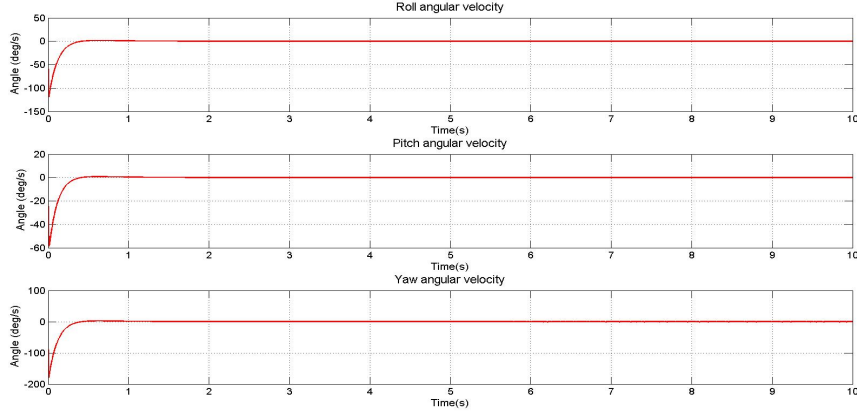


Figure 5.4: Angular Velocities with Backstepping Controller

that the quadrotor is a symmetrical rigid body. However, in the real platform as shown in Chapter 4, based on the layout of several electronic circuits, the quadrotor is not a complete symmetrical rigid body. Also, the measurement of inertial moments is basically dependent on the mass of the quadrotor. The mass can not change when the measurement is done, not to mention the measurement errors. Therefore, the moment of inertia  $I_\phi$ ,  $I_\theta$ , and  $I_\psi$  can not be accurately measured, so they are treated as unknown parameters in this thesis.

Motivated by [12, 13, 46, 47], a fuzzy adaptive integral backstepping controller with Euler angle representation has been proposed to handle the nonlinearities  $\dot{\theta}\dot{\psi} \left( \frac{I_\theta - I_\psi}{I_\phi} \right)$ ,  $\dot{\phi}\dot{\psi} \left( \frac{I_\psi - I_\phi}{I_\theta} \right)$ , and  $\dot{\phi}\dot{\theta} \left( \frac{I_\phi - I_\theta}{I_\psi} \right)$  and unknown parameters  $I_\phi$ ,  $I_\theta$ , and  $I_\psi$  in the quadrotor. A FLS consists of four parts: the knowledge base, the fuzzifier, the fuzzy inference engine, and the defuzzifier. The knowledge base is composed of a collection of fuzzy IF-THEN rules in the following form:

$$R^k : \mathbf{IF} \ x_1 \in \mathbf{A}_1^k, x_2 \in \mathbf{A}_2^k, \dots, x_n \in \mathbf{A}_n^k, \mathbf{THEN} \ y \in \mathbf{B}^k \quad (5.15)$$

where  $x = [x_1 \ x_2 \ \dots \ x_n]^T$  is the input vector,  $y$  is the output variable,  $\mu_{A_i^k}(x_i)$  is the fuzzy membership function of fuzzy set  $A_i^k$ ,  $\mu_{B^k}(y)$  is the fuzzy membership function of fuzzy set  $B^k$ ,  $k = 1, 2, \dots, N$  with  $N$  being the number of the IF-THEN rules.

By using singleton fuzzifier, product inference engine, and center average defuzzification, the fuzzy logic system can be formulated as follows

$$y^* = \frac{\sum_{k=1}^N \bar{y}_k [\prod_{i=1}^n \mu_{A_i^k}(x_i)]}{\sum_{k=1}^N [\prod_{i=1}^n \mu_{A_i^k}(x_i)]} \quad (5.16)$$

where  $\bar{y}_k$  is the maximum value of  $\mu_{B^k}(y)$ , that is,  $\bar{y}_k = \max_{y \in R} \mu_{B^k}(y)$ .

Define the fuzzy basic function as:

$$S_k(x) = \frac{\prod_{i=1}^n \mu_{A_i^k}(x_i)}{\sum_{k=1}^N [\prod_{i=1}^n \mu_{A_i^k}(x_i)]}, \quad k = 1, 2, \dots, N \quad (5.17)$$

In this thesis, in order to reduce the computation burden, the following trapezoidal membership function is used.

$$\mu(x; a, b, c, d) = \begin{cases} 0, & x < a \text{ or } x > d \\ \frac{x-a}{b-a}, & a \leq x \leq b \\ 1, & b \leq x \leq c \\ \frac{d-x}{d-c}, & c \leq x \leq d \end{cases} \quad (5.18)$$

Then, the fuzzy logic system in (5.16) can be rewritten as:

$$f(x) = \eta^T S(x) \quad (5.19)$$

where  $\eta = [\bar{y}_1 \ \bar{y}_2 \ \cdots \ \bar{y}_N]^T$ ,  $S(x) = [S_1(x) \ S_2(x) \ \cdots \ S_N(x)]^T$ .

Assume that the parameters  $I_\phi$ ,  $I_\theta$ , and  $I_\psi$  are unknown and the nonlinear terms  $\dot{\theta}\dot{\psi} \left( \frac{I_\theta - I_\psi}{I_\phi} \right)$ ,  $\dot{\phi}\dot{\psi} \left( \frac{I_\psi - I_\phi}{I_\theta} \right)$ , and  $\dot{\phi}\dot{\theta} \left( \frac{I_\phi - I_\theta}{I_\psi} \right)$  are unknown as well.

The unknown nonlinear terms can be estimated by the following fuzzy logic systems.

$$\dot{\theta}\dot{\psi} \left( \frac{I_\theta - I_\psi}{I_\phi} \right) = \eta_1^T S_1(\dot{\theta}, \dot{\psi}) + \delta_1 \quad (5.20)$$

$$\dot{\phi}\dot{\psi} \left( \frac{I_\psi - I_\phi}{I_\theta} \right) = \eta_2^T S_2(\dot{\phi}, \dot{\psi}) + \delta_2 \quad (5.21)$$

$$\dot{\phi}\dot{\theta} \left( \frac{I_\phi - I_\theta}{I_\psi} \right) = \eta_3^T S_3(\dot{\phi}, \dot{\theta}) + \delta_3 \quad (5.22)$$

where  $\delta_1$ ,  $\delta_2$ ,  $\delta_3$  are the approximation errors, which are bounded by a positive constant  $\delta_{\max}$  [16], that is,  $\delta_i \leq \delta_{\max}$ ,  $i = 1, 2, 3$ .

In this thesis,

$$\begin{aligned} S_1 &= [S_{11}, S_{12}, S_{13}, S_{14}, S_{15}, S_{16}, S_{17}, S_{18}, S_{19}]^T \\ S_2 &= [S_{21}, S_{22}, S_{23}, S_{24}, S_{25}, S_{26}, S_{27}, S_{28}, S_{29}]^T \\ S_3 &= [S_{31}, S_{32}, S_{33}, S_{34}, S_{35}, S_{36}, S_{37}, S_{38}, S_{39}]^T \end{aligned} \quad (5.23)$$

where

$$\begin{aligned}
 S_{11} &= \frac{\mu_N(\dot{\theta})\mu_N(\dot{\psi})}{D_1}, S_{21} = \frac{\mu_N(\dot{\phi})\mu_N(\dot{\psi})}{D_2}, S_{31} = \frac{\mu_N(\dot{\phi})\mu_N(\dot{\theta})}{D_3} \\
 S_{12} &= \frac{\mu_N(\dot{\theta})\mu_Z(\dot{\psi})}{D_1}, S_{22} = \frac{\mu_N(\dot{\phi})\mu_Z(\dot{\psi})}{D_2}, S_{32} = \frac{\mu_N(\dot{\phi})\mu_Z(\dot{\theta})}{D_3} \\
 S_{13} &= \frac{\mu_N(\dot{\theta})\mu_P(\dot{\psi})}{D_1}, S_{23} = \frac{\mu_N(\dot{\phi})\mu_P(\dot{\psi})}{D_2}, S_{33} = \frac{\mu_N(\dot{\phi})\mu_P(\dot{\theta})}{D_3} \\
 S_{14} &= \frac{\mu_Z(\dot{\theta})\mu_N(\dot{\psi})}{D_1}, S_{24} = \frac{\mu_Z(\dot{\phi})\mu_N(\dot{\psi})}{D_2}, S_{34} = \frac{\mu_Z(\dot{\phi})\mu_N(\dot{\theta})}{D_3} \\
 S_{15} &= \frac{\mu_Z(\dot{\theta})\mu_Z(\dot{\psi})}{D_1}, S_{25} = \frac{\mu_Z(\dot{\phi})\mu_Z(\dot{\psi})}{D_2}, S_{35} = \frac{\mu_Z(\dot{\phi})\mu_Z(\dot{\theta})}{D_3} \\
 S_{16} &= \frac{\mu_Z(\dot{\theta})\mu_P(\dot{\psi})}{D_1}, S_{26} = \frac{\mu_Z(\dot{\phi})\mu_P(\dot{\psi})}{D_2}, S_{36} = \frac{\mu_Z(\dot{\phi})\mu_P(\dot{\theta})}{D_3} \\
 S_{17} &= \frac{\mu_P(\dot{\theta})\mu_N(\dot{\psi})}{D_1}, S_{27} = \frac{\mu_P(\dot{\phi})\mu_N(\dot{\psi})}{D_2}, S_{37} = \frac{\mu_P(\dot{\phi})\mu_N(\dot{\theta})}{D_3} \\
 S_{18} &= \frac{\mu_P(\dot{\theta})\mu_Z(\dot{\psi})}{D_1}, S_{28} = \frac{\mu_P(\dot{\phi})\mu_Z(\dot{\psi})}{D_2}, S_{38} = \frac{\mu_P(\dot{\phi})\mu_Z(\dot{\theta})}{D_3} \\
 S_{19} &= \frac{\mu_P(\dot{\theta})\mu_P(\dot{\psi})}{D_1}, S_{29} = \frac{\mu_P(\dot{\phi})\mu_P(\dot{\psi})}{D_2}, S_{39} = \frac{\mu_P(\dot{\phi})\mu_P(\dot{\theta})}{D_3} \tag{5.24}
 \end{aligned}$$

with

$$\begin{aligned}
 D_1 &= \mu_N(\dot{\theta})\mu_N(\dot{\psi}) + \mu_N(\dot{\theta})\mu_Z(\dot{\psi}) + \mu_N(\dot{\theta})\mu_P(\dot{\psi}) + \mu_Z(\dot{\theta})\mu_N(\dot{\psi}) + \mu_Z(\dot{\theta})\mu_Z(\dot{\psi}) \\
 &\quad + \mu_Z(\dot{\theta})\mu_P(\dot{\psi}) + \mu_P(\dot{\theta})\mu_N(\dot{\psi}) + \mu_P(\dot{\theta})\mu_Z(\dot{\psi}) + \mu_P(\dot{\theta})\mu_P(\dot{\psi}) \\
 D_2 &= \mu_N(\dot{\phi})\mu_N(\dot{\psi}) + \mu_N(\dot{\phi})\mu_Z(\dot{\psi}) + \mu_N(\dot{\phi})\mu_P(\dot{\psi}) + \mu_Z(\dot{\phi})\mu_N(\dot{\psi}) + \mu_Z(\dot{\phi})\mu_Z(\dot{\psi}) \\
 &\quad + \mu_Z(\dot{\phi})\mu_P(\dot{\psi}) + \mu_P(\dot{\phi})\mu_N(\dot{\psi}) + \mu_P(\dot{\phi})\mu_Z(\dot{\psi}) + \mu_P(\dot{\phi})\mu_P(\dot{\psi}) \\
 D_3 &= \mu_N(\dot{\phi})\mu_N(\dot{\theta}) + \mu_N(\dot{\phi})\mu_Z(\dot{\theta}) + \mu_N(\dot{\phi})\mu_P(\dot{\theta}) + \mu_Z(\dot{\phi})\mu_N(\dot{\theta}) + \mu_Z(\dot{\phi})\mu_Z(\dot{\theta}) \\
 &\quad + \mu_Z(\dot{\phi})\mu_P(\dot{\theta}) + \mu_P(\dot{\phi})\mu_N(\dot{\theta}) + \mu_P(\dot{\phi})\mu_Z(\dot{\theta}) + \mu_P(\dot{\phi})\mu_P(\dot{\theta}) \tag{5.25}
 \end{aligned}$$

The fuzzy sets N, Z, P are defined for  $\dot{\phi}, \dot{\theta}, \dot{\psi}$  as shown in Figs. 5.5 - 5.7.

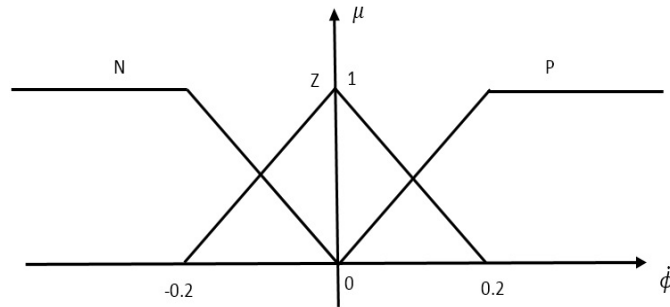
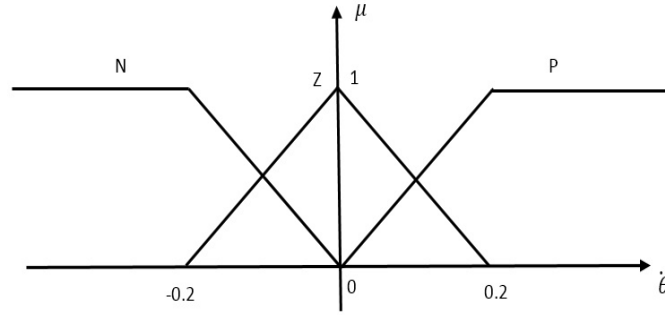
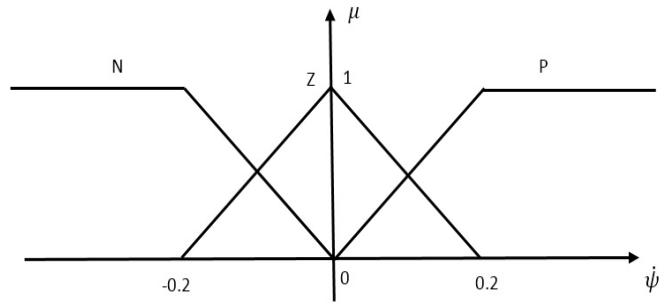


Figure 5.5: The Fuzzy Sets for  $\dot{\phi}$


 Figure 5.6: The Fuzzy Sets for  $\dot{\theta}$ 

 Figure 5.7: The Fuzzy Sets for  $\dot{\psi}$ 

The fuzzy rule base for (5.20) is given below.

- $R^{11}$  : **IF**  $\dot{\theta} \in \mathbf{N}$ ,  $\dot{\psi} \in \mathbf{N}$ , **THEN**  $\mathbf{y} \in \mathbf{B}^{11}$
- $R^{12}$  : **IF**  $\dot{\theta} \in \mathbf{N}$ ,  $\dot{\psi} \in \mathbf{Z}$ , **THEN**  $\mathbf{y} \in \mathbf{B}^{12}$
- $R^{13}$  : **IF**  $\dot{\theta} \in \mathbf{N}$ ,  $\dot{\psi} \in \mathbf{P}$ , **THEN**  $\mathbf{y} \in \mathbf{B}^{13}$
- $R^{14}$  : **IF**  $\dot{\theta} \in \mathbf{Z}$ ,  $\dot{\psi} \in \mathbf{N}$ , **THEN**  $\mathbf{y} \in \mathbf{B}^{14}$
- $R^{15}$  : **IF**  $\dot{\theta} \in \mathbf{Z}$ ,  $\dot{\psi} \in \mathbf{Z}$ , **THEN**  $\mathbf{y} \in \mathbf{B}^{15}$
- $R^{16}$  : **IF**  $\dot{\theta} \in \mathbf{Z}$ ,  $\dot{\psi} \in \mathbf{P}$ , **THEN**  $\mathbf{y} \in \mathbf{B}^{16}$
- $R^{17}$  : **IF**  $\dot{\theta} \in \mathbf{P}$ ,  $\dot{\psi} \in \mathbf{N}$ , **THEN**  $\mathbf{y} \in \mathbf{B}^{17}$
- $R^{18}$  : **IF**  $\dot{\theta} \in \mathbf{P}$ ,  $\dot{\psi} \in \mathbf{Z}$ , **THEN**  $\mathbf{y} \in \mathbf{B}^{18}$
- $R^{19}$  : **IF**  $\dot{\theta} \in \mathbf{P}$ ,  $\dot{\psi} \in \mathbf{P}$ , **THEN**  $\mathbf{y} \in \mathbf{B}^{19}$

The fuzzy rule base for (5.21) is given below.

$$\begin{aligned}
 R^{21} &: \text{IF } \dot{\phi} \in \mathbf{N}, \dot{\psi} \in \mathbf{N}, \text{ THEN } \mathbf{y} \in \mathbf{B}^{21} \\
 R^{22} &: \text{IF } \dot{\phi} \in \mathbf{N}, \dot{\psi} \in \mathbf{Z}, \text{ THEN } \mathbf{y} \in \mathbf{B}^{22} \\
 R^{23} &: \text{IF } \dot{\phi} \in \mathbf{N}, \dot{\psi} \in \mathbf{P}, \text{ THEN } \mathbf{y} \in \mathbf{B}^{23} \\
 R^{24} &: \text{IF } \dot{\phi} \in \mathbf{Z}, \dot{\psi} \in \mathbf{N}, \text{ THEN } \mathbf{y} \in \mathbf{B}^{24} \\
 R^{25} &: \text{IF } \dot{\phi} \in \mathbf{Z}, \dot{\psi} \in \mathbf{Z}, \text{ THEN } \mathbf{y} \in \mathbf{B}^{25} \\
 R^{26} &: \text{IF } \dot{\phi} \in \mathbf{Z}, \dot{\psi} \in \mathbf{P}, \text{ THEN } \mathbf{y} \in \mathbf{B}^{26} \\
 R^{27} &: \text{IF } \dot{\phi} \in \mathbf{P}, \dot{\psi} \in \mathbf{N}, \text{ THEN } \mathbf{y} \in \mathbf{B}^{27} \\
 R^{28} &: \text{IF } \dot{\phi} \in \mathbf{P}, \dot{\psi} \in \mathbf{Z}, \text{ THEN } \mathbf{y} \in \mathbf{B}^{28} \\
 R^{29} &: \text{IF } \dot{\phi} \in \mathbf{P}, \dot{\psi} \in \mathbf{P}, \text{ THEN } \mathbf{y} \in \mathbf{B}^{29}
 \end{aligned}$$

The fuzzy rule base for (5.22) is given below.

$$\begin{aligned}
 R^{31} &: \text{IF } \dot{\phi} \in \mathbf{N}, \dot{\theta} \in \mathbf{N}, \text{ THEN } \mathbf{y} \in \mathbf{B}^{31} \\
 R^{32} &: \text{IF } \dot{\phi} \in \mathbf{N}, \dot{\theta} \in \mathbf{Z}, \text{ THEN } \mathbf{y} \in \mathbf{B}^{32} \\
 R^{33} &: \text{IF } \dot{\phi} \in \mathbf{N}, \dot{\theta} \in \mathbf{P}, \text{ THEN } \mathbf{y} \in \mathbf{B}^{33} \\
 R^{34} &: \text{IF } \dot{\phi} \in \mathbf{Z}, \dot{\theta} \in \mathbf{N}, \text{ THEN } \mathbf{y} \in \mathbf{B}^{34} \\
 R^{35} &: \text{IF } \dot{\phi} \in \mathbf{Z}, \dot{\theta} \in \mathbf{Z}, \text{ THEN } \mathbf{y} \in \mathbf{B}^{35} \\
 R^{36} &: \text{IF } \dot{\phi} \in \mathbf{Z}, \dot{\theta} \in \mathbf{P}, \text{ THEN } \mathbf{y} \in \mathbf{B}^{36} \\
 R^{37} &: \text{IF } \dot{\phi} \in \mathbf{P}, \dot{\theta} \in \mathbf{N}, \text{ THEN } \mathbf{y} \in \mathbf{B}^{37} \\
 R^{38} &: \text{IF } \dot{\phi} \in \mathbf{P}, \dot{\theta} \in \mathbf{Z}, \text{ THEN } \mathbf{y} \in \mathbf{B}^{38} \\
 R^{39} &: \text{IF } \dot{\phi} \in \mathbf{P}, \dot{\theta} \in \mathbf{P}, \text{ THEN } \mathbf{y} \in \mathbf{B}^{39}
 \end{aligned}$$

$\eta_1, \eta_2, \eta_3$  in (5.20)-(5.22) are defined as follows

$$\begin{aligned}
 \eta_1 &= [\eta_{11}, \eta_{12}, \eta_{13}, \eta_{14}, \eta_{15}, \eta_{16}, \eta_{17}, \eta_{18}, \eta_{19}]^T \\
 \eta_2 &= [\eta_{21}, \eta_{22}, \eta_{23}, \eta_{24}, \eta_{25}, \eta_{26}, \eta_{27}, \eta_{28}, \eta_{29}]^T \\
 \eta_3 &= [\eta_{31}, \eta_{32}, \eta_{33}, \eta_{34}, \eta_{35}, \eta_{36}, \eta_{37}, \eta_{38}, \eta_{39}]^T
 \end{aligned} \tag{5.26}$$

where  $\eta_{ij}$  is the center of the fuzzy set  $\mathbf{B}^{ij}$  and will be estimated, as an adaptive parameter, by an adaptive law later,  $i = 1, 2, 3$  and  $j = 1, 2, \dots, 9$ .

The unknown parameters  $I_\phi$ ,  $I_\theta$ , and  $I_\psi$  are estimated through parameters

$$\beta_1 = \frac{1}{I_\phi} \tag{5.27}$$

$$\beta_2 = \frac{1}{I_\theta} \tag{5.28}$$

$$\beta_3 = \frac{1}{I_\psi} \tag{5.29}$$

For simplicity in derivations, define

$$u_1 = -J_r \dot{\theta} \Omega + l \tau_\phi \quad (5.30)$$

$$u_2 = J_r \dot{\phi} \Omega + l \tau_\theta \quad (5.31)$$

$$u_3 = \tau_\psi \quad (5.32)$$

Then, with (5.20)-(5.32), (3.12) can be rewritten as

$$\begin{aligned} \ddot{\phi} &= \dot{\theta} \dot{\psi} \left( \frac{I_\theta - I_\psi}{I_\phi} \right) - \frac{J_r}{I_\phi} \dot{\theta} \Omega + \frac{l}{I_\phi} \tau_\phi \\ &= \eta_1^T S_1 + \delta_1 + \beta_1 u_1 \end{aligned} \quad (5.33)$$

$$\begin{aligned} \ddot{\theta} &= \dot{\phi} \dot{\psi} \left( \frac{I_\psi - I_\phi}{I_\theta} \right) + \frac{J_r}{I_\theta} \dot{\phi} \Omega + \frac{l}{I_\theta} \tau_\theta \\ &= \eta_2^T S_2 + \delta_2 + \beta_2 u_2 \end{aligned} \quad (5.34)$$

$$\begin{aligned} \ddot{\psi} &= \dot{\phi} \dot{\theta} \left( \frac{I_\phi - I_\theta}{I_\psi} \right) + \frac{1}{I_\psi} \tau_\psi \\ &= \eta_3^T S_3 + \delta_3 + \beta_3 u_3 \end{aligned} \quad (5.35)$$

The block diagram of the adaptive fuzzy logic estimator with Euler angle representation is shown in Figs. 5.8-5.10.

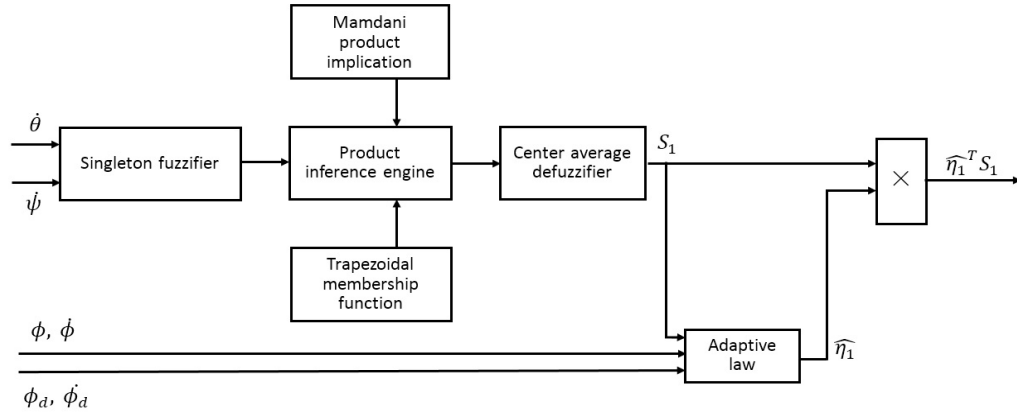
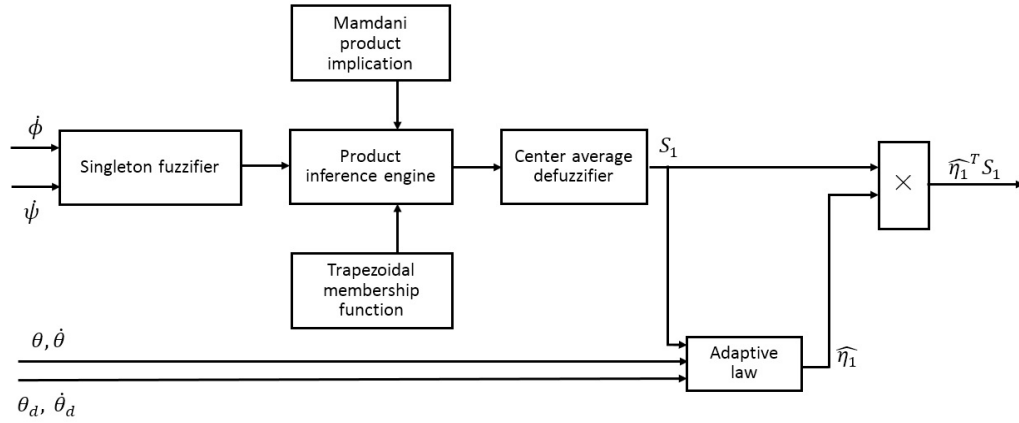
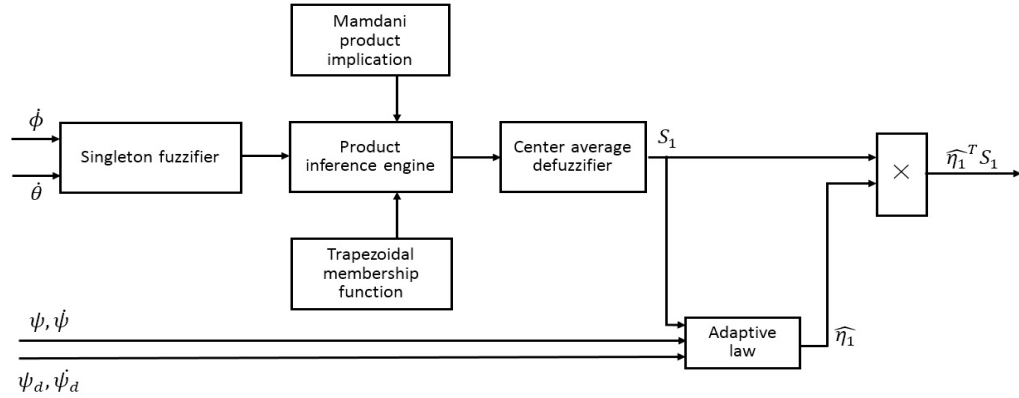


Figure 5.8: The Fuzzy Logic Estimator for  $\dot{\theta} \dot{\psi} \left( \frac{I_\theta - I_\psi}{I_\phi} \right)$


 Figure 5.9: The Fuzzy Logic Estimator for  $\dot{\phi}\dot{\psi} \left( \frac{I_\psi - I_\phi}{I_\theta} \right)$ 

 Figure 5.10: The Fuzzy Logic Estimator for  $\dot{\phi}\dot{\theta} \left( \frac{I_\phi - I_\theta}{I_\psi} \right)$ 

Define the errors as follows

$$\begin{aligned}
 e_a &= \int (\phi - \phi_d) dt \\
 e_1 &= \phi - \phi_d = \dot{e}_a \\
 e_2 &= \dot{\phi} - \dot{\phi}_d = \dot{e}_1 \\
 e_b &= \int (\theta - \theta_d) dt \\
 e_3 &= \theta - \theta_d = \dot{e}_b \\
 e_4 &= \dot{\theta} - \dot{\theta}_d = \dot{e}_3 \\
 e_c &= \int (\psi - \psi_d) dt \\
 e_5 &= \psi - \psi_d = \dot{e}_c \\
 e_6 &= \dot{\psi} - \dot{\psi}_d = \dot{e}_5
 \end{aligned} \tag{5.36}$$

Step 1

Define a positive definite Lyapunov function  $V_1$

$$V_1 = \frac{1}{2}e_a^2 + \frac{1}{2}e_b^2 + \frac{1}{2}e_c^2 \quad (5.37)$$

The derivative of  $V_1$  with respect to time is given by

$$\begin{aligned} \dot{V}_1 &= e_a \dot{e}_a + e_b \dot{e}_b + e_c \dot{e}_c \\ &= e_a e_1 + e_b e_3 + e_c e_5 \\ &= e_a(e_1 - k_a e_a + k_a e_a) + e_b(e_3 - k_b e_b + k_b e_b) + e_c(e_5 - k_c e_c + k_c e_c) \\ &= -k_a e_a^2 - k_b e_b^2 - k_c e_c^2 + e_a(e_1 + k_a e_a) + e_b(e_3 + k_b e_b) + e_c(e_5 + k_c e_c) \end{aligned} \quad (5.38)$$

where  $k_a$ ,  $k_b$ , and  $k_c$  are the positive gains and  $k_a e_a$ ,  $k_b e_b$ , and  $k_c e_c$  are called virtual control. For convenience, define

$$\begin{aligned} \alpha_1 &= -k_a e_a \\ \alpha_3 &= -k_b e_b \\ \alpha_5 &= -k_c e_c \end{aligned} \quad (5.39)$$

and

$$\begin{aligned} \bar{e}_1 &= e_1 + k_a e_a \\ \bar{e}_3 &= e_3 + k_b e_b \\ \bar{e}_5 &= e_5 + k_c e_c \end{aligned} \quad (5.40)$$

Then, (5.38) can be rewritten as

$$\dot{V}_1 = -k_a e_a^2 - k_b e_b^2 - k_c e_c^2 + e_a \bar{e}_1 + e_b \bar{e}_3 + e_c \bar{e}_5 \quad (5.41)$$

It is clear that  $\dot{V}_1$  is a negative definite if  $\bar{e}_1$ ,  $\bar{e}_3$ , and  $\bar{e}_5$  are equal to zero. Differentiating (5.40), which will be used at Step 2, produces

$$\begin{aligned} \dot{\bar{e}}_1 &= e_2 + k_a e_1 \\ \dot{\bar{e}}_3 &= e_4 + k_b e_3 \\ \dot{\bar{e}}_5 &= e_6 + k_c e_5 \end{aligned} \quad (5.42)$$

Step 2

Define a positive definite Lyapunov function  $V_2$ :

$$V_2 = V_1 + \frac{1}{2}\bar{e}_1^2 + \frac{1}{2}\bar{e}_3^2 + \frac{1}{2}\bar{e}_5^2 \quad (5.43)$$

Substituting (5.41) and (5.42) into (5.43), the derivative of  $V_2$  with respect to time becomes:

$$\begin{aligned}
 \dot{V}_2 &= \dot{V}_1 + \bar{e}_1 \dot{\bar{e}}_1 + \bar{e}_3 \dot{\bar{e}}_3 + \bar{e}_5 \dot{\bar{e}}_5 \\
 &= -k_a e_a^2 - k_b e_b^2 - k_c e_c^2 + e_a \bar{e}_1 + e_b \bar{e}_3 + e_c \bar{e}_5 + \bar{e}_1 \dot{\bar{e}}_1 + \bar{e}_3 \dot{\bar{e}}_3 + \bar{e}_5 \dot{\bar{e}}_5 \\
 &= -k_a e_a^2 - k_b e_b^2 - k_c e_c^2 + \bar{e}_1 (e_a + \dot{\bar{e}}_1) + \bar{e}_3 (e_b + \dot{\bar{e}}_3) + \bar{e}_5 (e_c + \dot{\bar{e}}_5) \\
 &= -k_a e_a^2 - k_b e_b^2 - k_c e_c^2 \\
 &\quad + \bar{e}_1 (e_a + e_2 + k_a e_1) + \bar{e}_3 (e_b + e_4 + k_b e_3) + \bar{e}_5 (e_c + e_6 + k_c e_5)
 \end{aligned} \tag{5.44}$$

Define the virtual control  $\alpha_2$ ,  $\alpha_4$ , and  $\alpha_6$

$$\begin{aligned}
 \alpha_2 &= -k_1 \bar{e}_1 - e_a - k_a e_1 \\
 \alpha_4 &= -k_3 \bar{e}_3 - e_b - k_b e_3 \\
 \alpha_6 &= -k_5 \bar{e}_5 - e_c - k_c e_5
 \end{aligned} \tag{5.45}$$

where  $k_1$ ,  $k_3$ , and  $k_5$  are the positive gains. Then, (5.44) can be rewritten as

$$\begin{aligned}
 \dot{V}_2 &= -k_a e_a^2 - k_b e_b^2 - k_c e_c^2 \\
 &\quad + \bar{e}_1 (-k_1 \bar{e}_1 + e_2 - \alpha_2) + \bar{e}_3 (-k_3 \bar{e}_3 + e_4 - \alpha_4) + \bar{e}_5 (-k_5 \bar{e}_5 + e_6 - \alpha_6)
 \end{aligned} \tag{5.46}$$

Set

$$\begin{aligned}
 \bar{e}_2 &= e_2 - \alpha_2 \\
 \bar{e}_4 &= e_4 - \alpha_4 \\
 \bar{e}_6 &= e_6 - \alpha_6
 \end{aligned} \tag{5.47}$$

As a result,  $\dot{V}_2$  can be expressed as

$$\begin{aligned}
 \dot{V}_2 &= -k_a e_a^2 - k_b e_b^2 - k_c e_c^2 - k_1 \bar{e}_1^2 - k_3 \bar{e}_3^2 - k_5 \bar{e}_5^2 \\
 &\quad + \bar{e}_1 \bar{e}_2 + \bar{e}_3 \bar{e}_4 + \bar{e}_5 \bar{e}_6
 \end{aligned} \tag{5.48}$$

which is a negative definite if  $\bar{e}_1$ ,  $\bar{e}_3$ , and  $\bar{e}_5$  equal zero. Differentiating (5.47), which will be used at Step 3, yields:

$$\begin{aligned}
 \dot{\bar{e}}_2 &= \dot{\phi} - \ddot{\phi}_d - \dot{\alpha}_2 \\
 \dot{\bar{e}}_4 &= \dot{\theta} - \ddot{\theta}_d - \dot{\alpha}_4 \\
 \dot{\bar{e}}_6 &= \dot{\psi} - \ddot{\psi}_d - \dot{\alpha}_6
 \end{aligned} \tag{5.49}$$

Step 3

Define a positive definite Lyapunov function  $V_3$  with the estimation errors added

$$\begin{aligned}
 V_3 &= V_2 + \frac{1}{2} \bar{e}_2^2 + \frac{1}{2} \bar{e}_4^2 + \frac{1}{2} \bar{e}_6^2 \\
 &\quad + \frac{1}{2} \sum_{i=1}^3 (\eta_i - \hat{\eta}_i)^T \Gamma_i (\eta_i - \hat{\eta}_i) + \frac{1}{2} \sum_{i=1}^3 \lambda_i \beta_i (\xi_i - \hat{\xi}_i)^2
 \end{aligned} \tag{5.50}$$

where  $\hat{\eta}_i$  are the estimations of the parameters  $\eta_1, \eta_2$ , and  $\eta_3$ ,  $\hat{\xi}_1, \hat{\xi}_2$ , and  $\hat{\xi}_3$  are the estimations of the parameters  $\xi_1 = I_\phi, \xi_2 = I_\theta$ , and  $\xi_3 = I_\psi$ , respectively,  $\Gamma_i$ , and  $\lambda_i, i = 1, 2, 3$ , are positive constants. It follows from (5.27)-(5.29) that

$$\beta_i = \frac{1}{\hat{\xi}_i}, i = 1, 2, 3 \quad (5.51)$$

Motivated by [48], define

$$\begin{aligned} \bar{u}_1 &= \frac{u_1}{\hat{\xi}_1} \\ \bar{u}_2 &= \frac{u_2}{\hat{\xi}_2} \\ \bar{u}_3 &= \frac{u_3}{\hat{\xi}_3} \end{aligned} \quad (5.52)$$

Then, it can be verified that the following are true.

$$\begin{aligned} \beta_1 u_1 &= \bar{u}_1 - \beta_1(\xi_1 - \hat{\xi}_1)\bar{u}_1 \\ \beta_2 u_2 &= \bar{u}_2 - \beta_2(\xi_2 - \hat{\xi}_2)\bar{u}_2 \\ \beta_3 u_3 &= \bar{u}_3 - \beta_3(\xi_3 - \hat{\xi}_3)\bar{u}_3 \end{aligned} \quad (5.53)$$

For instance,  $\beta_1 u_1 = \frac{1}{\hat{\xi}_1} \hat{\xi}_1 \bar{u}_1 = \frac{1}{\hat{\xi}_1} (\hat{\xi}_1 - \xi_1 + \xi_1) \bar{u}_1 = \bar{u}_1 - \frac{1}{\hat{\xi}_1} (\xi_1 - \hat{\xi}_1) \bar{u}_1 = \bar{u}_1 - \beta_1(\xi_1 - \hat{\xi}_1)\bar{u}_1$ . Substituting (5.53) into (5.33)-(5.35) produces

$$\begin{aligned} \ddot{\phi} &= \eta_1^T S_1 + \delta_1 + \beta_1 u_1 \\ &= \eta_1^T S_1 + \delta_1 + \bar{u}_1 - \beta_1(\xi_1 - \hat{\xi}_1)\bar{u}_1 \end{aligned} \quad (5.54)$$

$$\begin{aligned} \ddot{\theta} &= \eta_2^T S_2 + \delta_2 + \beta_2 u_2 \\ &= \eta_2^T S_2 + \delta_2 + \bar{u}_2 - \beta_2(\xi_2 - \hat{\xi}_2)\bar{u}_2 \end{aligned} \quad (5.55)$$

$$\begin{aligned} \ddot{\psi} &= \eta_3^T S_3 + \delta_3 + \beta_3 u_3 \\ &= \eta_3^T S_3 + \delta_3 + \bar{u}_3 - \beta_3(\xi_3 - \hat{\xi}_3)\bar{u}_3 \end{aligned} \quad (5.56)$$

Substituting (5.48), and (5.49) into (5.50), it can be shown that the derivative of  $V_3$  with respect to time is given by

$$\begin{aligned}
 \dot{V}_3 &= \dot{V}_2 + \bar{e}_2 \dot{\bar{e}}_2 + \bar{e}_4 \dot{\bar{e}}_4 + \bar{e}_6 \dot{\bar{e}}_6 \\
 &\quad + \sum_{i=1}^3 (\eta_i - \hat{\eta}_i)^T \Gamma_i (-\dot{\hat{\eta}}_i) + \sum_{i=1}^3 \lambda_i \beta_i (\xi_i - \hat{\xi}_i) (-\dot{\hat{\xi}}_i) \\
 &= -k_a e_a^2 - k_1 \bar{e}_1^2 + \bar{e}_1 \bar{e}_2 + \bar{e}_2 \dot{\bar{e}}_2 + (\eta_1 - \hat{\eta}_1)^T \Gamma_1 (-\dot{\hat{\eta}}_1) \\
 &\quad - k_b e_b^2 - k_3 \bar{e}_3^2 + \bar{e}_3 \bar{e}_4 + \bar{e}_4 \dot{\bar{e}}_4 + (\eta_2 - \hat{\eta}_2)^T \Gamma_2 (-\dot{\hat{\eta}}_2) \\
 &\quad - k_c e_c^2 - k_5 \bar{e}_5^2 + \bar{e}_5 \bar{e}_6 + \bar{e}_6 \dot{\bar{e}}_6 + (\eta_3 - \hat{\eta}_3)^T \Gamma_3 (-\dot{\hat{\eta}}_3) \\
 &\quad + \lambda_1 \beta_1 (\xi_1 - \hat{\xi}_1) (-\dot{\hat{\xi}}_1) + \lambda_2 \beta_2 (\xi_2 - \hat{\xi}_2) (-\dot{\hat{\xi}}_2) + \lambda_3 \beta_3 (\xi_3 - \hat{\xi}_3) (-\dot{\hat{\xi}}_3) \\
 &= -k_a e_a^2 - k_1 \bar{e}_1^2 + \bar{e}_2 (\bar{e}_1 + \ddot{\phi} - \ddot{\phi}_d - \dot{\alpha}_2) + (\eta_1 - \hat{\eta}_1)^T \Gamma_1 (-\dot{\hat{\eta}}_1) \\
 &\quad - k_b e_b^2 - k_3 \bar{e}_3^2 + \bar{e}_4 (\bar{e}_3 + \ddot{\theta} - \ddot{\theta}_d - \dot{\alpha}_4) + (\eta_2 - \hat{\eta}_2)^T \Gamma_2 (-\dot{\hat{\eta}}_2) \\
 &\quad - k_c e_c^2 - k_5 \bar{e}_5^2 + \bar{e}_6 (\bar{e}_5 + \ddot{\psi} - \ddot{\psi}_d - \dot{\alpha}_6) + (\eta_3 - \hat{\eta}_3)^T \Gamma_3 (-\dot{\hat{\eta}}_3) \\
 &\quad + \lambda_1 \beta_1 (\xi_1 - \hat{\xi}_1) (-\dot{\hat{\xi}}_1) + \lambda_2 \beta_2 (\xi_2 - \hat{\xi}_2) (-\dot{\hat{\xi}}_2) + \lambda_3 \beta_3 (\xi_3 - \hat{\xi}_3) (-\dot{\hat{\xi}}_3) \quad (5.57)
 \end{aligned}$$

Substituting (5.54)-(5.56) into (5.57), (5.58) holds

$$\begin{aligned}
 \dot{V}_3 &= -k_a e_a^2 - k_1 \bar{e}_1^2 + (\eta_1 - \hat{\eta}_1)^T \Gamma_1 (-\dot{\hat{\eta}}_1) + \lambda_1 \beta_1 (\xi_1 - \hat{\xi}_1) (-\dot{\hat{\xi}}_1) \\
 &\quad - k_b e_b^2 - k_3 \bar{e}_3^2 + (\eta_2 - \hat{\eta}_2)^T \Gamma_2 (-\dot{\hat{\eta}}_2) + \lambda_2 \beta_2 (\xi_2 - \hat{\xi}_2) (-\dot{\hat{\xi}}_2) \\
 &\quad - k_c e_c^2 - k_5 \bar{e}_5^2 + (\eta_3 - \hat{\eta}_3)^T \Gamma_3 (-\dot{\hat{\eta}}_3) + \lambda_3 \beta_3 (\xi_3 - \hat{\xi}_3) (-\dot{\hat{\xi}}_3) \\
 &\quad + \bar{e}_2 (\bar{e}_1 + \eta_1^T S_1 + \delta_1 + \bar{u}_1 - \beta_1 (\xi_1 - \hat{\xi}_1) \bar{u}_1 - \ddot{\phi}_d - \dot{\alpha}_2) \\
 &\quad + \bar{e}_4 (\bar{e}_3 + \eta_2^T S_2 + \delta_2 + \bar{u}_2 - \beta_2 (\xi_2 - \hat{\xi}_2) \bar{u}_2 - \ddot{\theta}_d - \dot{\alpha}_4) \\
 &\quad + \bar{e}_6 (\bar{e}_5 + \eta_3^T S_3 + \delta_3 + \bar{u}_3 - \beta_3 (\xi_3 - \hat{\xi}_3) \bar{u}_3 - \ddot{\psi}_d - \dot{\alpha}_6) \\
 &= -k_a e_a^2 - k_1 \bar{e}_1^2 + (\eta_1 - \hat{\eta}_1)^T \Gamma_1 (-\dot{\hat{\eta}}_1) + \lambda_1 \beta_1 (\xi_1 - \hat{\xi}_1) (-\lambda_1^{-1} \bar{u}_1 \bar{e}_2 - \dot{\hat{\xi}}_1) \\
 &\quad - k_b e_b^2 - k_3 \bar{e}_3^2 + (\eta_2 - \hat{\eta}_2)^T \Gamma_2 (-\dot{\hat{\eta}}_2) + \lambda_2 \beta_2 (\xi_2 - \hat{\xi}_2) (-\lambda_2^{-1} \bar{u}_2 \bar{e}_4 - \dot{\hat{\xi}}_2) \\
 &\quad - k_c e_c^2 - k_5 \bar{e}_5^2 + (\eta_3 - \hat{\eta}_3)^T \Gamma_3 (-\dot{\hat{\eta}}_3) + \lambda_3 \beta_3 (\xi_3 - \hat{\xi}_3) (-\lambda_3^{-1} \bar{u}_3 \bar{e}_6 - \dot{\hat{\xi}}_3) \\
 &\quad + \bar{e}_2 [\bar{e}_1 + (\eta_1 - \hat{\eta}_1)^T S_1 + \hat{\eta}_1^T S_1 + \delta_1 + \bar{u}_1 - \ddot{\phi}_d - \dot{\alpha}_2] \\
 &\quad + \bar{e}_4 [\bar{e}_3 + (\eta_2 - \hat{\eta}_2)^T S_2 + \hat{\eta}_2^T S_2 + \delta_2 + \bar{u}_2 - \ddot{\theta}_d - \dot{\alpha}_4] \\
 &\quad + \bar{e}_6 [\bar{e}_5 + (\eta_3 - \hat{\eta}_3)^T S_3 + \hat{\eta}_3^T S_3 + \delta_3 + \bar{u}_3 - \ddot{\psi}_d - \dot{\alpha}_6] \quad (5.58)
 \end{aligned}$$

which can be rewritten as

$$\begin{aligned}
 \dot{V}_3 = & -k_a e_a^2 - k_1 \bar{e}_1^2 + (\eta_1 - \hat{\eta}_1)^T \Gamma_1 (\Gamma_1^{-1} \bar{e}_2 S_1 - \dot{\hat{\eta}}_1) + \lambda_1 \beta_1 (\xi_1 - \hat{\xi}_1) (-\lambda_1^{-1} \bar{u}_1 \bar{e}_2 - \dot{\hat{\xi}}_1) \\
 & -k_b e_b^2 - k_3 \bar{e}_3^2 + (\eta_2 - \hat{\eta}_2)^T \Gamma_2 (\Gamma_2^{-1} \bar{e}_4 S_2 - \dot{\hat{\eta}}_2) + \lambda_2 \beta_2 (\xi_2 - \hat{\xi}_2) (-\lambda_2^{-1} \bar{u}_2 \bar{e}_4 - \dot{\hat{\xi}}_2) \\
 & -k_c e_c^2 - k_5 \bar{e}_5^2 + (\eta_3 - \hat{\eta}_3)^T \Gamma_3 (\Gamma_3^{-1} \bar{e}_6 S_3 - \dot{\hat{\eta}}_3) + \lambda_3 \beta_3 (\xi_3 - \hat{\xi}_3) (-\lambda_3^{-1} \bar{u}_3 \bar{e}_6 - \dot{\hat{\xi}}_3) \\
 & + \bar{e}_2 [\bar{e}_1 + \hat{\eta}_1^T S_1 + \bar{u}_1 - \ddot{\phi}_d - \dot{\alpha}_2] + \bar{e}_2 \delta_1 \\
 & + \bar{e}_4 [\bar{e}_3 + \hat{\eta}_2^T S_2 + \bar{u}_2 - \ddot{\theta}_d - \dot{\alpha}_4] + \bar{e}_4 \delta_2 \\
 & + \bar{e}_6 [\bar{e}_5 + \hat{\eta}_3^T S_3 + \bar{u}_3 - \ddot{\psi}_d - \dot{\alpha}_6] + \bar{e}_6 \delta_3
 \end{aligned} \tag{5.59}$$

The following adaptation laws are introduced

$$\begin{aligned}
 \dot{\hat{\eta}}_1 &= \Gamma_1^{-1} \bar{e}_2 S_1 - \sigma_1 \hat{\eta}_1 \\
 \dot{\hat{\eta}}_2 &= \Gamma_2^{-1} \bar{e}_4 S_2 - \sigma_2 \hat{\eta}_2 \\
 \dot{\hat{\eta}}_3 &= \Gamma_3^{-1} \bar{e}_6 S_3 - \sigma_3 \hat{\eta}_3
 \end{aligned} \tag{5.60}$$

and

$$\begin{aligned}
 \dot{\hat{\xi}}_1 &= -\lambda_1^{-1} \bar{u}_1 \bar{e}_2 - \varrho_1 \hat{\xi}_1 \\
 \dot{\hat{\xi}}_2 &= -\lambda_2^{-1} \bar{u}_2 \bar{e}_4 - \varrho_2 \hat{\xi}_2 \\
 \dot{\hat{\xi}}_3 &= -\lambda_3^{-1} \bar{u}_3 \bar{e}_6 - \varrho_3 \hat{\xi}_3
 \end{aligned} \tag{5.61}$$

Then, (5.59) can be rewritten as

$$\begin{aligned}
 \dot{V}_3 = & -k_a e_a^2 - k_1 \bar{e}_1^2 + \sigma_1 (\eta_1 - \hat{\eta}_1)^T \Gamma_1 \hat{\eta}_1 + \varrho_1 \lambda_1 \beta_1 (\xi_1 - \hat{\xi}_1) \hat{\xi}_1 \\
 & -k_b e_b^2 - k_3 \bar{e}_3^2 + \sigma_2 (\eta_2 - \hat{\eta}_2)^T \Gamma_2 \hat{\eta}_2 + \varrho_2 \lambda_2 \beta_2 (\xi_2 - \hat{\xi}_2) \hat{\xi}_2 \\
 & -k_c e_c^2 - k_5 \bar{e}_5^2 + \sigma_3 (\eta_3 - \hat{\eta}_3)^T \Gamma_3 \hat{\eta}_3 + \varrho_3 \lambda_3 \beta_3 (\xi_3 - \hat{\xi}_3) \hat{\xi}_3 \\
 & + \bar{e}_2 [\bar{e}_1 + \hat{\eta}_1^T S_1 + \bar{u}_1 - \ddot{\phi}_d - \dot{\alpha}_2] + \bar{e}_2 \delta_1 \\
 & + \bar{e}_4 [\bar{e}_3 + \hat{\eta}_2^T S_2 + \bar{u}_2 - \ddot{\theta}_d - \dot{\alpha}_4] + \bar{e}_4 \delta_2 \\
 & + \bar{e}_6 [\bar{e}_5 + \hat{\eta}_3^T S_3 + \bar{u}_3 - \ddot{\psi}_d - \dot{\alpha}_6] + \bar{e}_6 \delta_3
 \end{aligned} \tag{5.62}$$

Due to the relations  $\hat{\eta}_i = \eta_i - (\eta_i - \hat{\eta}_i)$  and  $\hat{\xi}_i = \xi_i - (\xi_i - \hat{\xi}_i)$ ,  $\dot{V}_3$  in (5.62) can be re-expressed as

$$\begin{aligned}
 \dot{V}_3 = & -k_a e_a^2 - k_1 \bar{e}_1^2 + \sigma_1 (\eta_1 - \hat{\eta}_1)^T \Gamma_1 \eta_1 + \varrho_1 \lambda_1 \beta_1 (\xi_1 - \hat{\xi}_1) \xi_1 \\
 & -k_b e_b^2 - k_3 \bar{e}_3^2 + \sigma_2 (\eta_2 - \hat{\eta}_2)^T \Gamma_2 \eta_2 + \varrho_2 \lambda_2 \beta_2 (\xi_2 - \hat{\xi}_2) \xi_2 \\
 & -k_c e_c^2 - k_5 \bar{e}_5^2 + \sigma_3 (\eta_3 - \hat{\eta}_3)^T \Gamma_3 \eta_3 + \varrho_3 \lambda_3 \beta_3 (\xi_3 - \hat{\xi}_3) \xi_3 \\
 & -\sigma_1 (\eta_1 - \hat{\eta}_1)^T \Gamma_1 (\eta_1 - \hat{\eta}_1) - \sigma_2 (\eta_2 - \hat{\eta}_2)^T \Gamma_2 (\eta_2 - \hat{\eta}_2) - \sigma_3 (\eta_3 - \hat{\eta}_3)^T \Gamma_3 (\eta_3 - \hat{\eta}_3) \\
 & + \bar{e}_2 [\bar{e}_1 + \hat{\eta}_1^T S_1 + \bar{u}_1 - \ddot{\phi}_d - \dot{\alpha}_2] + \bar{e}_2 \delta_1 - \varrho_1 \lambda_1 \beta_1 (\xi_1 - \hat{\xi}_1)^2 \\
 & + \bar{e}_4 [\bar{e}_3 + \hat{\eta}_2^T S_2 + \bar{u}_2 - \ddot{\theta}_d - \dot{\alpha}_4] + \bar{e}_4 \delta_2 - \varrho_2 \lambda_2 \beta_2 (\xi_2 - \hat{\xi}_2)^2 \\
 & + \bar{e}_6 [\bar{e}_5 + \hat{\eta}_3^T S_3 + \bar{u}_3 - \ddot{\psi}_d - \dot{\alpha}_6] + \bar{e}_6 \delta_3 - \varrho_3 \lambda_3 \beta_3 (\xi_3 - \hat{\xi}_3)^2
 \end{aligned} \tag{5.63}$$

Using Young's inequality  $xy \leq \frac{1}{2}(x^2 + y^2)$ , it follows that

$$\begin{aligned}\bar{e}_2\delta_1 &\leq \frac{1}{2}\bar{e}_2^2 + \frac{1}{2}\delta_1^2 \\ \bar{e}_4\delta_2 &\leq \frac{1}{2}\bar{e}_4^2 + \frac{1}{2}\delta_2^2 \\ \bar{e}_6\delta_3 &\leq \frac{1}{2}\bar{e}_6^2 + \frac{1}{2}\delta_3^2\end{aligned}\tag{5.64}$$

and

$$\begin{aligned}(\xi_1 - \hat{\xi}_1)\xi_1 &\leq \frac{1}{2}(\xi_1 - \hat{\xi}_1)^2 + \frac{1}{2}\xi_1^2 \\ (\xi_2 - \hat{\xi}_2)\xi_2 &\leq \frac{1}{2}(\xi_2 - \hat{\xi}_2)^2 + \frac{1}{2}\xi_2^2 \\ (\xi_3 - \hat{\xi}_3)\xi_3 &\leq \frac{1}{2}(\xi_3 - \hat{\xi}_3)^2 + \frac{1}{2}\xi_3^2\end{aligned}\tag{5.65}$$

Using Young's inequality theory  $x^T\Gamma y \leq \frac{1}{2}x^T\Gamma x + \frac{1}{2}y^T\Gamma y$  once more, it follows:

$$\begin{aligned}(\eta_1 - \hat{\eta}_1)^T\Gamma_1\eta_1 &\leq \frac{1}{2}(\eta_1 - \hat{\eta}_1)^T\Gamma_1(\eta_1 - \hat{\eta}_1) + \frac{1}{2}\eta_1^T\Gamma_1\eta_1 \\ (\eta_2 - \hat{\eta}_2)^T\Gamma_2\eta_2 &\leq \frac{1}{2}(\eta_2 - \hat{\eta}_2)^T\Gamma_2(\eta_2 - \hat{\eta}_2) + \frac{1}{2}\eta_2^T\Gamma_2\eta_2 \\ (\eta_3 - \hat{\eta}_3)^T\Gamma_3\eta_3 &\leq \frac{1}{2}(\eta_3 - \hat{\eta}_3)^T\Gamma_3(\eta_3 - \hat{\eta}_3) + \frac{1}{2}\eta_3^T\Gamma_3\eta_3\end{aligned}\tag{5.66}$$

Substituting (5.64), (5.65), and (5.66) into (5.63),  $\dot{V}_3$  becomes

$$\begin{aligned}&\dot{V}_3 \\ \leq &-k_a e_a^2 - k_1 \bar{e}_1^2 + \frac{1}{2}\sigma_1 ((\eta_1 - \hat{\eta}_1)^T\Gamma_1(\eta_1 - \hat{\eta}_1) + \eta_1^T\Gamma_1\eta_1) + \frac{1}{2}\varrho_1\lambda_1\beta_1 ((\xi_1 - \hat{\xi}_1)^2 + \xi_1^2) \\ &-k_b e_b^2 - k_3 \bar{e}_3^2 + \frac{1}{2}\sigma_2 ((\eta_2 - \hat{\eta}_2)^T\Gamma_2(\eta_2 - \hat{\eta}_2) + \eta_2^T\Gamma_2\eta_2) + \frac{1}{2}\varrho_2\lambda_2\beta_2 ((\xi_2 - \hat{\xi}_2)^2 + \xi_2^2) \\ &-k_c e_c^2 - k_5 \bar{e}_5^2 + \frac{1}{2}\sigma_3 ((\eta_3 - \hat{\eta}_3)^T\Gamma_3(\eta_3 - \hat{\eta}_3) + \eta_3^T\Gamma_3\eta_3) + \frac{1}{2}\varrho_3\lambda_3\beta_3 ((\xi_3 - \hat{\xi}_3)^2 + \xi_3^2) \\ &-\sigma_1(\eta_1 - \hat{\eta}_1)^T\Gamma_1(\eta_1 - \hat{\eta}_1) - \sigma_2(\eta_2 - \hat{\eta}_2)^T\Gamma_2(\eta_2 - \hat{\eta}_2) - \sigma_3(\eta_3 - \hat{\eta}_3)^T\Gamma_3(\eta_3 - \hat{\eta}_3) \\ &+\bar{e}_2[\bar{e}_1 + \hat{\eta}_1^T S_1 + \bar{u}_1 - \ddot{\phi}_d - \dot{\alpha}_2] + \frac{1}{2}\bar{e}_2^2 + \frac{1}{2}\delta_1^2 - \varrho_1\lambda_1\beta_1(\xi_1 - \hat{\xi}_1)^2 \\ &+\bar{e}_4[\bar{e}_3 + \hat{\eta}_2^T S_2 + \bar{u}_2 - \ddot{\theta}_d - \dot{\alpha}_4] + \frac{1}{2}\bar{e}_4^2 + \frac{1}{2}\delta_2^2 - \varrho_2\lambda_2\beta_2(\xi_2 - \hat{\xi}_2)^2 \\ &+\bar{e}_6[\bar{e}_5 + \hat{\eta}_3^T S_3 + \bar{u}_3 - \ddot{\psi}_d - \dot{\alpha}_6] + \frac{1}{2}\bar{e}_6^2 + \frac{1}{2}\delta_3^2 - \varrho_3\lambda_3\beta_3(\xi_3 - \hat{\xi}_3)^2\end{aligned}\tag{5.67}$$

After some operations on (5.67), it follows that  $\dot{V}_3$  can be rewritten as

$$\begin{aligned}
& \dot{V}_3 \\
\leq & -k_a e_a^2 - k_1 \bar{e}_1^2 + \frac{1}{2} \sigma_1 \eta_1^T \Gamma_1 \eta_1 + \frac{1}{2} \varrho_1 \lambda_1 \beta_1 \xi_1^2 - \frac{1}{2} \varrho_1 \lambda_1 \beta_1 (\xi_1 - \hat{\xi}_1)^2 \\
& -k_b e_b^2 - k_3 \bar{e}_3^2 + \frac{1}{2} \sigma_2 \eta_2^T \Gamma_2 \eta_2 + \frac{1}{2} \varrho_2 \lambda_2 \beta_2 \xi_2^2 - \frac{1}{2} \varrho_2 \lambda_2 \beta_2 (\xi_2 - \hat{\xi}_2)^2 \\
& -k_c e_c^2 - k_5 \bar{e}_5^2 + \frac{1}{2} \sigma_3 \eta_3^T \Gamma_3 \eta_3 + \frac{1}{2} \varrho_3 \lambda_3 \beta_3 \xi_3^2 - \frac{1}{2} \varrho_3 \lambda_3 \beta_3 (\xi_3 - \hat{\xi}_3)^2 \\
& -\frac{1}{2} \sigma_1 (\eta_1 - \hat{\eta}_1)^T \Gamma_1 (\eta_1 - \hat{\eta}_1) - \frac{1}{2} \sigma_2 (\eta_2 - \hat{\eta}_2)^T \Gamma_2 (\eta_2 - \hat{\eta}_2) - \frac{1}{2} \sigma_3 (\eta_3 - \hat{\eta}_3)^T \Gamma_3 (\eta_3 - \hat{\eta}_3) \\
& + \bar{e}_2 \left( \bar{e}_1 + \hat{\eta}_1^T S_1 + \bar{u}_1 - \ddot{\phi}_d - \dot{\alpha}_2 + \frac{1}{2} \bar{e}_2 \right) + \frac{1}{2} \delta_1^2 \\
& + \bar{e}_4 \left( \bar{e}_3 + \hat{\eta}_2^T S_2 + \bar{u}_2 - \ddot{\theta}_d - \dot{\alpha}_4 + \frac{1}{2} \bar{e}_4 \right) + \frac{1}{2} \delta_2^2 \\
& + \bar{e}_6 \left( \bar{e}_5 + \hat{\eta}_3^T S_3 + \bar{u}_3 - \ddot{\psi}_d - \dot{\alpha}_6 + \frac{1}{2} \bar{e}_6 \right) + \frac{1}{2} \delta_3^2
\end{aligned} \tag{5.68}$$

Due to (5.51),  $\dot{V}_3$  in (5.68) can be simplified as

$$\begin{aligned}
& \dot{V}_3 \\
\leq & -k_a e_a^2 - k_1 \bar{e}_1^2 + \frac{1}{2} \sigma_1 \eta_1^T \Gamma_1 \eta_1 + \frac{1}{2} \varrho_1 \lambda_1 \xi_1^2 - \frac{1}{2} \varrho_1 \lambda_1 \beta_1 (\xi_1 - \hat{\xi}_1)^2 \\
& -k_b e_b^2 - k_3 \bar{e}_3^2 + \frac{1}{2} \sigma_2 \eta_2^T \Gamma_2 \eta_2 + \frac{1}{2} \varrho_2 \lambda_2 \xi_2^2 - \frac{1}{2} \varrho_2 \lambda_2 \beta_2 (\xi_2 - \hat{\xi}_2)^2 \\
& -k_c e_c^2 - k_5 \bar{e}_5^2 + \frac{1}{2} \sigma_3 \eta_3^T \Gamma_3 \eta_3 + \frac{1}{2} \varrho_3 \lambda_3 \xi_3^2 - \frac{1}{2} \varrho_3 \lambda_3 \beta_3 (\xi_3 - \hat{\xi}_3)^2 \\
& -\frac{1}{2} \sigma_1 (\eta_1 - \hat{\eta}_1)^T \Gamma_1 (\eta_1 - \hat{\eta}_1) - \frac{1}{2} \sigma_2 (\eta_2 - \hat{\eta}_2)^T \Gamma_2 (\eta_2 - \hat{\eta}_2) - \frac{1}{2} \sigma_3 (\eta_3 - \hat{\eta}_3)^T \Gamma_3 (\eta_3 - \hat{\eta}_3) \\
& + \bar{e}_2 \left( \bar{e}_1 + \hat{\eta}_1^T S_1 + \bar{u}_1 - \ddot{\phi}_d - \dot{\alpha}_2 + \frac{1}{2} \bar{e}_2 \right) + \frac{1}{2} \delta_1^2 \\
& + \bar{e}_4 \left( \bar{e}_3 + \hat{\eta}_2^T S_2 + \bar{u}_2 - \ddot{\theta}_d - \dot{\alpha}_4 + \frac{1}{2} \bar{e}_4 \right) + \frac{1}{2} \delta_2^2 \\
& + \bar{e}_6 \left( \bar{e}_5 + \hat{\eta}_3^T S_3 + \bar{u}_3 - \ddot{\psi}_d - \dot{\alpha}_6 + \frac{1}{2} \bar{e}_6 \right) + \frac{1}{2} \delta_3^2
\end{aligned} \tag{5.69}$$

To get the control law, set

$$\begin{aligned}
-k_2 \bar{e}_2 &= \bar{e}_1 + \hat{\eta}_1^T S_1 + \bar{u}_1 - \ddot{\phi}_d - \dot{\alpha}_2 + \frac{1}{2} \bar{e}_2 \\
-k_4 \bar{e}_4 &= \bar{e}_3 + \hat{\eta}_2^T S_2 + \bar{u}_2 - \ddot{\theta}_d - \dot{\alpha}_4 + \frac{1}{2} \bar{e}_4 \\
-k_6 \bar{e}_6 &= \bar{e}_5 + \hat{\eta}_3^T S_3 + \bar{u}_3 - \ddot{\psi}_d - \dot{\alpha}_6 + \frac{1}{2} \bar{e}_6
\end{aligned} \tag{5.70}$$

where  $\ddot{\phi}_d = \ddot{\theta}_d = \ddot{\psi}_d = 0$ , (5.70) can be rewritten as

$$\begin{aligned}\bar{u}_1 &= \dot{\alpha}_2 - \bar{e}_1 - \hat{\eta}_1^T S_1 - \left(\frac{1}{2} + k_2\right) \bar{e}_2 \\ \bar{u}_2 &= \dot{\alpha}_4 - \bar{e}_3 - \hat{\eta}_2^T S_2 - \left(\frac{1}{2} + k_4\right) \bar{e}_4 \\ \bar{u}_3 &= \dot{\alpha}_6 - \bar{e}_5 - \hat{\eta}_3^T S_3 - \left(\frac{1}{2} + k_6\right) \bar{e}_6\end{aligned}\quad (5.71)$$

Using (5.70), (5.69) can be simplified as

$$\begin{aligned}& \dot{V}_3 \\ \leq & -k_a e_a^2 - k_b e_b^2 - k_c e_c^2 - k_1 \bar{e}_1^2 - k_2 \bar{e}_2^2 - k_3 \bar{e}_3^2 - k_4 \bar{e}_4^2 - k_5 \bar{e}_5^2 - k_6 \bar{e}_6^2 \\ & - \frac{1}{2} \sigma_1 (\eta_1 - \hat{\eta}_1)^T \Gamma_1 (\eta_1 - \hat{\eta}_1) - \frac{1}{2} \sigma_2 (\eta_2 - \hat{\eta}_2)^T \Gamma_2 (\eta_2 - \hat{\eta}_2) - \frac{1}{2} \sigma_3 (\eta_3 - \hat{\eta}_3)^T \Gamma_3 (\eta_3 - \hat{\eta}_3) \\ & - \frac{1}{2} \lambda_1 \varrho_1 \beta_1 (\xi_1 - \hat{\xi}_1)^2 - \frac{1}{2} \lambda_2 \varrho_2 \beta_2 (\xi_2 - \hat{\xi}_2)^2 - \frac{1}{2} \lambda_3 \varrho_3 \beta_3 (\xi_3 - \hat{\xi}_3)^2 \\ & + \frac{1}{2} \sigma_1 \eta_1^T \Gamma_1 \eta_1 + \frac{1}{2} \sigma_2 \eta_2^T \Gamma_2 \eta_2 + \frac{1}{2} \sigma_3 \eta_3^T \Gamma_3 \eta_3 + \frac{1}{2} \delta_1^2 + \frac{1}{2} \delta_2^2 + \frac{1}{2} \delta_3^2 \\ & + \frac{1}{2} \lambda_1 \varrho_1 \xi_1 + \frac{1}{2} \lambda_2 \varrho_2 \xi_2 + \frac{1}{2} \lambda_3 \varrho_3 \xi_3 \\ \leq & -a V_3 + b\end{aligned}\quad (5.72)$$

where

$$\begin{aligned}a &= 2 \min\{k_a, k_b, k_c, k_1, k_2, k_3, k_4, k_5, k_6, \frac{1}{2} \sigma_1, \frac{1}{2} \sigma_2, \frac{1}{2} \sigma_3, \frac{1}{2} \varrho_1, \frac{1}{2} \varrho_2, \frac{1}{2} \varrho_3\} \\ b &= \frac{1}{2} \sigma_1 \eta_1^T \Gamma_1 \eta_1 + \frac{1}{2} \sigma_2 \eta_2^T \Gamma_2 \eta_2 + \frac{1}{2} \sigma_3 \eta_3^T \Gamma_3 \eta_3 \\ & + \frac{1}{2} \delta_1^2 + \frac{1}{2} \delta_2^2 + \frac{1}{2} \delta_3^2 + \frac{1}{2} \lambda_1 \varrho_1 \xi_1 + \frac{1}{2} \lambda_2 \varrho_2 \xi_2 + \frac{1}{2} \lambda_3 \varrho_3 \xi_3\end{aligned}\quad (5.73)$$

Multiplying (5.72) by  $e^{at}$  gives

$$e^{at} \frac{dV_3}{dt} + a V_3 e^{at} \leq b e^{at}\quad (5.74)$$

which is equivalent to

$$\frac{d(e^{at} V_3)}{dt} \leq b e^{at}\quad (5.75)$$

Integrating both sides of the inequality above produces

$$\int_0^t d(e^{at} V_3) \leq \int_0^t b e^{at} dt\quad (5.76)$$

that is,

$$e^{at} V_3(t) - V_3(0) \leq \frac{b}{a} e^{at} - \frac{b}{a}\quad (5.77)$$

which can be rewritten as

$$V_3(t) \leq \frac{b}{a} + e^{-at} \left[ V_3(0) - \frac{b}{a} \right] \quad (5.78)$$

As a result,  $V_3$  is bounded by  $V_3(0)$  [49]. Therefore, all the error terms in  $V_3$  are bounded.

Combining (5.30)-(5.32) and (5.52) with (5.71) yeilds:

$$\begin{aligned} u_1 &= -J_r \dot{\theta} \Omega + l \tau_\phi = \hat{\xi}_1 \bar{u}_1 = \hat{\xi}_1 \left[ \dot{\alpha}_2 - \bar{e}_1 - \left( \frac{1}{2} + k_2 \right) \bar{e}_2 - \hat{\eta}_1^T S_1 \right] \\ u_2 &= J_r \dot{\phi} \Omega + l \tau_\theta = \hat{\xi}_2 \bar{u}_2 = \hat{\xi}_2 \left[ \dot{\alpha}_4 - \bar{e}_3 - \left( \frac{1}{2} + k_4 \right) \bar{e}_4 - \hat{\eta}_2^T S_2 \right] \\ u_3 &= \tau_\psi = \hat{\xi}_3 \bar{u}_3 = \hat{\xi}_3 \left[ \dot{\alpha}_6 - \bar{e}_5 - \left( \frac{1}{2} + k_6 \right) \bar{e}_6 - \hat{\eta}_3^T S_3 \right] \end{aligned} \quad (5.79)$$

which means that the control law can be given as follows.

$$\begin{aligned} \tau_\phi &= \frac{1}{l} \left[ \hat{\xi}_1 \left( \dot{\alpha}_2 - \bar{e}_1 - \left( \frac{1}{2} + k_2 \right) \bar{e}_2 - \hat{\eta}_1^T S_1 \right) + J_r \dot{\theta} \Omega \right] \\ \tau_\theta &= \frac{1}{l} \left[ \hat{\xi}_2 \left( \dot{\alpha}_4 - \bar{e}_3 - \left( \frac{1}{2} + k_4 \right) \bar{e}_4 - \hat{\eta}_2^T S_2 \right) - J_r \dot{\phi} \Omega \right] \\ \tau_\psi &= \hat{\xi}_3 \left[ \dot{\alpha}_6 - \bar{e}_5 - \left( \frac{1}{2} + k_6 \right) \bar{e}_6 - \hat{\eta}_3^T S_3 \right] \end{aligned} \quad (5.80)$$

Using (3.8), the motor speeds  $\Omega_1, \Omega_2, \Omega_3$  and  $\Omega_4$  can be calculated by

$$\begin{aligned} b(\Omega_1^2 + \Omega_2^2 + \Omega_3^2 + \Omega_4^2) &= U_1 \\ bl(\Omega_2^2 - \Omega_4^2) - \frac{1}{l} J_r \dot{\theta} \Omega &= \frac{1}{l} \left[ \hat{\xi}_1 \left( \dot{\alpha}_2 - \bar{e}_1 - \left( \frac{1}{2} + k_2 \right) \bar{e}_2 - \hat{\eta}_1^T S_1 \right) \right] \\ bl(\Omega_1^2 - \Omega_3^2) + \frac{1}{l} J_r \dot{\phi} \Omega &= \frac{1}{l} \left[ \hat{\xi}_2 \left( \dot{\alpha}_4 - \bar{e}_3 - \left( \frac{1}{2} + k_4 \right) \bar{e}_4 - \hat{\eta}_2^T S_2 \right) \right] \\ k(\Omega_1^2 - \Omega_2^2 + \Omega_3^2 - \Omega_4^2) &= \hat{\xi}_3 \left[ \dot{\alpha}_6 - \bar{e}_5 - \left( \frac{1}{2} + k_6 \right) \bar{e}_6 - \hat{\eta}_3^T S_3 \right] \end{aligned} \quad (5.81)$$

where

$$\begin{aligned} \dot{\alpha}_2 &= -k_a e_2 - k_1(e_2 + k_a e_1) - e_1 \\ \dot{\alpha}_4 &= -k_b e_4 - k_3(e_4 + k_b e_3) - e_3 \\ \dot{\alpha}_6 &= -k_c e_6 - k_5(e_6 + k_c e_5) - e_5 \end{aligned} \quad (5.82)$$

and

$$\begin{aligned} \bar{e}_2 &= e_2 + (k_a + k_1)e_1 + (k_1 k_a + 1)e_a \\ \bar{e}_4 &= e_4 + (k_b + k_3)e_3 + (k_3 k_b + 1)e_b \\ \bar{e}_6 &= e_6 + (k_c + k_5)e_5 + (k_5 k_c + 1)e_c \end{aligned} \quad (5.83)$$

The block diagram of the adaptive fuzzy integral backstepping controller with Euler angle representation is shown in Fig. 5.11.

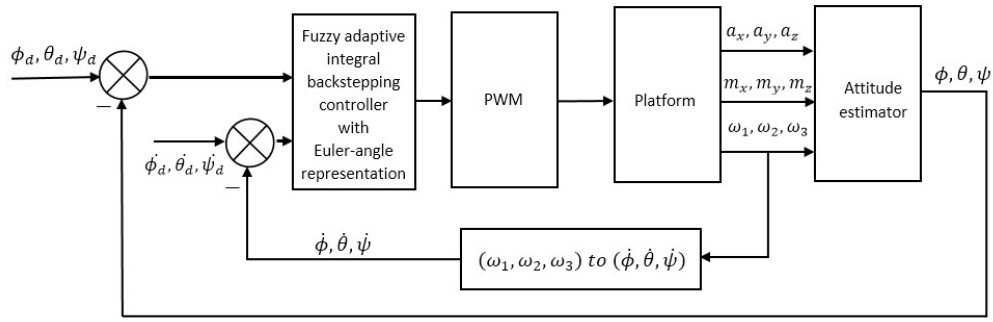
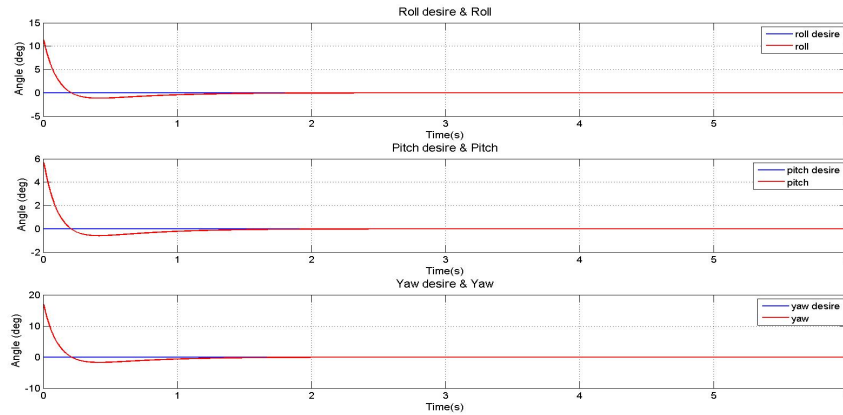


Figure 5.11: Adaptive Fuzzy Integral Backstepping Controller with Euler Angle Representation

### 5.2.2 Simulation Results

After tuning by trial and error method, the parameters of the proposed controller are set to  $k_a = k_b = k_c = 10$ ,  $k_1 = k_3 = k_5 = 2$ ,  $k_2 = k_4 = k_6 = 100$ ,  $\Gamma_1 = \Gamma_2 = \Gamma_3 = 50I_9$ ,  $\sigma_1 = \sigma_2 = \sigma_3 = 0.01$ ,  $\lambda_1 = \lambda_2 = \lambda_3 = 10$ , and  $\varrho_1 = \varrho_2 = \varrho_3 = 0.01$  for the simulation study, where  $I_9$  is the identity matrix. The inertial Euler angles are chosen randomly as 0.2, 0.1, and 0.3 rad. Simulation results are provided in Figs. 5.12 - 5.14. The stability is achieved and the performance of the proposed controller is satisfactory. As for tracking the angles  $\phi$ ,  $\theta$ , and  $\psi$ , comparing to a backstepping controller, the controller with integrator and fuzzy estimation terms share the similar tracking errors. To simulate if the proposed controller will track the desired angles properly, a sine wave desired angle has been added to the controller. As shown in Fig. 5.15, the response time is about 1.5s and the 3 angles can follow the desired angles satisfactorily.


 Figure 5.12:  $\phi$ ,  $\theta$ , and  $\psi$  with Fuzzy Adaptive Integral Backstepping Controller

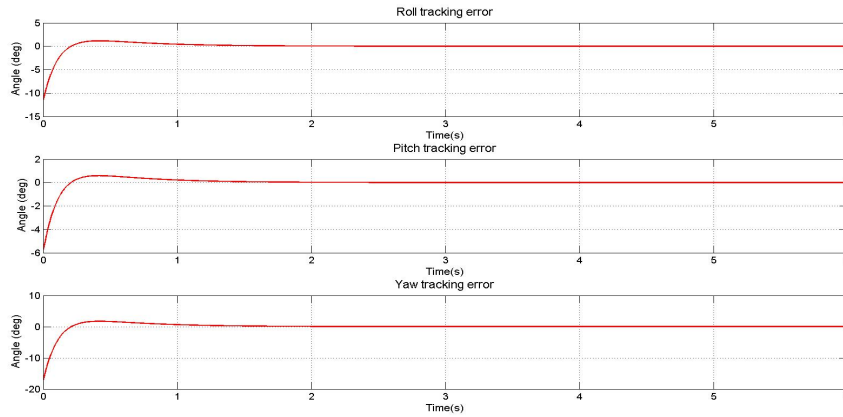


Figure 5.13: Tracking Errors with Fuzzy Adaptive Integral Backstepping Controller

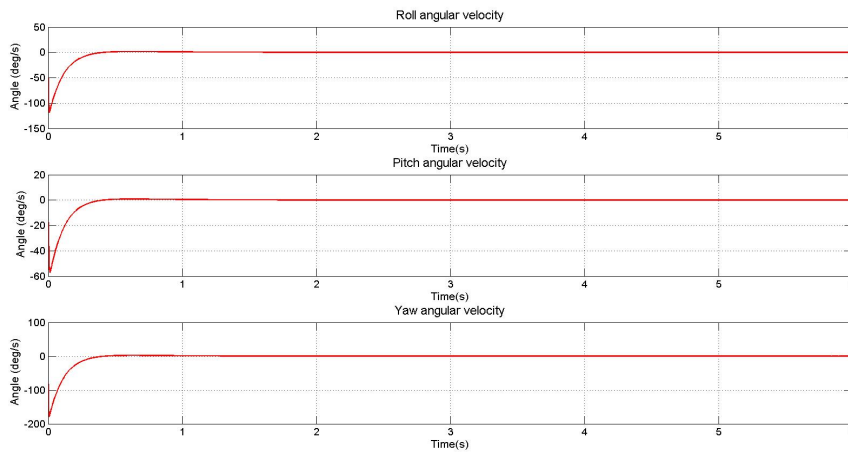


Figure 5.14: Angular Velocities with Fuzzy Adaptive Integral Backstepping Controller

## 5.3 Backstepping Design with Unit Quaternion Representation

### 5.3.1 Controller Design

In this section, a backstepping controller based on quaternion representation will be discussed because it is singularity-free. The basic mathematical procedure around backstepping is similar to the controller with Euler angle representation.

Let  $Q = [q_0 \ q^T]^T$  and  $Q_d = [q_{d0} \ q_d^T]^T$  be the actual and desired attitude in unit quaternion representation with  $q = [q_1 \ q_2 \ q_3]^T$  and  $q_d = [q_{d1} \ q_{d2} \ q_{d3}]^T$ .  $q_0$  and  $q_{d0}$  are constant components, which can be determined from (2.10), together with  $\|Q\| = 1$  and  $\|Q_d\| = 1$ . Let  $\omega = [\omega_1 \ \omega_2 \ \omega_3]^T$  and  $\omega_d = [\omega_{d1} \ \omega_{d2} \ \omega_{d3}]^T$  denote the angular velocities and

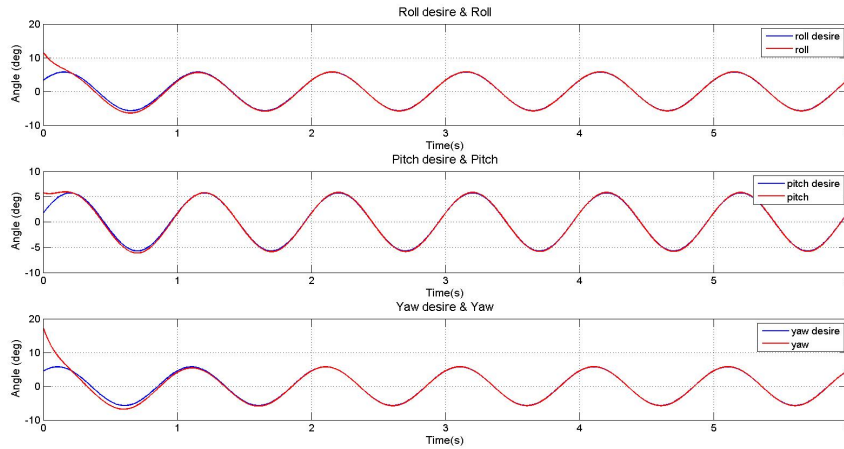


Figure 5.15: Tracking for  $\phi$ ,  $\theta$ , and  $\psi$  with Fuzzy Adaptive Integral Backstepping Controller

desired angular velocities corresponding to the actual and desired attitude. Let  $R$  and  $R_d$  stand for the rotation matrices associated with  $Q$  and  $Q_d$ .

The differential equations for  $Q$  and  $Q_d$  are given by

$$\begin{aligned}\dot{Q} &= \frac{1}{2}Q \odot Q_\omega \\ &= \frac{1}{2} \begin{bmatrix} -q^T \\ q_0 I_{3 \times 3} + S(q) \end{bmatrix} \omega\end{aligned}\quad (5.84)$$

$$\begin{aligned}\dot{Q}_d &= \frac{1}{2}Q_d \odot Q_{d\omega} \\ &= \frac{1}{2} \begin{bmatrix} -q_d^T \\ q_{d0} I_{3 \times 3} + S(q_d) \end{bmatrix} \omega_d\end{aligned}\quad (5.85)$$

The unit-quaternion tracking error  $Q_e = [q_{e0} \quad q_e^T]^T$ , which describes the discrepancy between the actual quaternion and desired quaternion, can be determined by

$$Q_e = Q_d^{-1} \odot Q \quad (5.86)$$

$$\begin{bmatrix} q_{e0} \\ q_e \end{bmatrix} = \begin{bmatrix} q_{d0}q_0 + q^T q_d \\ q_{d0}q - q_0q_d - q_d \times q \end{bmatrix} \quad (5.87)$$

It follows from (5.86)  $Q = Q_d \odot Q_e$ , which can be differentiated to obtain (5.88)

$$\dot{Q} = \dot{Q}_d \odot Q_e + Q_d \odot \dot{Q}_e \quad (5.88)$$

from which, according to [20], the following equation can be derived.

$$\dot{Q}_e = \frac{1}{2} Q_e \odot Q_{\tilde{\omega}}$$

where  $\tilde{\omega} = \omega - \bar{\omega}_d$  with  $\bar{\omega}_d = R^T(Q_e)\omega_d$ .

Following [26],  $\omega_d \approx 0$ ,  $\omega_e = \omega - \omega_d = \omega$ , the time derivative of  $Q_e$  with respect to time can be given by

$$\dot{Q}_e = \begin{bmatrix} \dot{q}_{e0} \\ \dot{q}_e \end{bmatrix} = \frac{1}{2} \begin{bmatrix} -q_e^T \omega \\ q_{e0} \omega + S(q_e) \omega \end{bmatrix} \quad (5.89)$$

With the property  $S(\omega)q_e = -S(q_e)\omega$ , one can rewrite (5.89) as:

$$\dot{Q}_e = \begin{bmatrix} \dot{q}_{e0} \\ \dot{q}_e \end{bmatrix} = \frac{1}{2} \begin{bmatrix} -q_e^T \omega \\ q_{e0} \omega - S(\omega)q_e \end{bmatrix} \quad (5.90)$$

Step 1

Define a positive definite Lyapunov function  $V_1$

$$V_1 = q_e^T q_e + (q_{e0} - 1)^2 \quad (5.91)$$

The derivative of  $V_1$  with respect with time is given by

$$\dot{V}_1 = 2q_e^T \dot{q}_e + 2(q_{e0} - 1)\dot{q}_{e0} \quad (5.92)$$

Substituting (5.90) into (5.92)

$$\begin{aligned} \dot{V}_1 &= q_e^T (q_{e0} \omega - S(\omega)q_e) - (q_{e0} - 1)q_e^T \omega \\ &= q_{e0} q_e^T \omega - q_e^T S(\omega)q_e - q_{e0} q_e^T \omega + q_e^T \omega \\ &= -q_e^T S(\omega)q_e + q_e^T \omega \end{aligned} \quad (5.93)$$

By using the property  $S(\omega)q_e = -S(q_e)\omega$ , (5.93) can be rewritten as

$$\begin{aligned} \dot{V}_1 &= -q_e^T S(\omega)q_e + q_e^T \omega \\ &= q_e^T S(q_e)\omega + q_e^T \omega \\ &= q_e^T \omega + q_e^T \omega^* - q_e^T \omega^* \\ &= q_e^T \omega^* + q_e^T (\omega - \omega^*) \\ &= q_e^T \omega^* + (\omega - \omega^*)^T q_e \end{aligned} \quad (5.94)$$

Note that  $\omega^*$  is the virtual control defined by

$$\omega^* = \begin{bmatrix} \omega_1^* \\ \omega_2^* \\ \omega_3^* \end{bmatrix} = -\gamma_1 q_e = \begin{bmatrix} -k_1 q_{e1} \\ -k_2 q_{e2} \\ -k_3 q_{e3} \end{bmatrix} \quad (5.95)$$

where  $\gamma_1 = \begin{bmatrix} k_1 & 0 & 0 \\ 0 & k_2 & 0 \\ 0 & 0 & k_3 \end{bmatrix} > 0$  with  $k_1, k_2$ , and  $k_3$  being positive control parameters. The derivative of virtual control with respect to time is given by

$$\dot{\omega}^* = \begin{bmatrix} \dot{\omega}_1^* \\ \dot{\omega}_2^* \\ \dot{\omega}_3^* \end{bmatrix} = -\gamma_1 \dot{q}_e = \begin{bmatrix} -k_1 \dot{q}_{e1} \\ -k_2 \dot{q}_{e2} \\ -k_3 \dot{q}_{e3} \end{bmatrix} \quad (5.96)$$

Then, (5.94) can be rewritten as :

$$\dot{V}_1 = -q_e^T \gamma_1 q_e + (\omega - \omega^*)^T q_e \quad (5.97)$$

Step 2

Define a positive definite function  $V_2$

$$V_2 = V_1 + \frac{1}{2}(\omega - \omega^*)^T (\omega - \omega^*) \quad (5.98)$$

The derivative of  $V_2$  with respect to time is derived as

$$\begin{aligned} \dot{V}_2 &= \dot{V}_1 + (\omega - \omega^*)^T (\dot{\omega} - \dot{\omega}^*) \\ &= -q_e^T \gamma_1 q_e + (\omega - \omega^*)^T q_e + (\omega - \omega^*)^T (\dot{\omega} - \dot{\omega}^*) \\ &= -q_e^T \gamma_1 q_e + (\omega - \omega^*)^T (q_e + \dot{\omega} - \dot{\omega}^*) \\ &= -q_e^T \gamma_1 q_e - (\omega - \omega^*)^T \gamma_2 (\omega - \omega^*) + (\omega - \omega^*)^T \gamma_2 (\omega - \omega^*) \\ &\quad + (\omega - \omega^*)^T (q_e + \dot{\omega} - \dot{\omega}^*) \\ &= -q_e^T \gamma_1 q_e - (\omega - \omega^*)^T \gamma_2 (\omega - \omega^*) \\ &\quad + (\omega - \omega^*)^T [\gamma_2 (\omega - \omega^*) + q_e + \dot{\omega} - \dot{\omega}^*] \end{aligned} \quad (5.99)$$

where  $\gamma_2 = \begin{bmatrix} k_4 & 0 & 0 \\ 0 & k_5 & 0 \\ 0 & 0 & k_6 \end{bmatrix} > 0$  with  $k_4, k_5$ , and  $k_6$  being positive gains. Setting the last term in (5.99) to zero gives (5.100),

$$\gamma_2 (\omega - \omega^*) + q_e + \dot{\omega} - \dot{\omega}^* = 0 \quad (5.100)$$

which makes

$$\dot{V}_2 = -q_e^T \gamma_1 q_e - (\omega - \omega^*)^T \gamma_2 (\omega - \omega^*) < 0 \quad (5.101)$$

Then, (5.100) can be rewritten as

$$\begin{aligned} \dot{\omega} &= -\gamma_2 (\omega - \omega^*) - q_e + \dot{\omega}^* \\ &= -\begin{bmatrix} k_4 & 0 & 0 \\ 0 & k_5 & 0 \\ 0 & 0 & k_6 \end{bmatrix} \begin{bmatrix} \omega_1 - \omega_1^* \\ \omega_2 - \omega_2^* \\ \omega_3 - \omega_3^* \end{bmatrix} - \begin{bmatrix} q_{e1} \\ q_{e2} \\ q_{e3} \end{bmatrix} + \begin{bmatrix} \dot{\omega}_1^* \\ \dot{\omega}_2^* \\ \dot{\omega}_3^* \end{bmatrix} \\ &= \begin{bmatrix} -k_4(\omega_1 - \omega_1^*) - q_{e1} + \dot{\omega}_1^* \\ -k_5(\omega_2 - \omega_2^*) - q_{e2} + \dot{\omega}_2^* \\ -k_6(\omega_3 - \omega_3^*) - q_{e3} + \dot{\omega}_3^* \end{bmatrix} \end{aligned} \quad (5.102)$$

Substituting (3.24) into (5.102) yeilds:

$$\begin{bmatrix} \frac{1}{I_\phi} [\tau_\phi + \omega_2 \omega_3 (I_\theta - I_\psi) - J_r \omega_2 \Omega] \\ \frac{1}{I_\theta} [\tau_\theta + \omega_1 \omega_3 (I_\psi - I_\phi) + J_r \omega_1 \Omega] \\ \frac{1}{I_\psi} [\tau_\psi + \omega_1 \omega_2 (I_\phi - I_\theta)] \end{bmatrix} = \begin{bmatrix} -k_4 (\omega_1 - \omega_1^*) - q_{e1} + \dot{\omega}_1^* \\ -k_5 (\omega_2 - \omega_2^*) - q_{e2} + \dot{\omega}_2^* \\ -k_6 (\omega_3 - \omega_3^*) - q_{e3} + \dot{\omega}_3^* \end{bmatrix} \quad (5.103)$$

from which the following control law can be derived.

$$\tau = \begin{bmatrix} \tau_\phi \\ \tau_\theta \\ \tau_\psi \end{bmatrix} = \begin{bmatrix} I_\phi [-k_4 (\omega_1 - \omega_1^*) - q_{e1} + \dot{\omega}_1^*] - \omega_2 \omega_3 (I_\theta - I_\psi) + J_r \omega_2 \Omega \\ I_\theta [-k_5 (\omega_2 - \omega_2^*) - q_{e2} + \dot{\omega}_2^*] - \omega_1 \omega_3 (I_\psi - I_\phi) - J_r \omega_1 \Omega \\ I_\psi [-k_6 (\omega_3 - \omega_3^*) - q_{e3} + \dot{\omega}_3^*] - \omega_1 \omega_2 (I_\phi - I_\theta) \end{bmatrix} \quad (5.104)$$

Considering the motor speeds in (3.8), (5.104) can be rewritten as

$$\begin{bmatrix} bl(\Omega_2^2 - \Omega_4^2) - J_r \omega_2 \Omega \\ bl(\Omega_1^2 - \Omega_3^2) + J_r \omega_1 \Omega \\ k(\Omega_1^2 - \Omega_2^2 + \Omega_3^2 - \Omega_4^2) \\ k(\Omega_1^2 + \Omega_2^2 + \Omega_3^2 + \Omega_4^2) \end{bmatrix} = \begin{bmatrix} I_\phi [-k_4 (\omega_1 - \omega_1^*) - q_{e1} + \dot{\omega}_1^*] - \omega_2 \omega_3 (I_\theta - I_\psi) \\ I_\theta [-k_5 (\omega_2 - \omega_2^*) - q_{e2} + \dot{\omega}_2^*] - \omega_1 \omega_3 (I_\psi - I_\phi) \\ I_\psi [-k_6 (\omega_3 - \omega_3^*) - q_{e3} + \dot{\omega}_3^*] - \omega_1 \omega_2 (I_\phi - I_\theta) \\ U_1 \end{bmatrix} \quad (5.105)$$

where  $\Omega = \Omega_1 - \Omega_2 - \Omega_3 + \Omega_4$ . The motor speeds  $\Omega_1, \Omega_2, \Omega_3, \Omega_4$  can be determined from (5.105). By tuning the gains  $k_1, \dots, k_6$  with trial and error method, the quadrotor can be stabilized around the desired attitude. The block diagram of the backstepping controller with unit quaternion representation is shown in Fig. 5.16.

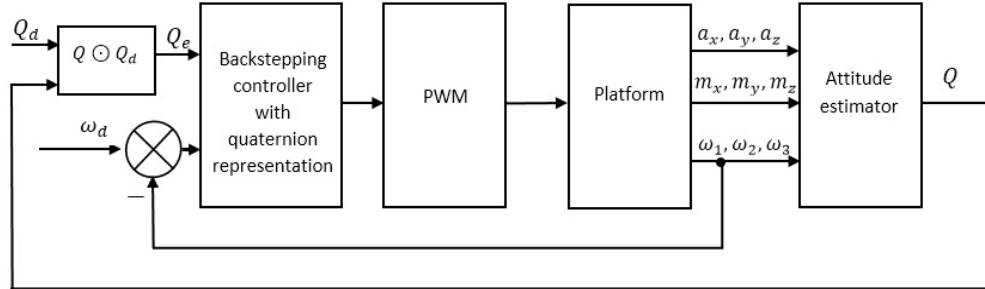


Figure 5.16: Backsteppig Controller with Unit Quaternion Representation

### 5.3.2 Experimental Results

According to the control algorithm, which is designed in this section, the corresponding code was downloaded to the APM 2.6. The altitude is manipulated by the remote controller and the attitude is controlled by the proposed controller with the gain  $k_1 = 1700, k_2 = 170, k_3 = 6, k_4 = 7, k_5 = 8, k_6 = 650$ . Some tests were conducted and test data were recorded by Arduino via the 3DR telemetry radio.

Performance of the controllers for the roll, pitch, and yaw angles were tested separately before testing the whole system. The experimental results are shown in Fig. 5.17. To test

the ability of disturbance attenuation, several sudden changes in roll, pitch, and yaw angles were created by exerting some external forces to the roll, pitch, and yaw directions. The corresponding test results for the roll, pitch, and yaw controllers can be observed from the sections of 0-650, 0-500, and 500-950 seconds in the graphs shown in Fig. 5.17. For step responses, the remote control was used to create the changes of the setpoints for the roll, pitch, and yaw angles, which can be seen from the parts of 650-1400, 950-1200, and 0-600 seconds of the response curves shown in Fig. 5.17.

The test results on attitude control, while the quadrotor flying, are shown in Fig. 5.18 - 5.19. It can be seen that the variations in  $\phi$ ,  $\theta$ , and  $\psi$  fall within 10, 11 and 19 degrees, which are presented in Fig. 5.18. Also, angular velocities are controlled within an acceptable range.

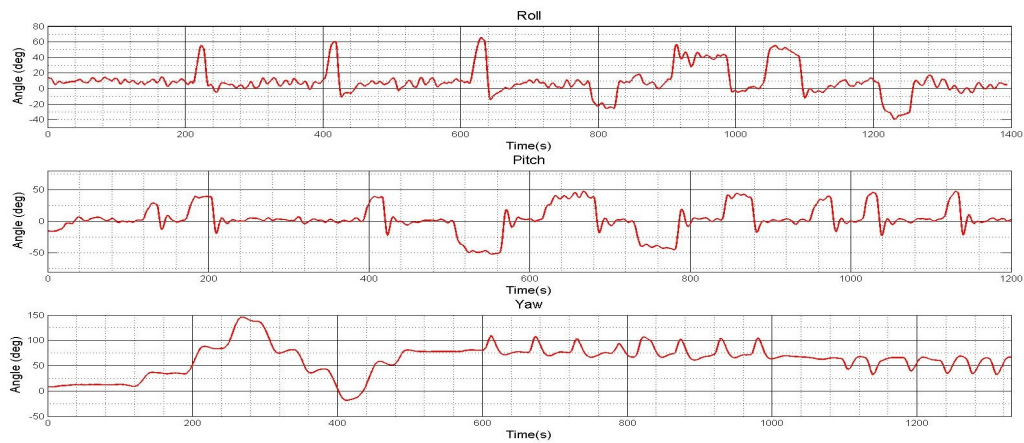


Figure 5.17: Separate Tests with Backstepping Controller-Quaternion Representation

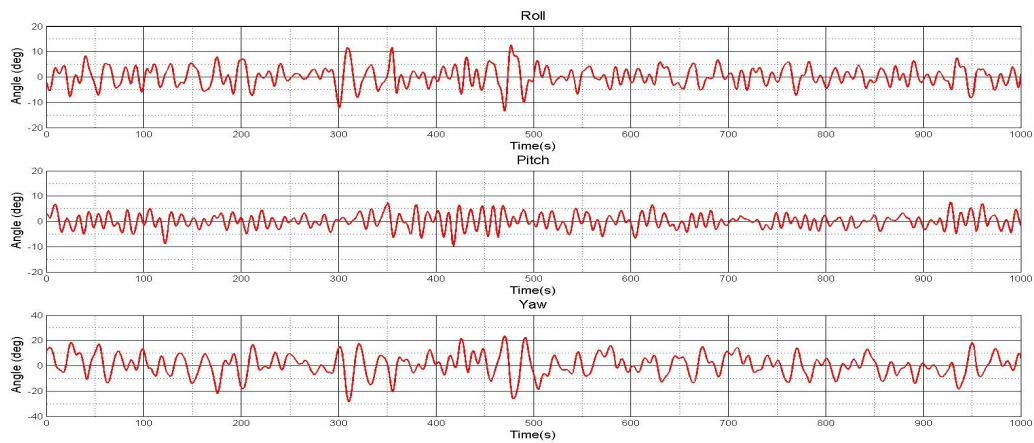


Figure 5.18:  $\phi$ ,  $\theta$ , and  $\psi$  with Backstepping Controller-Quaternion Representation

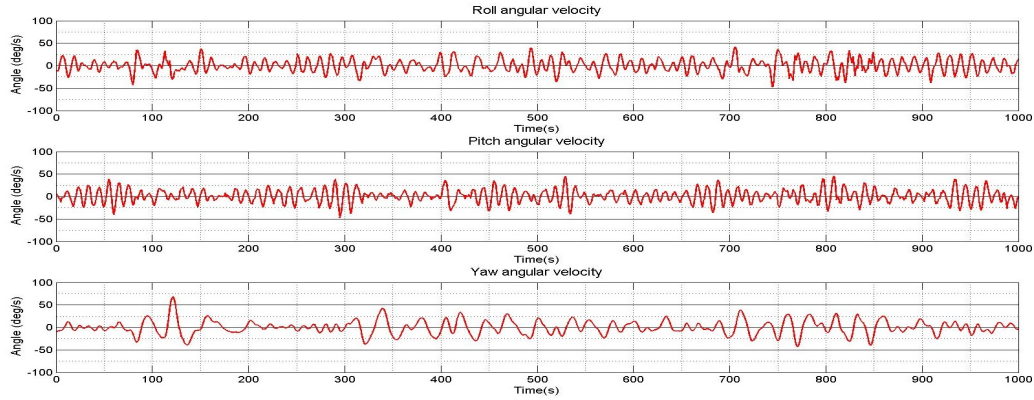


Figure 5.19: Angular Velocities with Backstepping Controller-Quaternion Representation

## 5.4 Adaptive Fuzzy Backstepping Design with Quaternion Representation

### 5.4.1 Controller Design

In this section, based on the unit quaternion representation, an adaptive backstepping controller with fuzzy logic is proposed. The basic mathematical procedure is similar to the controller design with Euler angle representation given in Section 5.2.

Similar to Section 5.2, assume that the parameters  $I_\phi$ ,  $I_\theta$ , and  $I_\psi$  are unknown and the nonlinear terms  $\left(\frac{I_\theta - I_\psi}{I_\phi}\right)\omega_2\omega_3$ ,  $\left(\frac{I_\psi - I_\phi}{I_\theta}\right)\omega_1\omega_3$ , and  $\left(\frac{I_\phi - I_\theta}{I_\psi}\right)\omega_1\omega_2$  are unknown as well.

The unknown nonlinear terms can be estimated by the following fuzzy logic systems.

$$\left(\frac{I_\theta - I_\psi}{I_\phi}\right)\omega_2\omega_3 = \eta_1^T S_1(\omega_2, \omega_3) + \delta_1 \quad (5.106)$$

$$\left(\frac{I_\psi - I_\phi}{I_\theta}\right)\omega_1\omega_3 = \eta_2^T S_2(\omega_1, \omega_3) + \delta_2 \quad (5.107)$$

$$\left(\frac{I_\phi - I_\theta}{I_\psi}\right)\omega_1\omega_2 = \eta_3^T S_3(\omega_1, \omega_2) + \delta_3 \quad (5.108)$$

where  $\delta_1$ ,  $\delta_2$ ,  $\delta_3$  are the approximation errors, which are bounded by a positive constant  $\delta_{\max}$  [16], that is,  $\delta_i \leq \delta_{\max}$ ,  $i = 1, 2, 3$ .

In this thesis,

$$\begin{aligned} S_1 &= [S_{11}, S_{12}, S_{13}, S_{14}, S_{15}, S_{16}, S_{17}, S_{18}, S_{19}]^T \\ S_2 &= [S_{21}, S_{22}, S_{23}, S_{24}, S_{25}, S_{26}, S_{27}, S_{28}, S_{29}]^T \\ S_3 &= [S_{31}, S_{32}, S_{33}, S_{34}, S_{35}, S_{36}, S_{37}, S_{38}, S_{39}]^T \end{aligned} \quad (5.109)$$

where

$$\begin{aligned}
S_{11} &= \frac{\mu_N(\omega_2)\mu_N(\omega_3)}{D_1}, S_{21} = \frac{\mu_N(\omega_1)\mu_N(\omega_3)}{D_2}, S_{31} = \frac{\mu_N(\omega_1)\mu_N(\omega_2)}{D_3} \\
S_{12} &= \frac{\mu_N(\omega_2)\mu_Z(\omega_3)}{D_1}, S_{22} = \frac{\mu_N(\omega_1)\mu_Z(\omega_3)}{D_2}, S_{32} = \frac{\mu_N(\omega_1)\mu_Z(\omega_2)}{D_3} \\
S_{13} &= \frac{\mu_N(\omega_2)\mu_P(\omega_3)}{D_1}, S_{23} = \frac{\mu_N(\omega_1)\mu_P(\omega_3)}{D_2}, S_{33} = \frac{\mu_N(\omega_1)\mu_P(\omega_2)}{D_3} \\
S_{14} &= \frac{\mu_Z(\omega_2)\mu_N(\omega_3)}{D_1}, S_{24} = \frac{\mu_Z(\omega_1)\mu_N(\omega_3)}{D_2}, S_{34} = \frac{\mu_Z(\omega_1)\mu_N(\omega_2)}{D_3} \\
S_{15} &= \frac{\mu_Z(\omega_2)\mu_Z(\omega_3)}{D_1}, S_{25} = \frac{\mu_Z(\omega_1)\mu_Z(\omega_3)}{D_2}, S_{35} = \frac{\mu_Z(\omega_1)\mu_Z(\omega_2)}{D_3} \\
S_{16} &= \frac{\mu_Z(\omega_2)\mu_P(\omega_3)}{D_1}, S_{26} = \frac{\mu_Z(\omega_1)\mu_P(\omega_3)}{D_2}, S_{36} = \frac{\mu_Z(\omega_1)\mu_P(\omega_2)}{D_3} \\
S_{17} &= \frac{\mu_P(\omega_2)\mu_N(\omega_3)}{D_1}, S_{27} = \frac{\mu_P(\omega_1)\mu_N(\omega_3)}{D_2}, S_{37} = \frac{\mu_P(\omega_1)\mu_N(\omega_2)}{D_3} \\
S_{18} &= \frac{\mu_P(\omega_2)\mu_Z(\omega_3)}{D_1}, S_{28} = \frac{\mu_P(\omega_1)\mu_Z(\omega_3)}{D_2}, S_{38} = \frac{\mu_P(\omega_1)\mu_Z(\omega_2)}{D_3} \\
S_{19} &= \frac{\mu_P(\omega_2)\mu_P(\omega_3)}{D_1}, S_{29} = \frac{\mu_P(\omega_1)\mu_P(\omega_3)}{D_2}, S_{39} = \frac{\mu_P(\omega_1)\mu_P(\omega_2)}{D_3} \quad (5.110)
\end{aligned}$$

with

$$\begin{aligned}
D_1 &= \mu_N(\omega_2)\mu_N(\omega_3) + \mu_N(\omega_2)\mu_Z(\omega_3) + \mu_N(\omega_2)\mu_P(\omega_3) + \mu_Z(\omega_2)\mu_N(\omega_3) + \mu_Z(\omega_2)\mu_Z(\omega_3) \\
&\quad + \mu_Z(\omega_2)\mu_P(\omega_3) + \mu_P(\omega_2)\mu_N(\omega_3) + \mu_P(\omega_2)\mu_Z(\omega_3) + \mu_P(\omega_2)\mu_P(\omega_3) \\
D_2 &= \mu_N(\omega_1)\mu_N(\omega_3) + \mu_N(\omega_1)\mu_Z(\omega_3) + \mu_N(\omega_1)\mu_P(\omega_3) + \mu_Z(\omega_1)\mu_N(\omega_3) + \mu_Z(\omega_1)\mu_Z(\omega_3) \\
&\quad + \mu_Z(\omega_1)\mu_P(\omega_3) + \mu_P(\omega_1)\mu_N(\omega_3) + \mu_P(\omega_1)\mu_Z(\omega_3) + \mu_P(\omega_1)\mu_P(\omega_3) \\
D_3 &= \mu_N(\omega_1)\mu_N(\omega_2) + \mu_N(\omega_1)\mu_Z(\omega_2) + \mu_N(\omega_1)\mu_P(\omega_2) + \mu_Z(\omega_1)\mu_N(\omega_2) + \mu_Z(\omega_1)\mu_Z(\omega_2) \\
&\quad + \mu_Z(\omega_1)\mu_P(\omega_2) + \mu_P(\omega_1)\mu_N(\omega_2) + \mu_P(\omega_1)\mu_Z(\omega_2) + \mu_P(\omega_1)\mu_P(\omega_2) \quad (5.111)
\end{aligned}$$

The fuzzy sets N, Z, P are defined for  $\omega_1, \omega_2, \omega_3$  as shown in Figs. 5.20 - 5.22.

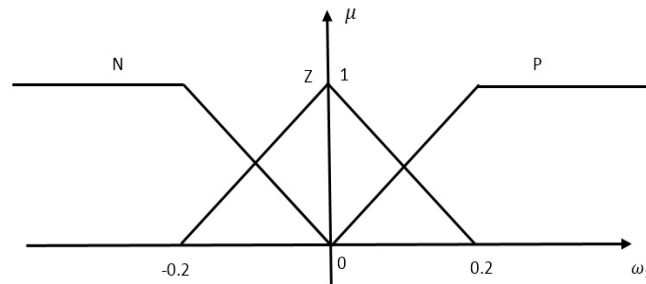
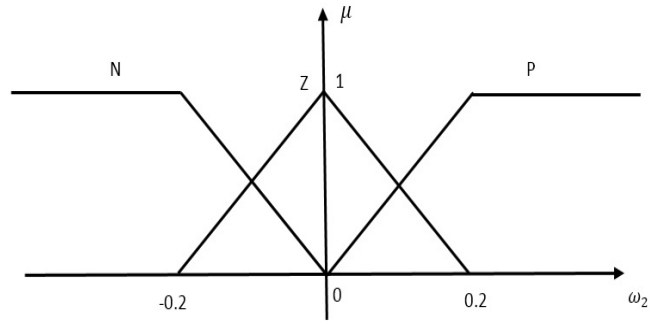
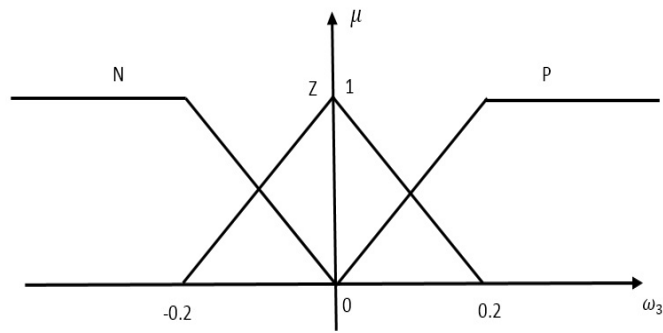


Figure 5.20: The Fuzzy Sets for  $\omega_1$

Figure 5.21: The Fuzzy Sets for  $\omega_2$ Figure 5.22: The Fuzzy Sets for  $\omega_3$ 

The fuzzy rule base for (5.106) is given below.

- $R^{11}$  : **IF**  $\omega_2 \in \mathbf{N}, \omega_3 \in \mathbf{N}$ , **THEN**  $\mathbf{y} \in \mathbf{B}^{11}$
- $R^{12}$  : **IF**  $\omega_2 \in \mathbf{N}, \omega_3 \in \mathbf{Z}$ , **THEN**  $\mathbf{y} \in \mathbf{B}^{12}$
- $R^{13}$  : **IF**  $\omega_2 \in \mathbf{N}, \omega_3 \in \mathbf{P}$ , **THEN**  $\mathbf{y} \in \mathbf{B}^{13}$
- $R^{14}$  : **IF**  $\omega_2 \in \mathbf{Z}, \omega_3 \in \mathbf{N}$ , **THEN**  $\mathbf{y} \in \mathbf{B}^{14}$
- $R^{15}$  : **IF**  $\omega_2 \in \mathbf{Z}, \omega_3 \in \mathbf{Z}$ , **THEN**  $\mathbf{y} \in \mathbf{B}^{15}$
- $R^{16}$  : **IF**  $\omega_2 \in \mathbf{Z}, \omega_3 \in \mathbf{P}$ , **THEN**  $\mathbf{y} \in \mathbf{B}^{16}$
- $R^{17}$  : **IF**  $\omega_2 \in \mathbf{P}, \omega_3 \in \mathbf{N}$ , **THEN**  $\mathbf{y} \in \mathbf{B}^{17}$
- $R^{18}$  : **IF**  $\omega_2 \in \mathbf{P}, \omega_3 \in \mathbf{Z}$ , **THEN**  $\mathbf{y} \in \mathbf{B}^{18}$
- $R^{19}$  : **IF**  $\omega_2 \in \mathbf{P}, \omega_3 \in \mathbf{P}$ , **THEN**  $\mathbf{y} \in \mathbf{B}^{19}$

The fuzzy rule base for (5.107) is given below.

$$\begin{aligned}
R^{21} &: \text{IF } \omega_1 \in \mathbf{N}, \omega_3 \in \mathbf{N}, \text{ THEN } \mathbf{y} \in \mathbf{B}^{21} \\
R^{22} &: \text{IF } \omega_1 \in \mathbf{N}, \omega_3 \in \mathbf{Z}, \text{ THEN } \mathbf{y} \in \mathbf{B}^{22} \\
R^{23} &: \text{IF } \omega_1 \in \mathbf{N}, \omega_3 \in \mathbf{P}, \text{ THEN } \mathbf{y} \in \mathbf{B}^{23} \\
R^{24} &: \text{IF } \omega_1 \in \mathbf{Z}, \omega_3 \in \mathbf{N}, \text{ THEN } \mathbf{y} \in \mathbf{B}^{24} \\
R^{25} &: \text{IF } \omega_1 \in \mathbf{Z}, \omega_3 \in \mathbf{Z}, \text{ THEN } \mathbf{y} \in \mathbf{B}^{25} \\
R^{26} &: \text{IF } \omega_1 \in \mathbf{Z}, \omega_3 \in \mathbf{P}, \text{ THEN } \mathbf{y} \in \mathbf{B}^{26} \\
R^{27} &: \text{IF } \omega_1 \in \mathbf{P}, \omega_3 \in \mathbf{N}, \text{ THEN } \mathbf{y} \in \mathbf{B}^{27} \\
R^{28} &: \text{IF } \omega_1 \in \mathbf{P}, \omega_3 \in \mathbf{Z}, \text{ THEN } \mathbf{y} \in \mathbf{B}^{28} \\
R^{29} &: \text{IF } \omega_1 \in \mathbf{P}, \omega_3 \in \mathbf{P}, \text{ THEN } \mathbf{y} \in \mathbf{B}^{29}
\end{aligned}$$

The fuzzy rule base for (5.108) is given below.

$$\begin{aligned}
R^{31} &: \text{IF } \omega_1 \in \mathbf{N}, \omega_2 \in \mathbf{N}, \text{ THEN } \mathbf{y} \in \mathbf{B}^{31} \\
R^{32} &: \text{IF } \omega_1 \in \mathbf{N}, \omega_2 \in \mathbf{Z}, \text{ THEN } \mathbf{y} \in \mathbf{B}^{32} \\
R^{33} &: \text{IF } \omega_1 \in \mathbf{N}, \omega_2 \in \mathbf{P}, \text{ THEN } \mathbf{y} \in \mathbf{B}^{33} \\
R^{34} &: \text{IF } \omega_1 \in \mathbf{Z}, \omega_2 \in \mathbf{N}, \text{ THEN } \mathbf{y} \in \mathbf{B}^{34} \\
R^{35} &: \text{IF } \omega_1 \in \mathbf{Z}, \omega_2 \in \mathbf{Z}, \text{ THEN } \mathbf{y} \in \mathbf{B}^{35} \\
R^{36} &: \text{IF } \omega_1 \in \mathbf{Z}, \omega_2 \in \mathbf{P}, \text{ THEN } \mathbf{y} \in \mathbf{B}^{36} \\
R^{37} &: \text{IF } \omega_1 \in \mathbf{P}, \omega_2 \in \mathbf{N}, \text{ THEN } \mathbf{y} \in \mathbf{B}^{37} \\
R^{38} &: \text{IF } \omega_1 \in \mathbf{P}, \omega_2 \in \mathbf{Z}, \text{ THEN } \mathbf{y} \in \mathbf{B}^{38} \\
R^{39} &: \text{IF } \omega_1 \in \mathbf{P}, \omega_2 \in \mathbf{P}, \text{ THEN } \mathbf{y} \in \mathbf{B}^{39}
\end{aligned}$$

$\eta_1, \eta_2, \eta_3$  in (5.106)-(5.108) are defined as follows

$$\begin{aligned}
\eta_1 &= [\eta_{11}, \eta_{12}, \eta_{13}, \eta_{14}, \eta_{15}, \eta_{16}, \eta_{17}, \eta_{18}, \eta_{19}]^T \\
\eta_2 &= [\eta_{21}, \eta_{22}, \eta_{23}, \eta_{24}, \eta_{25}, \eta_{26}, \eta_{27}, \eta_{28}, \eta_{29}]^T \\
\eta_3 &= [\eta_{31}, \eta_{32}, \eta_{33}, \eta_{34}, \eta_{35}, \eta_{36}, \eta_{37}, \eta_{38}, \eta_{39}]^T
\end{aligned} \tag{5.112}$$

where  $\eta_{ij}$  is the center of the fuzzy set  $\mathbf{B}^{ij}$  and will be estimated, as an adaptive parameter, by an adaptive law later,  $i = 1, 2, 3$  and  $j = 1, 2, \dots, 9$ .

The unknown parameters  $I_\phi$ ,  $I_\theta$ , and  $I_\psi$  are estimated through parameters

$$\beta_1 = \frac{1}{I_\phi} \tag{5.113}$$

$$\beta_2 = \frac{1}{I_\theta} \tag{5.114}$$

$$\beta_3 = \frac{1}{I_\psi} \tag{5.115}$$

For simplicity in derivations, define

$$u_1 = -J_r \omega_2 \Omega + \tau_\phi \quad (5.116)$$

$$u_2 = J_r \omega_1 \Omega + \tau_\theta \quad (5.117)$$

$$u_3 = \tau_\psi \quad (5.118)$$

Then, with (5.106)-(5.118), (3.24) can be rewritten as

$$\begin{aligned} \dot{\omega}_1 &= \left( \frac{I_\theta - I_\psi}{I_\phi} \right) \omega_2 \omega_3 - \frac{J_r}{I_\phi} \omega_2 \Omega + \frac{1}{I_\phi} \tau_\phi \\ &= \eta_1^T S_1 + \delta_1 + \beta_1 u_1 \end{aligned} \quad (5.119)$$

$$\begin{aligned} \dot{\omega}_2 &= \left( \frac{I_\psi - I_\phi}{I_\theta} \right) \omega_1 \omega_3 + \frac{J_r}{I_\theta} \omega_1 \Omega + \frac{1}{I_\theta} \tau_\theta \\ &= \eta_2^T S_2 + \delta_2 + \beta_2 u_2 \end{aligned} \quad (5.120)$$

$$\begin{aligned} \dot{\omega}_3 &= \left( \frac{I_\phi - I_\theta}{I_\psi} \right) \omega_1 \omega_2 + \frac{1}{I_\psi} \tau_\psi \\ &= \eta_3^T S_3 + \delta_3 + \beta_3 u_3 \end{aligned} \quad (5.121)$$

The block diagram of the adaptive fuzzy logic estimator with unit quaternion representation is shown in Fig. 5.23-5.25.

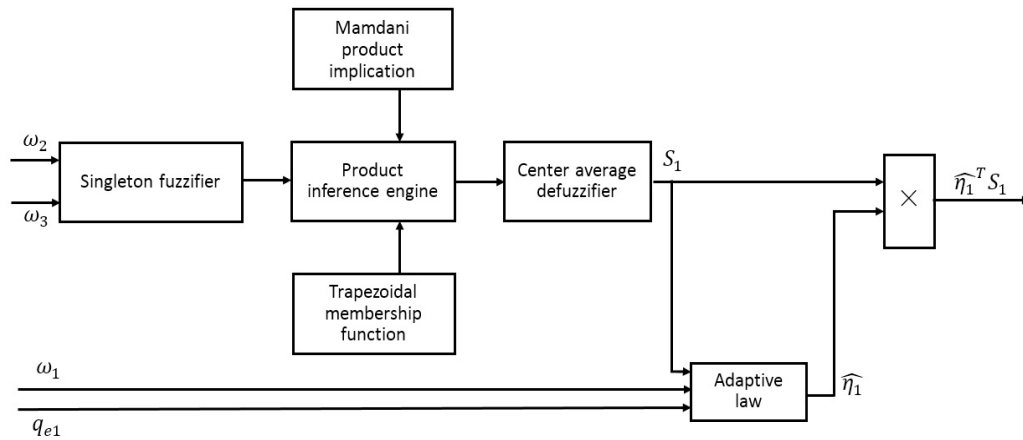
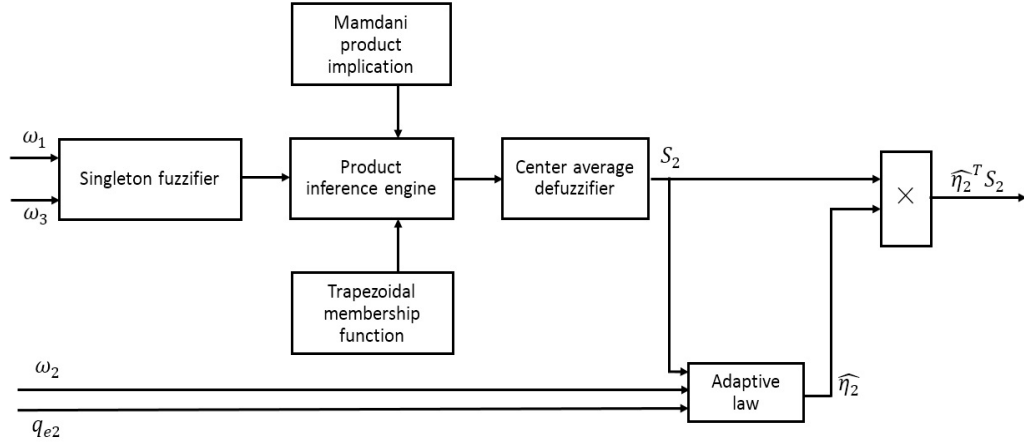
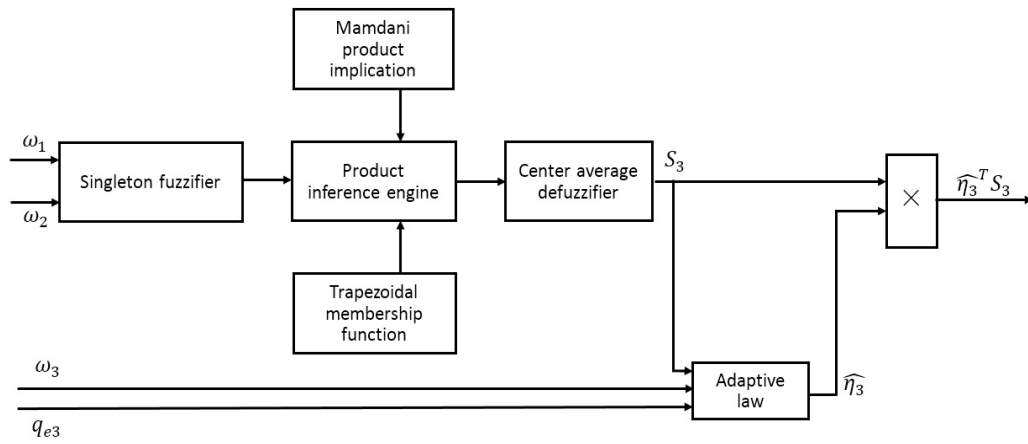


Figure 5.23: The Fuzzy Logic Estimator for  $\left( \frac{I_\theta - I_\psi}{I_\phi} \right) \omega_2 \omega_3$

Step 1

This step is the same as Step 1 in Section 5.3.

Step 2

Figure 5.24: The Fuzzy Logic Estimator for  $\left(\frac{I_\psi - I_\phi}{I_\theta}\right) \omega_1 \omega_3$ Figure 5.25: The Fuzzy Logic Estimator for  $\left(\frac{I_\phi - I_\theta}{I_\psi}\right) \omega_1 \omega_2$ 

Starting from (5.91) to (5.97), define a positive definite Lyapunov function  $V_2$  with the estimation errors added

$$\begin{aligned}
 V_2 = & V_1 + \frac{1}{2}(\omega - \omega^*)^T(\omega - \omega^*) \\
 & + \frac{1}{2} \sum_{i=1}^3 (\eta_i - \hat{\eta}_i)^T \Gamma_i (\eta_i - \hat{\eta}_i) + \frac{1}{2} \sum_{i=1}^3 \lambda_i \beta_i (\xi_i - \hat{\xi}_i)^2
 \end{aligned} \tag{5.122}$$

where  $\hat{\eta}_i$  are the estimations of the parameters  $\eta_1, \eta_2$ , and  $\eta_3$ ,  $\hat{\xi}_1, \hat{\xi}_2$ , and  $\hat{\xi}_3$  are the estimations of the parameters  $\xi_1 = I_\phi, \xi_2 = I_\theta$ , and  $\xi_3 = I_\psi$ , respectively,  $\Gamma_i$ , and  $\lambda_i, i = 1, 2, 3$ , are positive constants. It follows from (5.113)-(5.115) that

$$\beta_i = \frac{1}{\xi_i}, i = 1, 2, 3 \tag{5.123}$$

Motivated by [48], define

$$\begin{aligned}\bar{u}_1 &= \frac{u_1}{\hat{\xi}_1} \\ \bar{u}_2 &= \frac{u_2}{\hat{\xi}_2} \\ \bar{u}_3 &= \frac{u_3}{\hat{\xi}_3}\end{aligned}\quad (5.124)$$

Then, it can be verified that the following are true.

$$\begin{aligned}\beta_1 u_1 &= \bar{u}_1 - \beta_1(\xi_1 - \hat{\xi}_1)\bar{u}_1 \\ \beta_2 u_2 &= \bar{u}_2 - \beta_2(\xi_2 - \hat{\xi}_2)\bar{u}_2 \\ \beta_3 u_3 &= \bar{u}_3 - \beta_3(\xi_3 - \hat{\xi}_3)\bar{u}_3\end{aligned}\quad (5.125)$$

For instance,  $\beta_1 u_1 = \frac{1}{\hat{\xi}_1} \hat{\xi}_1 \bar{u}_1 = \frac{1}{\hat{\xi}_1} (\hat{\xi}_1 - \xi_1 + \xi_1) \bar{u}_1 = \bar{u}_1 - \frac{1}{\hat{\xi}_1} (\xi_1 - \hat{\xi}_1) \bar{u}_1 = \bar{u}_1 - \beta_1(\xi_1 - \hat{\xi}_1)\bar{u}_1$ .

Substituting (5.125) into (5.119)-(5.121) produces

$$\begin{aligned}\dot{\omega}_1 &= \eta_1^T S_1 + \delta_1 + \beta_1 u_1 \\ &= \eta_1^T S_1 + \delta_1 + \bar{u}_1 - \beta_1(\xi_1 - \hat{\xi}_1)\bar{u}_1\end{aligned}\quad (5.126)$$

$$\begin{aligned}\dot{\omega}_2 &= \eta_2^T S_2 + \delta_2 + \beta_2 u_2 \\ &= \eta_2^T S_2 + \delta_2 + \bar{u}_2 - \beta_2(\xi_2 - \hat{\xi}_2)\bar{u}_2\end{aligned}\quad (5.127)$$

$$\begin{aligned}\dot{\omega}_3 &= \eta_3^T S_3 + \delta_3 + \beta_3 u_3 \\ &= \eta_3^T S_3 + \delta_3 + \bar{u}_3 - \beta_3(\xi_3 - \hat{\xi}_3)\bar{u}_3\end{aligned}\quad (5.128)$$

Substituting (5.97) and (5.126)-(5.128) into (5.122), it can be shown that the derivative of  $V_2$  with respect to time is given by

$$\begin{aligned}\dot{V}_2 &= \dot{V}_1 + (\omega - \omega^*)^T (\dot{\omega} - \dot{\omega}^*) \\ &\quad + \sum_{i=1}^3 (\eta_i - \hat{\eta}_i)^T \Gamma_i (-\dot{\hat{\eta}}_i) + \sum_{i=1}^3 \lambda_i \beta_i (\xi_i - \hat{\xi}_i) (-\dot{\hat{\xi}}_i) \\ &= -q_e^T \gamma_1 q_e + (\omega - \omega^*)^T (q_e + \dot{\omega} - \dot{\omega}^*) \\ &\quad + (\eta_1 - \hat{\eta}_1)^T \Gamma_1 (-\dot{\hat{\eta}}_1) + (\eta_2 - \hat{\eta}_2)^T \Gamma_2 (-\dot{\hat{\eta}}_2) + (\eta_3 - \hat{\eta}_3)^T \Gamma_3 (-\dot{\hat{\eta}}_3) \\ &\quad + \lambda_1 \beta_1 (\xi_1 - \hat{\xi}_1) (-\dot{\hat{\xi}}_1) + \lambda_2 \beta_2 (\xi_2 - \hat{\xi}_2) (-\dot{\hat{\xi}}_2) + \lambda_3 \beta_3 (\xi_3 - \hat{\xi}_3) (-\dot{\hat{\xi}}_3) \\ &= -k_1 q_{e1}^2 - k_2 q_{e2}^2 - k_3 q_{e3}^2 \\ &\quad + (\omega_1 - \omega_1^*) (q_{e1} + \eta_1^T S_1 + \delta_1 + \bar{u}_1 - \beta_1(\xi_1 - \hat{\xi}_1)\bar{u}_1 - \dot{\omega}_1^*) \\ &\quad + (\omega_2 - \omega_2^*) (q_{e2} + \eta_2^T S_2 + \delta_2 + \bar{u}_2 - \beta_2(\xi_2 - \hat{\xi}_2)\bar{u}_2 - \dot{\omega}_2^*) \\ &\quad + (\omega_3 - \omega_3^*) (q_{e3} + \eta_3^T S_3 + \delta_3 + \bar{u}_3 - \beta_3(\xi_3 - \hat{\xi}_3)\bar{u}_3 - \dot{\omega}_3^*) \\ &\quad + (\eta_1 - \hat{\eta}_1)^T \Gamma_1 (-\dot{\hat{\eta}}_1) + (\eta_2 - \hat{\eta}_2)^T \Gamma_2 (-\dot{\hat{\eta}}_2) + (\eta_3 - \hat{\eta}_3)^T \Gamma_3 (-\dot{\hat{\eta}}_3) \\ &\quad + \lambda_1 \beta_1 (\xi_1 - \hat{\xi}_1) (-\dot{\hat{\xi}}_1) + \lambda_2 \beta_2 (\xi_2 - \hat{\xi}_2) (-\dot{\hat{\xi}}_2) + \lambda_3 \beta_3 (\xi_3 - \hat{\xi}_3) (-\dot{\hat{\xi}}_3)\end{aligned}\quad (5.129)$$

(5.129) can be rewritten as

$$\begin{aligned}
\dot{V}_2 &= -k_1 q_{e1}^2 + (\eta_1 - \hat{\eta}_1)^T \Gamma_1 (-\dot{\hat{\eta}}_1) + \lambda_1 \beta_1 (\xi_1 - \hat{\xi}_1) (-\lambda_1^{-1} \bar{u}_1 (\omega_1 - \omega_1^*) - \dot{\hat{\xi}}_1) \\
&\quad - k_2 q_{e2}^2 + (\eta_2 - \hat{\eta}_2)^T \Gamma_2 (-\dot{\hat{\eta}}_2) + \lambda_2 \beta_2 (\xi_2 - \hat{\xi}_2) (-\lambda_2^{-1} \bar{u}_2 (\omega_2 - \omega_2^*) - \dot{\hat{\xi}}_2) \\
&\quad - k_3 q_{e3}^2 + (\eta_3 - \hat{\eta}_3)^T \Gamma_3 (-\dot{\hat{\eta}}_3) + \lambda_3 \beta_3 (\xi_3 - \hat{\xi}_3) (-\lambda_3^{-1} \bar{u}_3 (\omega_3 - \omega_3^*) - \dot{\hat{\xi}}_3) \\
&\quad + (\omega_1 - \omega_1^*) (q_{e1} + (\eta_1 - \hat{\eta}_1)^T S_1 + \hat{\eta}_1^T S_1 + \delta_1 + \bar{u}_1 - \dot{\omega}_1^*) \\
&\quad + (\omega_2 - \omega_2^*) (q_{e2} + (\eta_2 - \hat{\eta}_2)^T S_2 + \hat{\eta}_2^T S_2 + \delta_2 + \bar{u}_2 - \dot{\omega}_2^*) \\
&\quad + (\omega_3 - \omega_3^*) (q_{e3} + (\eta_3 - \hat{\eta}_3)^T S_3 + \hat{\eta}_3^T S_3 + \delta_3 + \bar{u}_3 - \dot{\omega}_3^*) \\
&= -k_1 q_{e1}^2 - k_2 q_{e2}^2 - k_3 q_{e3}^2 + (\omega_1 - \omega_1^*) \delta_1 + (\omega_2 - \omega_2^*) \delta_2 + (\omega_3 - \omega_3^*) \delta_3 \\
&\quad + (\eta_1 - \hat{\eta}_1)^T \Gamma_1 (\Gamma_1^{-1} (\omega_1 - \omega_1^*) S_1 - \dot{\hat{\eta}}_1) + \lambda_1 \beta_1 (\xi_1 - \hat{\xi}_1) (-\lambda_1^{-1} \bar{u}_1 (\omega_1 - \omega_1^*) - \dot{\hat{\xi}}_1) \\
&\quad + (\eta_2 - \hat{\eta}_2)^T \Gamma_2 (\Gamma_2^{-1} (\omega_2 - \omega_2^*) S_2 - \dot{\hat{\eta}}_2) + \lambda_2 \beta_2 (\xi_2 - \hat{\xi}_2) (-\lambda_2^{-1} \bar{u}_2 (\omega_2 - \omega_2^*) - \dot{\hat{\xi}}_2) \\
&\quad + (\eta_3 - \hat{\eta}_3)^T \Gamma_3 (\Gamma_3^{-1} (\omega_3 - \omega_3^*) S_3 - \dot{\hat{\eta}}_3) + \lambda_3 \beta_3 (\xi_3 - \hat{\xi}_3) (-\lambda_3^{-1} \bar{u}_3 (\omega_3 - \omega_3^*) - \dot{\hat{\xi}}_3) \\
&\quad + (\omega_1 - \omega_1^*) (q_{e1} + \hat{\eta}_1^T S_1 + \bar{u}_1 - \dot{\omega}_1^*) \\
&\quad + (\omega_2 - \omega_2^*) (q_{e2} + \hat{\eta}_2^T S_2 + \bar{u}_2 - \dot{\omega}_2^*) \\
&\quad + (\omega_3 - \omega_3^*) (q_{e3} + \hat{\eta}_3^T S_3 + \bar{u}_3 - \dot{\omega}_3^*) \tag{5.130}
\end{aligned}$$

The following adaptation laws are introduced

$$\begin{aligned}
\dot{\hat{\eta}}_1 &= \Gamma_1^{-1} (\omega_1 - \omega_1^*) S_1 - \sigma_1 \hat{\eta}_1 \\
\dot{\hat{\eta}}_2 &= \Gamma_2^{-1} (\omega_2 - \omega_2^*) S_2 - \sigma_2 \hat{\eta}_2 \\
\dot{\hat{\eta}}_3 &= \Gamma_3^{-1} (\omega_3 - \omega_3^*) S_3 - \sigma_3 \hat{\eta}_3 \tag{5.131}
\end{aligned}$$

$$\begin{aligned}
\dot{\hat{\xi}}_1 &= \lambda_1^{-1} \bar{u}_1 (\omega_1 - \omega_1^*) - \varrho_1 \hat{\xi}_1 \\
\dot{\hat{\xi}}_2 &= \lambda_2^{-1} \bar{u}_2 (\omega_2 - \omega_2^*) - \varrho_2 \hat{\xi}_2 \\
\dot{\hat{\xi}}_3 &= \lambda_3^{-1} \bar{u}_3 (\omega_3 - \omega_3^*) - \varrho_3 \hat{\xi}_3 \tag{5.132}
\end{aligned}$$

Then, (5.130) can be rewritten as

$$\begin{aligned}
\dot{V}_2 &= -k_1 q_{e1}^2 - k_2 q_{e2}^2 - k_3 q_{e3}^2 \\
&\quad + (\omega_1 - \omega_1^*) \delta_1 + (\omega_2 - \omega_2^*) \delta_2 + (\omega_3 - \omega_3^*) \delta_3 \\
&\quad + (\omega_1 - \omega_1^*) (q_{e1} + \hat{\eta}_1^T S_1 + \bar{u}_1 - \dot{\omega}_1^*) + \sigma_1 (\eta_1 - \hat{\eta}_1)^T \Gamma_1 \hat{\eta}_1 \\
&\quad + (\omega_2 - \omega_2^*) (q_{e2} + \hat{\eta}_2^T S_2 + \bar{u}_2 - \dot{\omega}_2^*) + \sigma_2 (\eta_2 - \hat{\eta}_2)^T \Gamma_2 \hat{\eta}_2 \\
&\quad + (\omega_3 - \omega_3^*) (q_{e3} + \hat{\eta}_3^T S_3 + \bar{u}_3 - \dot{\omega}_3^*) + \sigma_3 (\eta_3 - \hat{\eta}_3)^T \Gamma_3 \hat{\eta}_3 \\
&\quad + \varrho_1 \lambda_1 \beta_1 (\xi_1 - \hat{\xi}_1) \hat{\xi}_1 + \varrho_2 \lambda_2 \beta_2 (\xi_2 - \hat{\xi}_2) \hat{\xi}_2 + \varrho_3 \lambda_3 \beta_3 (\xi_3 - \hat{\xi}_3) \hat{\xi}_3 \tag{5.133}
\end{aligned}$$

Due to  $\hat{\eta}_i = \eta_i - (\eta_i - \hat{\eta}_i)$  and  $\hat{\xi}_i = \xi_i - (\xi_i - \hat{\xi}_i)$ ,  $\dot{V}_2$  in (5.133) can be re-expressed as

$$\begin{aligned}
\dot{V}_2 &= -k_1 q_{e1}^2 - k_2 q_{e2}^2 - k_3 q_{e3}^2 \\
&\quad + (\omega_1 - \omega_1^*)\delta_1 + (\omega_2 - \omega_2^*)\delta_2 + (\omega_3 - \omega_3^*)\delta_3 \\
&\quad + (\omega_1 - \omega_1^*)(q_{e1} + \hat{\eta}_1^T S_1 + \bar{u}_1 - \dot{\omega}_1^*) - \sigma_1(\eta_1 - \hat{\eta}_1)^T \Gamma_1(\eta_1 - \hat{\eta}_1) \\
&\quad + (\omega_2 - \omega_2^*)(q_{e2} + \hat{\eta}_2^T S_2 + \bar{u}_2 - \dot{\omega}_2^*) - \sigma_2(\eta_2 - \hat{\eta}_2)^T \Gamma_2(\eta_2 - \hat{\eta}_2) \\
&\quad + (\omega_3 - \omega_3^*)(q_{e3} + \hat{\eta}_3^T S_3 + \bar{u}_3 - \dot{\omega}_3^*) - \sigma_3(\eta_3 - \hat{\eta}_3)^T \Gamma_3(\eta_3 - \hat{\eta}_3) \\
&\quad + \sigma_1(\eta_1 - \hat{\eta}_1)^T \Gamma_1 \eta_1 + \sigma_2(\eta_2 - \hat{\eta}_2)^T \Gamma_2 \eta_2 + \sigma_3(\eta_3 - \hat{\eta}_3)^T \Gamma_3 \eta_3 \\
&\quad + \varrho_1 \lambda_1 \beta_1 (\xi_1 - \hat{\xi}_1) \xi_1 + \varrho_2 \lambda_2 \beta_2 (\xi_2 - \hat{\xi}_2) \xi_2 + \varrho_3 \lambda_3 \beta_3 (\xi_3 - \hat{\xi}_3) \xi_3 \\
&\quad - \varrho_1 \lambda_1 \beta_1 (\xi_1 - \hat{\xi}_1)^2 - \varrho_2 \lambda_2 \beta_2 (\xi_2 - \hat{\xi}_2)^2 - \varrho_3 \lambda_3 \beta_3 (\xi_3 - \hat{\xi}_3)^2 \tag{5.134} \\
&\leq -k_1 q_{e1}^2 + \sigma_1 \left( \frac{1}{2} (\eta_1 - \hat{\eta}_1)^T \Gamma_1 (\eta_1 - \hat{\eta}_1) + \frac{1}{2} \eta_1^T \Gamma_1 \eta_1 \right) + \varrho_1 \lambda_1 \beta_1 \left( \frac{1}{2} (\xi_1 - \hat{\xi}_1)^2 + \frac{1}{2} \xi_1^2 \right) \\
&\quad - k_2 q_{e2}^2 + \sigma_2 \left( \frac{1}{2} (\eta_2 - \hat{\eta}_2)^T \Gamma_2 (\eta_2 - \hat{\eta}_2) + \frac{1}{2} \eta_2^T \Gamma_2 \eta_2 \right) + \varrho_2 \lambda_2 \beta_2 \left( \frac{1}{2} (\xi_2 - \hat{\xi}_2)^2 + \frac{1}{2} \xi_2^2 \right) \\
&\quad - k_3 q_{e3}^2 + \sigma_3 \left( \frac{1}{2} (\eta_3 - \hat{\eta}_3)^T \Gamma_3 (\eta_3 - \hat{\eta}_3) + \frac{1}{2} \eta_3^T \Gamma_3 \eta_3 \right) + \varrho_3 \lambda_3 \beta_3 \left( \frac{1}{2} (\xi_3 - \hat{\xi}_3)^2 + \frac{1}{2} \xi_3^2 \right) \\
&\quad + (\omega_1 - \omega_1^*)(q_{e1} + \hat{\eta}_1^T S_1 + \bar{u}_1 - \dot{\omega}_1^*) + \frac{1}{2} (\omega_1 - \omega_1^*)^2 + \frac{1}{2} \delta_1^2 \\
&\quad + (\omega_2 - \omega_2^*)(q_{e2} + \hat{\eta}_2^T S_2 + \bar{u}_2 - \dot{\omega}_2^*) + \frac{1}{2} (\omega_2 - \omega_2^*)^2 + \frac{1}{2} \delta_2^2 \\
&\quad + (\omega_3 - \omega_3^*)(q_{e3} + \hat{\eta}_3^T S_3 + \bar{u}_3 - \dot{\omega}_3^*) + \frac{1}{2} (\omega_3 - \omega_3^*)^2 + \frac{1}{2} \delta_3^2 \\
&\quad - \sigma_1(\eta_1 - \hat{\eta}_1)^T \Gamma_1(\eta_1 - \hat{\eta}_1) - \sigma_2(\eta_2 - \hat{\eta}_2)^T \Gamma_2(\eta_2 - \hat{\eta}_2) - \sigma_3(\eta_3 - \hat{\eta}_3)^T \Gamma_3(\eta_3 - \hat{\eta}_3) \\
&\quad - \varrho_1 \lambda_1 \beta_1 (\xi_1 - \hat{\xi}_1)^2 - \varrho_2 \lambda_2 \beta_2 (\xi_2 - \hat{\xi}_2)^2 - \varrho_3 \lambda_3 \beta_3 (\xi_3 - \hat{\xi}_3)^2 \tag{5.135}
\end{aligned}$$

where the following Young's inequalities are used to obtain (5.135) from (5.134).

$$\begin{aligned}
(\omega_1 - \omega_1^*)\delta_1 &\leq \frac{1}{2} (\omega_1 - \omega_1^*)^2 + \frac{1}{2} \delta_1^2 \\
(\omega_2 - \omega_2^*)\delta_2 &\leq \frac{1}{2} (\omega_2 - \omega_2^*)^2 + \frac{1}{2} \delta_2^2 \\
(\omega_3 - \omega_3^*)\delta_3 &\leq \frac{1}{2} (\omega_3 - \omega_3^*)^2 + \frac{1}{2} \delta_3^2 \tag{5.136}
\end{aligned}$$

$$\begin{aligned}
(\xi_1 - \hat{\xi}_1)\xi_1 &\leq \frac{1}{2} (\xi_1 - \hat{\xi}_1)^2 + \frac{1}{2} \xi_1^2 \\
(\xi_2 - \hat{\xi}_2)\xi_2 &\leq \frac{1}{2} (\xi_2 - \hat{\xi}_2)^2 + \frac{1}{2} \xi_2^2 \\
(\xi_3 - \hat{\xi}_3)\xi_3 &\leq \frac{1}{2} (\xi_3 - \hat{\xi}_3)^2 + \frac{1}{2} \xi_3^2 \tag{5.137}
\end{aligned}$$

$$\begin{aligned}
(\eta_1 - \hat{\eta}_1)^T \Gamma_1 \eta_1 &\leq \frac{1}{2} (\eta_1 - \hat{\eta}_1)^T \Gamma_1 (\eta_1 - \hat{\eta}_1) + \frac{1}{2} \eta_1^T \Gamma_1 \eta_1 \\
(\eta_2 - \hat{\eta}_2)^T \Gamma_2 \eta_2 &\leq \frac{1}{2} (\eta_2 - \hat{\eta}_2)^T \Gamma_2 (\eta_2 - \hat{\eta}_2) + \frac{1}{2} \eta_2^T \Gamma_2 \eta_2 \\
(\eta_3 - \hat{\eta}_3)^T \Gamma_3 \eta_3 &\leq \frac{1}{2} (\eta_3 - \hat{\eta}_3)^T \Gamma_3 (\eta_3 - \hat{\eta}_3) + \frac{1}{2} \eta_3^T \Gamma_3 \eta_3 \tag{5.138}
\end{aligned}$$

due to  $xy \leq \frac{1}{2}(x^2 + y^2)$  and  $x^T \Gamma y \leq \frac{1}{2}x^T \Gamma x + \frac{1}{2}y^T \Gamma y$ .

After some operations on (5.135), it follows that  $\dot{V}_2$  can be rewritten as

$$\begin{aligned}
\dot{V}_2 \leq & -k_1 q_{e1}^2 + \frac{1}{2} \sigma_1 \eta_1^T \Gamma_1 \eta_1 + \frac{1}{2} \varrho_1 \lambda_1 \beta_1 \xi_1^2 - \frac{1}{2} \varrho_1 \lambda_1 \beta_1 (\xi_1 - \hat{\xi}_1)^2 \\
& -k_2 q_{e2}^2 + \frac{1}{2} \sigma_2 \eta_2^T \Gamma_2 \eta_2 + \frac{1}{2} \varrho_2 \lambda_2 \beta_2 \xi_2^2 - \frac{1}{2} \varrho_2 \lambda_2 \beta_2 (\xi_2 - \hat{\xi}_2)^2 \\
& -k_3 q_{e3}^2 + \frac{1}{2} \sigma_3 \eta_3^T \Gamma_3 \eta_3 + \frac{1}{2} \varrho_3 \lambda_3 \beta_3 \xi_3^2 - \frac{1}{2} \varrho_3 \lambda_3 \beta_3 (\xi_3 - \hat{\xi}_3)^2 \\
& -\frac{1}{2} \sigma_1 (\eta_1 - \hat{\eta}_1)^T \Gamma_1 (\eta_1 - \hat{\eta}_1) - \frac{1}{2} \sigma_2 (\eta_2 - \hat{\eta}_2)^T \Gamma_2 (\eta_2 - \hat{\eta}_2) - \frac{1}{2} \sigma_3 (\eta_3 - \hat{\eta}_3)^T \Gamma_3 (\eta_3 - \hat{\eta}_3) \\
& + (\omega_1 - \omega_1^*) \left( q_{e1} + \hat{\eta}_1^T S_1 + \bar{u}_1 - \dot{\omega}_1^* + \frac{1}{2} (\omega_1 - \omega_1^*) \right) + \frac{1}{2} \delta_1^2 \\
& + (\omega_2 - \omega_2^*) \left( q_{e2} + \hat{\eta}_2^T S_2 + \bar{u}_2 - \dot{\omega}_2^* + \frac{1}{2} (\omega_2 - \omega_2^*) \right) + \frac{1}{2} \delta_2^2 \\
& + (\omega_3 - \omega_3^*) \left( q_{e3} + \hat{\eta}_3^T S_3 + \bar{u}_3 - \dot{\omega}_3^* + \frac{1}{2} (\omega_3 - \omega_3^*) \right) + \frac{1}{2} \delta_3^2
\end{aligned} \tag{5.139}$$

Due to (5.123),  $\dot{V}_2$  in (5.139) can be simplified as

$$\begin{aligned}
\dot{V}_2 \leq & -k_1 q_{e1}^2 + \frac{1}{2} \sigma_1 \eta_1^T \Gamma_1 \eta_1 + \frac{1}{2} \varrho_1 \lambda_1 \xi_1 - \frac{1}{2} \varrho_1 \lambda_1 \beta_1 (\xi_1 - \hat{\xi}_1)^2 \\
& -k_2 q_{e2}^2 + \frac{1}{2} \sigma_2 \eta_2^T \Gamma_2 \eta_2 + \frac{1}{2} \varrho_2 \lambda_2 \xi_2 - \frac{1}{2} \varrho_2 \lambda_2 \beta_2 (\xi_2 - \hat{\xi}_2)^2 \\
& -k_3 q_{e3}^2 + \frac{1}{2} \sigma_3 \eta_3^T \Gamma_3 \eta_3 + \frac{1}{2} \varrho_3 \lambda_3 \xi_3 - \frac{1}{2} \varrho_3 \lambda_3 \beta_3 (\xi_3 - \hat{\xi}_3)^2 \\
& -\frac{1}{2} \sigma_1 (\eta_1 - \hat{\eta}_1)^T \Gamma_1 (\eta_1 - \hat{\eta}_1) - \frac{1}{2} \sigma_2 (\eta_2 - \hat{\eta}_2)^T \Gamma_2 (\eta_2 - \hat{\eta}_2) - \frac{1}{2} \sigma_3 (\eta_3 - \hat{\eta}_3)^T \Gamma_3 (\eta_3 - \hat{\eta}_3) \\
& + (\omega_1 - \omega_1^*) \left( q_{e1} + \hat{\eta}_1^T S_1 + \bar{u}_1 - \dot{\omega}_1^* + \frac{1}{2} (\omega_1 - \omega_1^*) \right) + \frac{1}{2} \delta_1^2 \\
& + (\omega_2 - \omega_2^*) \left( q_{e2} + \hat{\eta}_2^T S_2 + \bar{u}_2 - \dot{\omega}_2^* + \frac{1}{2} (\omega_2 - \omega_2^*) \right) + \frac{1}{2} \delta_2^2 \\
& + (\omega_3 - \omega_3^*) \left( q_{e3} + \hat{\eta}_3^T S_3 + \bar{u}_3 - \dot{\omega}_3^* + \frac{1}{2} (\omega_3 - \omega_3^*) \right) + \frac{1}{2} \delta_3^2
\end{aligned} \tag{5.140}$$

Note that (5.140) can be rewritten as follows.

$$\begin{aligned}
\dot{V}_2 &\leq -k_1 q_{e1}^2 + \frac{1}{2} \delta_1^2 + \frac{1}{2} \sigma_1 \eta_1^T \Gamma_1 \eta_1 + \frac{1}{2} \lambda_1 \varrho_1 \xi_1 - \frac{1}{2} \varrho_1 \lambda_1 \beta_1 (\xi_1 - \hat{\xi}_1)^2 \\
&\quad - k_2 q_{e2}^2 + \frac{1}{2} \delta_2^2 + \frac{1}{2} \sigma_2 \eta_2^T \Gamma_2 \eta_2 + \frac{1}{2} \lambda_2 \varrho_2 \xi_2 - \frac{1}{2} \varrho_2 \lambda_2 \beta_2 (\xi_2 - \hat{\xi}_2)^2 \\
&\quad - k_3 q_{e3}^2 + \frac{1}{2} \delta_3^2 + \frac{1}{2} \sigma_3 \eta_3^T \Gamma_3 \eta_3 + \frac{1}{2} \lambda_3 \varrho_3 \xi_3 - \frac{1}{2} \varrho_3 \lambda_3 \beta_3 (\xi_3 - \hat{\xi}_3)^2 \\
&\quad + (\omega_1 - \omega_1^*) \left( q_{e1} + \hat{\eta}_1^T S_1 + \bar{u}_1 - \dot{\omega}_1^* + \frac{1}{2} (\omega_1 - \omega_1^*) + k_4 (\omega_1 - \omega_1^*) - k_4 (\omega_1 - \omega_1^*) \right) \\
&\quad + (\omega_2 - \omega_2^*) \left( q_{e2} + \hat{\eta}_2^T S_2 + \bar{u}_2 - \dot{\omega}_2^* + \frac{1}{2} (\omega_2 - \omega_2^*) + k_5 (\omega_2 - \omega_2^*) - k_5 (\omega_2 - \omega_2^*) \right) \\
&\quad + (\omega_3 - \omega_3^*) \left( q_{e3} + \hat{\eta}_3^T S_3 + \bar{u}_3 - \dot{\omega}_3^* + \frac{1}{2} (\omega_3 - \omega_3^*) + k_6 (\omega_3 - \omega_3^*) - k_6 (\omega_3 - \omega_3^*) \right) \\
&\quad - \frac{1}{2} \sigma_1 (\eta_1 - \hat{\eta}_1)^T \Gamma_1 (\eta_1 - \hat{\eta}_1) - \frac{1}{2} \sigma_2 (\eta_2 - \hat{\eta}_2)^T \Gamma_2 (\eta_2 - \hat{\eta}_2) - \frac{1}{2} \sigma_3 (\eta_3 - \hat{\eta}_3)^T \Gamma_3 (\eta_3 - \hat{\eta}_3) \\
&= -k_1 q_{e1}^2 - k_4 (\omega_1 - \omega_1^*)^2 + \frac{1}{2} \delta_1^2 + \frac{1}{2} \sigma_1 \eta_1^T \Gamma_1 \eta_1 + \frac{1}{2} \lambda_1 \varrho_1 \xi_1 - \frac{1}{2} \varrho_1 \lambda_1 \beta_1 (\xi_1 - \hat{\xi}_1)^2 \\
&\quad - k_2 q_{e2}^2 - k_5 (\omega_2 - \omega_2^*)^2 + \frac{1}{2} \delta_2^2 + \frac{1}{2} \sigma_2 \eta_2^T \Gamma_2 \eta_2 + \frac{1}{2} \lambda_2 \varrho_2 \xi_2 - \frac{1}{2} \varrho_2 \lambda_2 \beta_2 (\xi_2 - \hat{\xi}_2)^2 \\
&\quad - k_3 q_{e3}^2 - k_6 (\omega_3 - \omega_3^*)^2 + \frac{1}{2} \delta_3^2 + \frac{1}{2} \sigma_3 \eta_3^T \Gamma_3 \eta_3 + \frac{1}{2} \lambda_3 \varrho_3 \xi_3 - \frac{1}{2} \varrho_3 \lambda_3 \beta_3 (\xi_3 - \hat{\xi}_3)^2 \\
&\quad - \frac{1}{2} \sigma_1 (\eta_1 - \hat{\eta}_1)^T \Gamma_1 (\eta_1 - \hat{\eta}_1) - \frac{1}{2} \sigma_2 (\eta_2 - \hat{\eta}_2)^T \Gamma_2 (\eta_2 - \hat{\eta}_2) - \frac{1}{2} \sigma_3 (\eta_3 - \hat{\eta}_3)^T \Gamma_3 (\eta_3 - \hat{\eta}_3) \\
&\quad + (\omega_1 - \omega_1^*) \left[ q_{e1} + \hat{\eta}_1^T S_1 + \bar{u}_1 - \dot{\omega}_1^* + \left( k_4 + \frac{1}{2} \right) (\omega_1 - \omega_1^*) \right] \\
&\quad + (\omega_2 - \omega_2^*) \left[ q_{e2} + \hat{\eta}_2^T S_2 + \bar{u}_2 - \dot{\omega}_2^* + \left( k_5 + \frac{1}{2} \right) (\omega_2 - \omega_2^*) \right] \\
&\quad + (\omega_3 - \omega_3^*) \left[ q_{e3} + \hat{\eta}_3^T S_3 + \bar{u}_3 - \dot{\omega}_3^* + \left( k_6 + \frac{1}{2} \right) (\omega_3 - \omega_3^*) \right] \tag{5.141}
\end{aligned}$$

where  $k_4, k_5, k_6$  are positive gains. To get the control law, set

$$\begin{aligned}
(\omega_1 - \omega_1^*) \left[ q_{e1} + \hat{\eta}_1^T S_1 + \bar{u}_1 - \dot{\omega}_1^* + \left( k_4 + \frac{1}{2} \right) (\omega_1 - \omega_1^*) \right] &= 0 \\
(\omega_2 - \omega_2^*) \left[ q_{e2} + \hat{\eta}_2^T S_2 + \bar{u}_2 - \dot{\omega}_2^* + \left( k_5 + \frac{1}{2} \right) (\omega_2 - \omega_2^*) \right] &= 0 \\
(\omega_3 - \omega_3^*) \left[ q_{e3} + \hat{\eta}_3^T S_3 + \bar{u}_3 - \dot{\omega}_3^* + \left( k_6 + \frac{1}{2} \right) (\omega_3 - \omega_3^*) \right] &= 0 \tag{5.142}
\end{aligned}$$

which can be rewritten as

$$\begin{aligned}
\bar{u}_1 &= -q_{e1} - \hat{\eta}_1^T S_1 + \dot{\omega}_1^* - \left( k_4 + \frac{1}{2} \right) (\omega_1 - \omega_1^*) \\
\bar{u}_2 &= -q_{e2} - \hat{\eta}_2^T S_2 + \dot{\omega}_2^* - \left( k_5 + \frac{1}{2} \right) (\omega_2 - \omega_2^*) \\
\bar{u}_3 &= -q_{e3} - \hat{\eta}_3^T S_3 + \dot{\omega}_3^* - \left( k_6 + \frac{1}{2} \right) (\omega_3 - \omega_3^*) \tag{5.143}
\end{aligned}$$

Using (5.142), (5.141) can be simplified as

$$\begin{aligned}
\dot{V}_2 &\leq -k_1 q_{e1}^2 - k_2 q_{e2}^2 - k_3 q_{e3}^2 - k_4 (\omega_1 - \omega_1^*)^2 - k_5 (\omega_2 - \omega_2^*)^2 - k_6 (\omega_3 - \omega_3^*)^2 \\
&\quad - \frac{1}{2} \sigma_1 (\eta_1 - \hat{\eta}_1)^T \Gamma_1 (\eta_1 - \hat{\eta}_1) - \frac{1}{2} \sigma_2 (\eta_2 - \hat{\eta}_2)^T \Gamma_2 (\eta_2 - \hat{\eta}_2) - \frac{1}{2} \sigma_3 (\eta_3 - \hat{\eta}_3)^T \Gamma_3 (\eta_3 - \hat{\eta}_3) \\
&\quad - \frac{1}{2} \varrho_1 \lambda_1 \beta_1 (\xi_1 - \hat{\xi}_1)^2 - \frac{1}{2} \varrho_2 \lambda_2 \beta_2 (\xi_2 - \hat{\xi}_2)^2 - \frac{1}{2} \varrho_3 \lambda_3 \beta_3 (\xi_3 - \hat{\xi}_3)^2 \\
&\quad + \frac{1}{2} \sigma_1 \eta_1^T \Gamma_1 \eta_1 + \frac{1}{2} \sigma_2 \eta_2^T \Gamma_2 \eta_2 + \frac{1}{2} \sigma_3 \eta_3^T \Gamma_3 \eta_3 \\
&\quad + \frac{1}{2} \lambda_1 \varrho_1 \xi_1 + \frac{1}{2} \lambda_2 \varrho_2 \xi_2 + \frac{1}{2} \lambda_3 \varrho_3 \xi_3 + \frac{1}{2} \delta_1^2 + \frac{1}{2} \delta_2^2 + \frac{1}{2} \delta_3^2 \\
&\leq -aV_2 + b
\end{aligned} \tag{5.144}$$

where

$$\begin{aligned}
a &= 2 \min \{k_1, k_2, k_3, k_4, k_5, k_6, \frac{1}{2} \sigma_1, \frac{1}{2} \sigma_2, \frac{1}{2} \sigma_3, \frac{1}{2} \varrho_1, \frac{1}{2} \varrho_2, \frac{1}{2} \varrho_3\} \\
b &= \frac{1}{2} \sigma_1 \eta_1^T \Gamma_1 \eta_1 + \frac{1}{2} \sigma_2 \eta_2^T \Gamma_2 \eta_2 + \frac{1}{2} \sigma_3 \eta_3^T \Gamma_3 \eta_3 + \frac{1}{2} \delta_1^2 + \frac{1}{2} \delta_2^2 \\
&\quad + \frac{1}{2} \delta_3^2 + \frac{1}{2} \lambda_1 \varrho_1 \xi_1 + \frac{1}{2} \lambda_2 \varrho_2 \xi_2 + \frac{1}{2} \lambda_3 \varrho_3 \xi_3
\end{aligned}$$

As a result,  $V_2$  is bounded by  $V_2(0)$  [49]. The detailed discussion for this result is given by (5.74)-(5.78) in Section 5.2. Therefore, all the error terms in  $V_2$  are bounded.

Combining (5.113)-(5.115) with (5.124) and (5.143) yields:

$$\begin{aligned}
u_1 &= -J_r \omega_2 \Omega + \tau_\phi = \hat{\xi}_1 \bar{u}_1 = \hat{\xi}_1 \left[ -q_{e1} - \hat{\eta}_1^T S_1 + \dot{\omega}_1^* - \left( k_4 + \frac{1}{2} \right) (\omega_1 - \omega_1^*) \right] \\
u_2 &= J_r \omega_1 \Omega + \tau_\theta = \hat{\xi}_2 \bar{u}_2 = \hat{\xi}_2 \left[ -q_{e2} - \hat{\eta}_2^T S_2 + \dot{\omega}_2^* - \left( k_5 + \frac{1}{2} \right) (\omega_2 - \omega_2^*) \right] \\
u_3 &= \tau_\psi = \hat{\xi}_3 \bar{u}_3 = \hat{\xi}_3 \left[ -q_{e3} - \hat{\eta}_3^T S_3 + \dot{\omega}_3^* - \left( k_6 + \frac{1}{2} \right) (\omega_3 - \omega_3^*) \right]
\end{aligned} \tag{5.145}$$

from which the following control law can be derived

$$\begin{aligned}
\tau_\phi &= \hat{\xi}_1 \left[ -q_{e1} - \hat{\eta}_1^T S_1 + \dot{\omega}_1^* - \left( k_4 + \frac{1}{2} \right) (\omega_1 - \omega_1^*) \right] + J_r \omega_2 \Omega \\
\tau_\theta &= \hat{\xi}_2 \left[ -q_{e2} - \hat{\eta}_2^T S_2 + \dot{\omega}_2^* - \left( k_5 + \frac{1}{2} \right) (\omega_2 - \omega_2^*) \right] - J_r \omega_1 \Omega \\
\tau_\psi &= \hat{\xi}_3 \left[ -q_{e3} - \hat{\eta}_3^T S_3 + \dot{\omega}_3^* - \left( k_6 + \frac{1}{2} \right) (\omega_3 - \omega_3^*) \right]
\end{aligned} \tag{5.146}$$

Using (3.8), the motor speeds  $\Omega_1, \Omega_2, \Omega_3,$  and  $\Omega_4$  can be calculated by

$$\begin{aligned}
 b(\Omega_1^2 + \Omega_2^2 + \Omega_3^2 + \Omega_4^2) &= U_1 \\
 bl(\Omega_2^2 - \Omega_4^2) - J_r \omega_2 \Omega &= \hat{\xi}_1 \left[ -q_{e1} - \hat{\eta}_1^T S_1 + \dot{\omega}_1^* - \left( k_4 + \frac{1}{2} \right) (\omega_1 - \omega_1^*) \right] \\
 bl(\Omega_1^2 - \Omega_3^2) + J_r \omega_1 \Omega &= \hat{\xi}_2 \left[ -q_{e2} - \hat{\eta}_2^T S_2 + \dot{\omega}_2^* - \left( k_5 + \frac{1}{2} \right) (\omega_2 - \omega_2^*) \right] \\
 k(\Omega_1^2 - \Omega_2^2 + \Omega_3^2 - \Omega_4^2) &= \hat{\xi}_3 \left[ -q_{e3} - \hat{\eta}_3^T S_3 + \dot{\omega}_3^* - \left( k_6 + \frac{1}{2} \right) (\omega_3 - \omega_3^*) \right] \quad (5.147)
 \end{aligned}$$

where  $\dot{\omega}_i^*$  and  $\omega_i^*$  are given by (5.95) and (5.96). The block diagram of the adaptive fuzzy backstepping controller with unit quaternion representation is shown in Fig. 5.26.

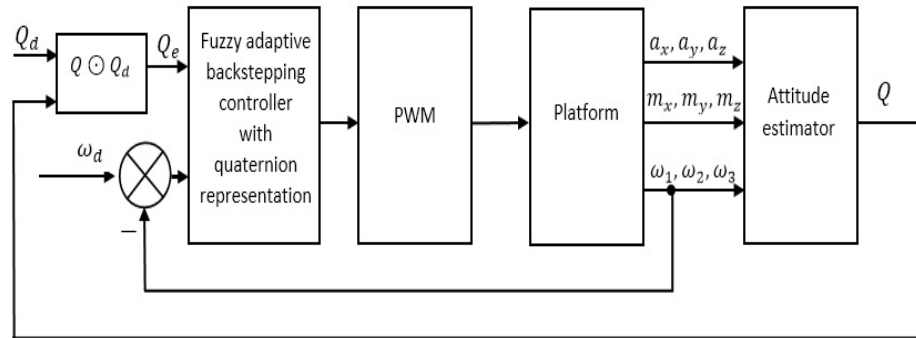


Figure 5.26: Adaptive Fuzzy Backstepping Controller with Unit Quaternion Representation

### 5.4.2 Experimental Results

Simulation results are also obtained for testing mathematical flexibility. However, in this section, experimental results are directly presented in Figs. 5.27 - 5.29. The real platform controlling method is similar to the backstepping controlling method, which is discussed in Section 5.2. The gain coefficients are  $k_1 = 160, k_2 = 160, k_3 = 6, k_4 = 7, k_5 = 7, k_6 = 650,$   $\Gamma_1 = \Gamma_3 = 0.001I_9, \Gamma_2 = 0.0001I_9, \lambda_1 = \lambda_2 = \lambda_3 = 1, \sigma_1 = \sigma_2 = 0.0001, \sigma_3 = 0.00007,$   $\varrho_1 = \varrho_2 = \varrho_3 = 1.$  Before testing the whole system, the performance of the controllers for the roll, pitch, and yaw angles are tested separately. The experimental results are shown in Fig. 5.27. As for the roll angle, it can be observed that the several sudden changes in the roll angle appear from 0 to 500 seconds, which are caused by adding external forces to the roll direction for creating some external disturbances and the roll angle settles down back to the desired value quickly after the changes due to the action of the adaptive controller. From 500 to 750 seconds, the setpoint for the roll angle was changed several times using the remote control to test the response of the adaptive controller along the roll direction. Similar tests were done to test the ability of disturbance attenuation of the adaptive controller for the pitch angle from 0 to 500 seconds and to examine the step response of the adaptive

controller from 500 to 950 seconds. As for the yaw angle, the step response was tested from 0 to 350 seconds and the disturbance test was conducted from 350 to 750 seconds.

The flying test results on attitude control are shown in Fig. 5.28 - 5.29. As shown in Fig. 5.28, despite some oscillations, it can be observed that the vibrations concerning  $\phi$ ,  $\theta$ , and  $\psi$  are controlled within a range of 10 degrees. Angular velocities are also within an acceptable range which is shown in Fig. 5.29.

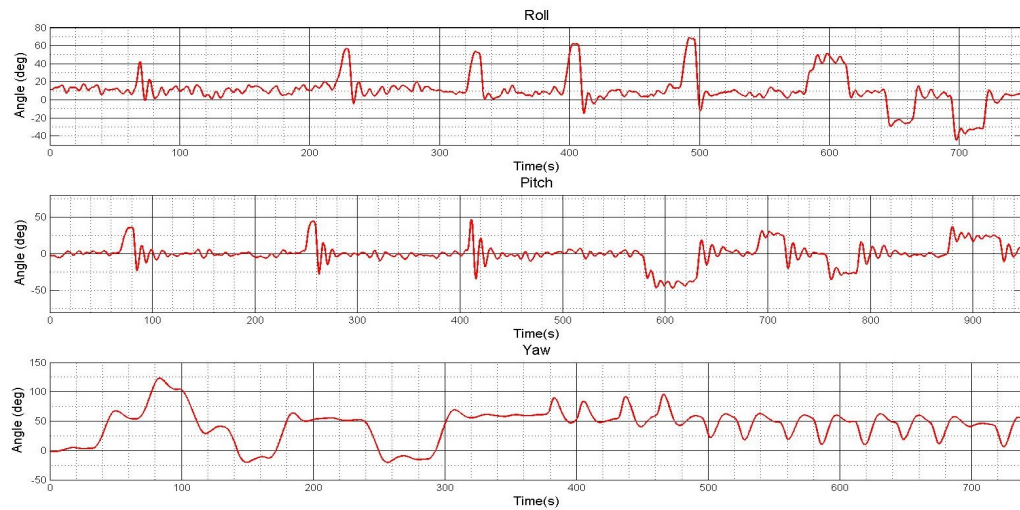


Figure 5.27: Separate Tests with Adaptive Fuzzy Backstepping Controller

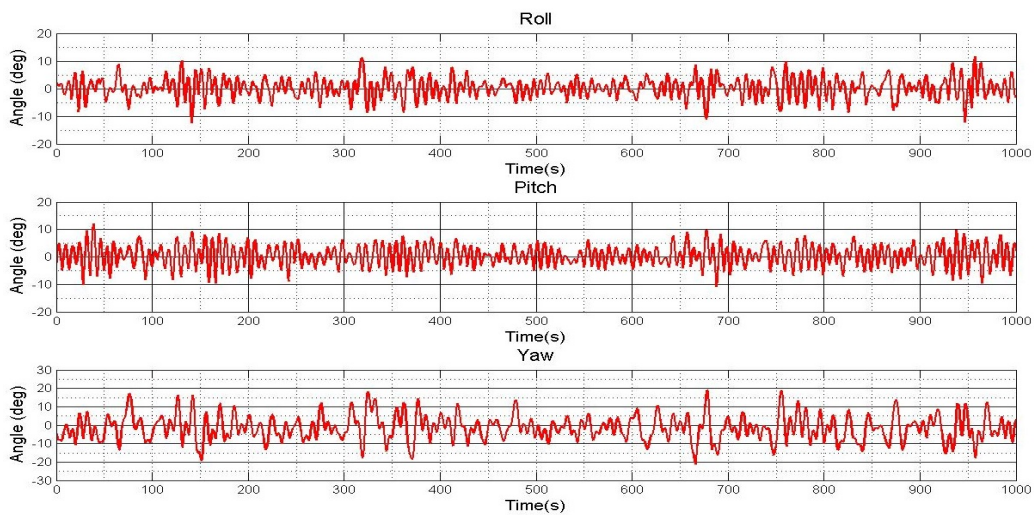


Figure 5.28:  $\phi$ ,  $\theta$ , and  $\psi$  with Adaptive Fuzzy Backstepping Controller

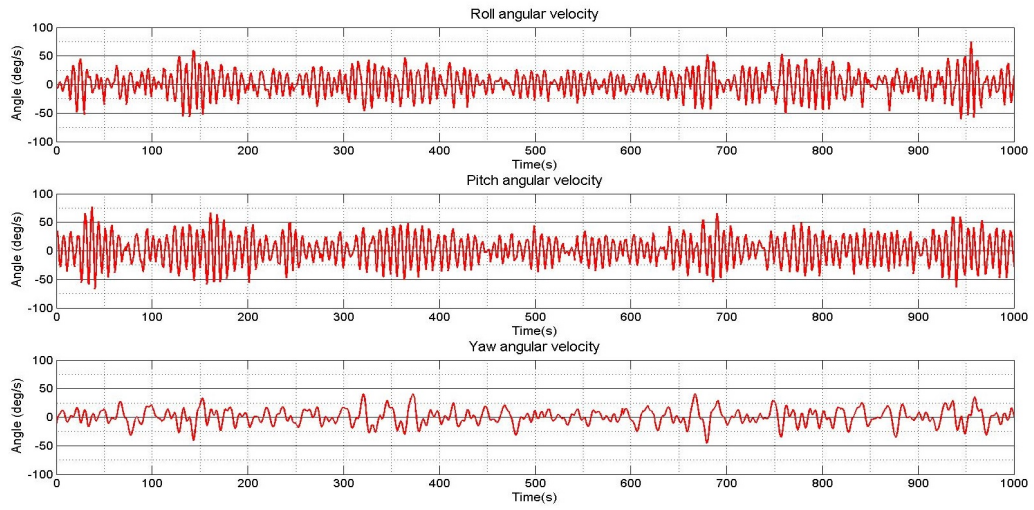


Figure 5.29: Angular Velocities with Adaptive Fuzzy Backstepping Controller

# Chapter 6

## Conclusion

### 6.1 Achievements of the Thesis

With the continuing development of high technology, the application field of UAV quadrotors is also becoming increasingly widespread. However, at the same time, one issue that should be considered is the stability of the controller. In this thesis, under the basic summarizing of a quadrotor research situation, some work has been done in this thesis.

The coordinate system and flight principles are discussed to show how the quadrotor flies. Three attitude representations are given in this thesis along with advantages and disadvantages. As mentioned in Chapter 2, because the Euler angle representation has a problem which is known as gimbal lock. So, the Euler angle representation is only used for simulation to verify the possibility of mathematical procedure. To deal with this problem, a unit quaternion representation is illustrated for its simple structure and computation amount which are used for the experimental platform. As for the dynamic model, an Euler Lagrangian formalism and a Newton-Euler formalism are introduced.

After the theoretical preparation, 4 controllers based on backstepping technique are discussed to stabilize the quadrotor. At first, two nonlinear controller with Euler angle representation are derived for testing theoretical feasibility and both of them are simulated. Because of the drawback of gimbal lock, controllers based on unit quaternion representation are then illustrated to solve this problem. When observing the dynamic model of the quadrotor, it is shown that the quadrotor is an under-actuated and coupling system with various uncertainties. Also, the measurement of inertial moments may possibly be inaccurate. An adaptive fuzzy estimator is added to the back-stepping controller to estimate unknown nonlinearities and unknown parameters. The fuzzy logic system consists of 9 fuzzy rules and there is no need for obtaining the full knowledge of inertial moments. As the experimental results shown, the attitude can be stabilized in a relatively satisfied range with the estimators. By comparing the test results, it has been observed that both backstepping and fuzzy adaptive backstepping controllers perform similarly.

## 6.2 Future Work

After this thesis, a couple of future work can be done. Also, plenty of improvements can be enriched to my thesis.

- Position controller design is also an important part of quadrotors. In this thesis, only attitude design is studied. The position controller not only include x, y direction, but also include the altitude control design. After that, the quadrotor can fly autonomously, which is determined by the ground station without the remote control transmitter.
- With the comparison of 3 kinds of representations, the unit quaternion has its own advantages. So, the position controller design need to be derived based on unit quaternion and implemented on a real quadrotor platform.
- Though trapezoidal membership function is used in this thesis, a comparison can be made to choose an optimal membership function. Also, more rules can be added to the fuzzy logic system.
- In this thesis, the quadrotor is tested while flying indoors. So, the flight environment is ideal, without extensive external disturbances. In the future study, external disturbances can be taken into consideration to test if the quadrotor can be stabilized outdoors by the designed controller.

# Bibliography

- [1] A. Chovancová, T. Fico, P. Hubinský, and F. Duchon, “Comparison of various quaternion-based control methods applied to quadrotor with disturbance observer and position estimator,” *Robotics and Autonomous Systems*, vol. 79, pp. 87–98, 2016.
- [2] A. Soumelidis, P. Gáspár, G. Regula, and B. Lantos, “Control of an experimental mini quad-rotor uav,” *IEEE 16th Mediterranean Conference on Control and Automation*, pp. 1252–1257, 2008.
- [3] J. Leishman, “Principles of helicopter aerodynamics,” *New York: Cambridge University Press*, 2000.
- [4] <https://gethover.com>.
- [5] A. Zulu and S. John, “A review of control algorithms for autonomous quadrotors,” *Open Journal of Applied Sciences*, vol. 79, pp. 547–556, 2014.
- [6] W. Jasim and D. Gu, “Integral backstepping controller for quadrotor path tracking,” *IEEE International Conference on Advanced Robotics*, pp. 593–598, July 2015.
- [7] H. An, J. Li, J. Wang, and H. Ma, “Backstepping-based inverse optimal attitude control of quadrotor,” *International Journal of Advanced Robotic Systems*, vol. 10, no. 5, pp. 223–232, May 2013.
- [8] P. D. Monte and B. Lohmann, “Trajectory tracking control for a quadrotor helicopter based on backstepping using a decoupling quaternion parametrization,” *IEEE 21th Mediterranean Conference on Control and Automation*, pp. 507–512, 2013.
- [9] S. Dolatabadi and M. Yazdanpanah, “Mimo sliding mode and backstepping control for a quadrotor uav,” *IEEE 23rd Iranian Conference on Electrical Engineering*, pp. 994–999, May 2015.
- [10] E. Fresk and G. Nikolakopoulos, “Experimental evaluation of a full quaternion based attitude quadrotor controller,” *IEEE 20th Conference on Emerging Technologies and Factory Automation*, pp. 1–4, Sept 2015.
- [11] F. Javidi-Niroumand and A. Fakharian, “Trajectory tracking via adaptive nonlinear control approach for a quadrotor mav,” *IEEE AI and Robotics*, pp. 1–7, 2015.

- [12] S. Tong, Y. Li, G. Feng, and T. Li, "Observer-based adaptive fuzzy backstepping dynamic surface control for a class of mimo nonlinear systems," *IEEE Transactions on Systems, Man, and Cybernetics, Part B (Cybernetics)*, vol. 41, no. 4, pp. 1124–1135, Aug 2011.
- [13] F. Yacef, O. Bouhali, and M. Hamerlain, "Adaptive fuzzy tracking control of unmanned quadrotor via backstepping," *IEEE 23rd International Symposium on Industrial Electronics*, pp. 40–45, June 2014.
- [14] F. Yacef, O. Bouhali, and M. Hamerlain, "Adaptive fuzzy backstepping control for trajectory tracking of unmanned aerial quadrotor," *IEEE International Conference on Unmanned Aircraft Systems*, pp. 920–927, 2014.
- [15] T. Madani and A. Benallegue, "Adaptive control via backstepping technique and neural networks of a quadrotor helicopter," *17th World Congress the International Federation of Automatic Control*, pp. 6513–6518, July 2008.
- [16] C. Coza and C. J. B. Macnab, "A new robust adaptive-fuzzy control method applied to quadrotor helicopter stabilization," *IEEE Fuzzy Information Processing Society*, pp. 454–458, 2006.
- [17] M. Bangura, R. Mahony, H. Lim, and H. J. Kim, "An open-source implementation of a unit quaternion based attitude and trajectory tracking for quadrotors," *Proceedings of the Australasian Conference on Robotics and Automation*, vol. 24, Dec 2014.
- [18] Y. C. Choi and H. S. Ahn, "Nonlinear control of quadrotor for point tracking: Actual implementation and experimental test," *IEEE/ASME Transactions on Mechatronics*, vol. 20, no. 3, pp. 1179–1192, June 2015.
- [19] H. Lim, J. Park, D. Lee, and H. J. Kim, "Build your own quadrotor," *IEEE Robotics and Automation Magazine*, vol. 19, no. 3, pp. 33–45, Sept 2012.
- [20] A. Tayebi, "Unit quaternion-based output feedback for the attitude tracking problem," *IEEE Transactions on Automatic Control*, vol. 56, no. 6, pp. 1516–1520, 2008.
- [21] X. Cui, "Intelligent backstepping quadrotor position control using neural network," *Master thesis, Lakehead University, Ontario, Canada*, 2016.
- [22] H. Huang, G. Hoffmann, S. Waslander, and C. Tomlin, "Aerodynamics and control of autonomous quadrotor helicopters in aggressive maneuvering," *IEEE International Conference on Robotics and Automation*, pp. 3277–3282, May 2009.
- [23] P. Bristeau, P. Martin, E. Salaun, and N. Petit, "The role of propeller aerodynamics in the model of a quadrotor uav," *IEEE European Control Conference*, pp. 683–688, Aug 2009.
- [24] M. Okasha and B. Newman, "Switching algorithm to avoid attitude representation singularity," *AIAA AtmosphericFlight Mechanics Conference*, pp. 1–17, Aug 2009.
- [25] F. Zhao and B. Wachem, "A novel quaternion integration approach for describing the behaviour of non-spherical particles," *Acta Mechanica*, vol. 224, no. 12, pp. 3091–3109, 2013.

- [26] M. Wang, "Attitude control of a quadrotor uav," *Master thesis, Lakehead University, Ontario, Canada*, 2015.
- [27] M. Shuster, "A survey of attitude representations," *Navigation*, vol. 8, no. 9, pp. 439–517, 1993.
- [28] B. C. Min, J. H. Hong, and E. T. Matson, "Adaptive robust control for an altitude control of a quadrotor type uav carrying an unknown payloads," *IEEE 11th International Conference on Control, Automation and Systems*, pp. 1147–1151, Oct 2011.
- [29] H. Bouadi, A. Aoudjif, and M. Guenifi, "Adaptive flight control for quadrotor uav in the presence of external disturbances," *IEEE 6th International Conference on Modeling, Simulation, and Applied Optimization*, pp. 1–6, 2015.
- [30] A. Dzaba and E. Schuster, "Nonlinear control of a dual-quadrotor assembly," *IEEE American Control Conference*, pp. 223–228, June 2013.
- [31] S. Bouabdallah, "Design and control of quadrotors with application to autonomous flying," *Ph.D. dissertation*, 2007.
- [32] G. V. Raffo, M. G. Ortega, and F. R. Rubio, "An underactuated  $h_{\infty}$  control strategy for a quadrotor helicopter," *IEEE European Control Conference*, pp. 3845–3850, Aug 2009.
- [33] A. Modirrousta and M. Khodabandeh, "Adaptive robust sliding mode controller design for full control of quadrotor with external disturbances," *IEEE Second RSI/ISM International Conference on Robotics and Mechatronics*, pp. 870–877, 2014.
- [34] T. Hamel and R. E. Mahony, "Dynamic modelling and configuration stabilization for an x4-flyer," *IFAC Proceedings*, vol. 35, no. 1, pp. 217–222, 2002.
- [35] L. R. G. Carrillo, A. E. D. López, R. Lozano, and C. Pégard, "Quad rotorcraft control, chapter 2," 2012.
- [36] <http://www.hobbyking.com>.
- [37] <http://www.robotshop.com/blog/en/make-uav-lesson-2-platform-14448>.
- [38] <http://www.atmel.com/>.
- [39] M. T. Köroglu, M. önkol, and M. Efe, "Experimental modelling of propulsion transients of a brushless dc motor and propeller pair under limited power conditions: A neural network based approach," *IFAC Proceedings*, vol. 42, no. 19, pp. 37–42, Sept 2009.
- [40] D. L. Gabriel, J. Meyer, and F. du Plessis, "Brushless dc motor characterisation and selection for a fixed wing uav," *IEEE AFRICON*, pp. 1–6, Sept 2011.
- [41] M. C. D. Simone, S. Russo, and A. Ruggiero, "Influence of aerodynamics on quadrotor dynamics," *Recent Researches in Mechanical and Transportation Systems Influence*, pp. 111–118, 2015.
- [42] <http://m-selig.ae.illinois.edu/props/volume-1/propDB-volume-1.html>.

- [43] Y. R. Mahony, V. Kumar, and P. Corke, “Multirotor aerial vehicles: modeling, estimation, and control of quadrotor,” *IEEE Robotics Automation Magazine*, vol. 19, no. 32, pp. 20–32, Sept 2012.
- [44] <https://alselectro.wordpress.com/category/quadcopter/>.
- [45] S. F. Desouky and H. M. Schwartz, “Q ( $\lambda$ )-learning adaptive fuzzy logic controllers for pursuit–evasion differential games,” *International Journal of Adaptive Control and Signal Processing*, vol. 25, no. 10, pp. 910–927, 2011.
- [46] Q. Zhou, P. Shi, J. Lu, and S. Xu, “Adaptive output-feedback fuzzy tracking control for a class of nonlinear systems,” *IEEE Transactions on Fuzzy Systems*, vol. 19, no. 5, pp. 972–982, Oct 2011.
- [47] L. Wang and J. M. Mendel, “Fuzzy basis functions, universal approximation, and orthogonal least-squares learning,” *IEEE Transactions on neural networks*, vol. 3, no. 5, pp. 807–814, 1992.
- [48] J. Zhou, C. Wen, and Y. Zhang, “Adaptive backstepping control of a class of uncertain nonlinear systems with unknown backlash-like hysteresis,” *IEEE transactions on Automatic Control*, vol. 49, no. 10, pp. 1751–1757, Oct 2004.
- [49] K. Gopalsamy, “Stability and oscillations in delay differential equations of population dynamic,” *Kluwer Academic, Dordrecht*, 1992.